CHAPTER III

RESULTS AND DISCUSSION

CHAPTER III

Contents *Page*

RESULTS AND DISCUSSION

The results of the experimental work that had been done in this study are presented in this chapter. The experimental work is divided into four main parts. The first part deals with the physical and chemical characteristics of the investigated samples. The second part deals with the sorption behavior of the selected radionuclides; of ^{134}Cs, ^{89}Sr, and ^{60}Co; and phenol onto the samples with batch technique. The third part deals with desorption behavior of phenol and the investigated radionuclides. The last part deals with column technique investigations.

III.1 Studied samples

In the current work two clay samples were collected from South-West of Allamine, Egypt and has a notation S_1 and from Baharia oasis, Egypt and has a notation S_2. In addition to a commercial activated carbon sample from Aldrich Company and this sample has a notation S_3.

III.2 Physical properties of samples

The specific surface area, moisture content and the point of zero charge are estimated and the data obtained are shown in the following items.

III.2.1 Specific surface area

The specific surface area for the investigated samples has been estimated at Microanalytical Center, Cairo University. The obtained data are presented in table (2).

Table (2): The specific surface area for the investigated samples

Sample	Specific surface area, m^2g^{-1}
S_1	407
S_2	350
S_3	610

III. 2. 2 The moisture content

The obtained data of moisture content of the investigated samples are shown in table (3). It is noticeable that S_3 has lower moisture content than clay samples (S_1 &S_2).

Table (3): The moisture content of the investigated samples

Sample	Moisture content %
S_1	4.5
S_2	5.1
S_3	1.3

III. 2. 3 point of zero charge (PZC) of the investigated samples

The data obtained for measurement of PZC of the investigated samples are shown in figures (13-15). The data reveal that the PZC of S_1, S_2 and S_3 are 5.8, 6.2 and 6.5, respectively. This means that their surface will, therefore, be negatively charged and have an electrostatic affinity for Cs^+, Co^{2+}, and Sr^{2+} from solution when the pH of the ambient solution is greater than the estimated value of the investigated sorbent **(Gary and Stephen, 2002)**.

Gary and Stephen (2002), reported that the sorption mechanism is described by the following equations:

$S\text{-}OH \leftrightarrow S\text{-}O^- + H^+$ .....(32)

$S\text{-}O^- + Cs^+ \leftrightarrow S\text{-}O\text{-}Cs$ ..... (33)

$S\text{-}O^- + Sr^{2+} \leftrightarrow S\text{-}O\text{-}Sr^+$ .....(34)

$S\text{-}O^- + Co^{2+} \leftrightarrow S\text{-}O\text{-}Co^+$ .....(35)

Where, S-OH denotes the surface site of the substrate. Eqn. (32) describes the deprotonation. Eqn. (33), (34) and (35) correspond to the sorption of Cs^+, Sr^{2+} and Co^{2+} onto the substrate.

III.3 Chemical analysis of the investigated clay samples

The chemical analysis of the investigated clay samples is shown in table (4). The data reveal that the elemental % of Al in S_1 is higher than that in S_2. The elemental % of Ca and Fe in S_2 is greater than that in S_1.

III.4 Total exchangeable metallic cations of the studied clays

The obtained data for the chemical analysis of the investigated clay samples as the milli equivalent (meq) of the total exchangeable metallic cations (TEMC) per 100g of each sample is presented in table (5). From this table it is observed that the sample of a notation S_1 has the higher exchangeable metallic cations than S_2.

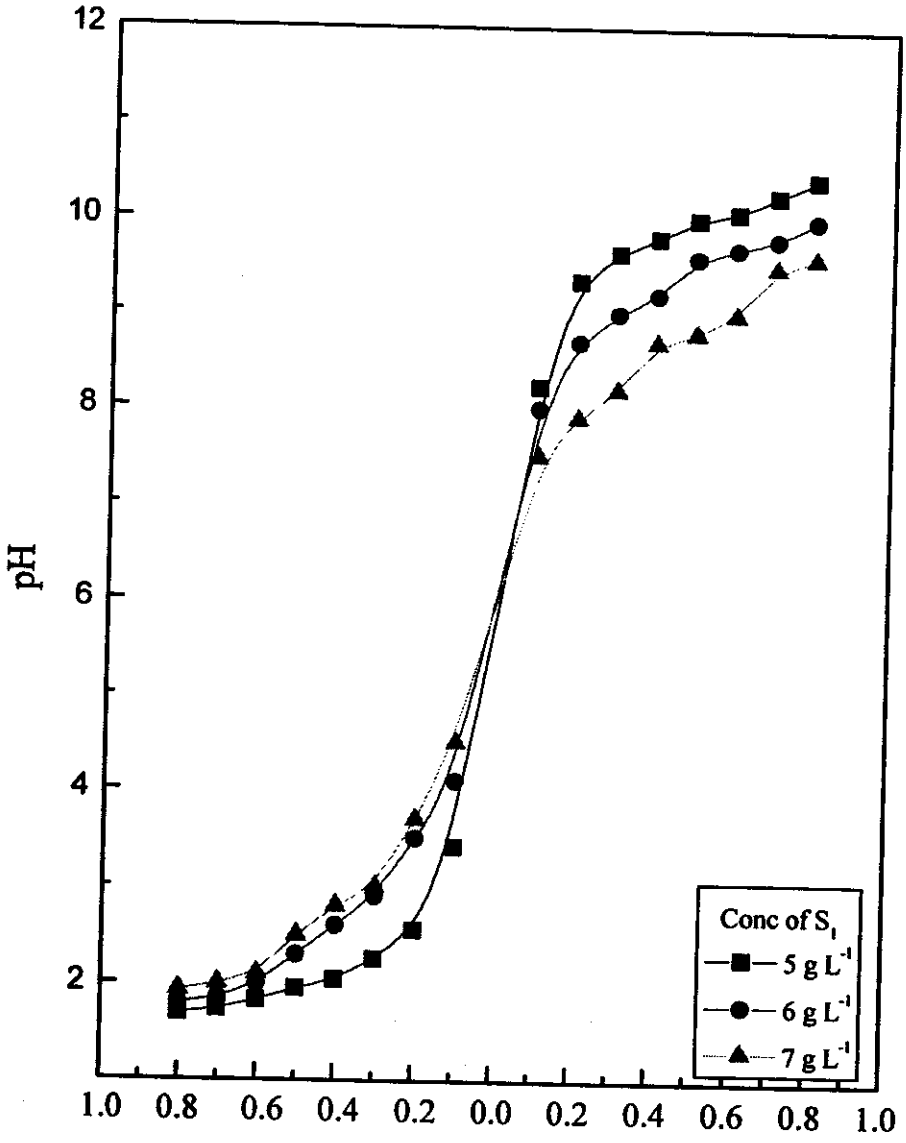

Amount of added acid and base

Fig. (13): Experimental measurment of PZC of S_1 sample.

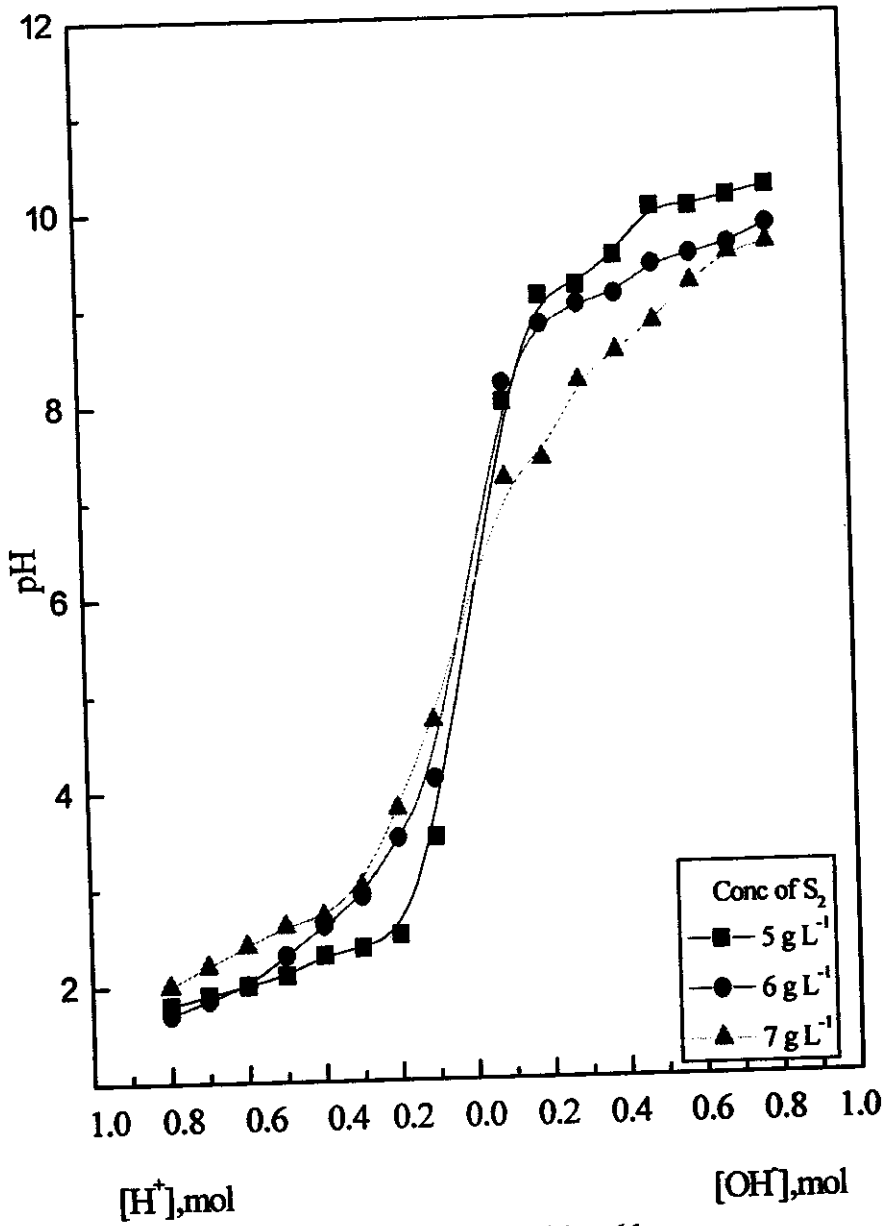

Fig. (14): Experimental measurment of PZC of S_2 sample.

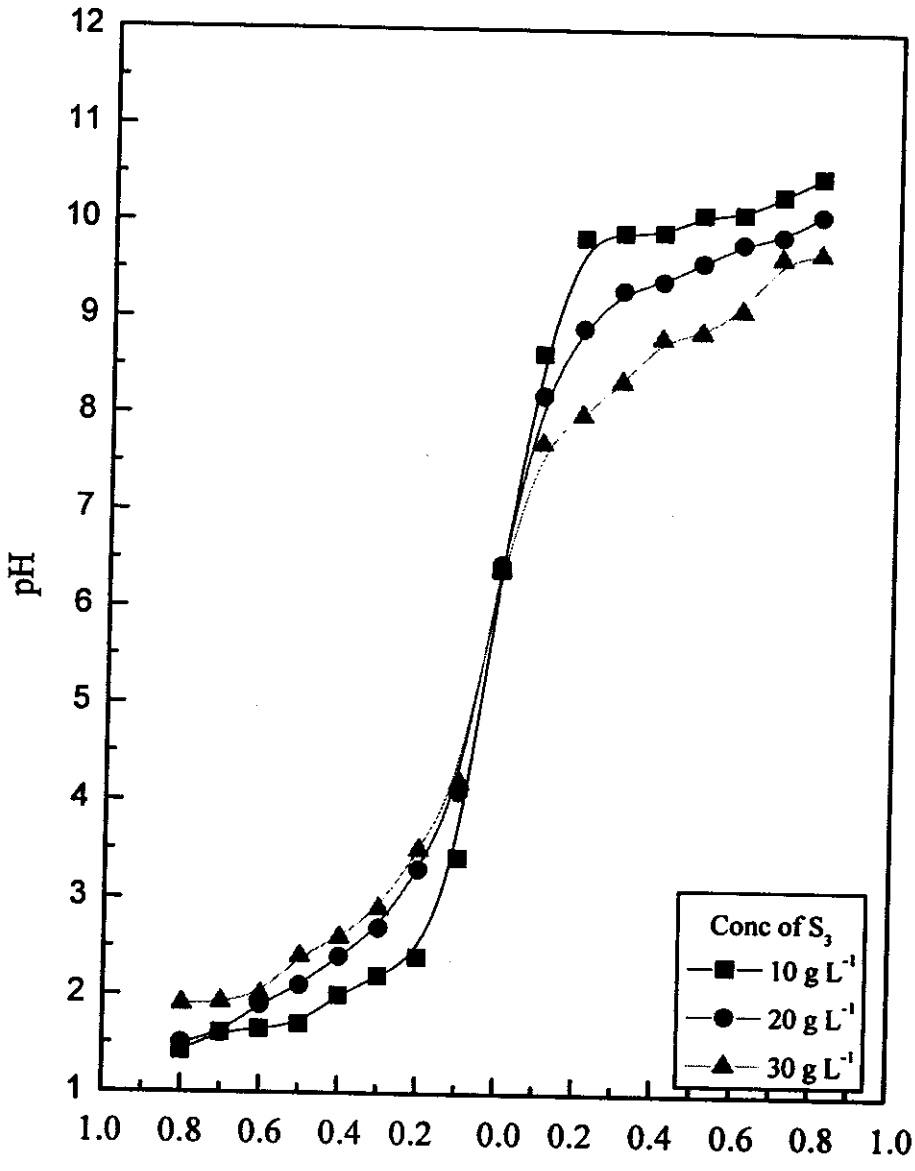

Amount of added acid and base

Fig. (15): Experimental measurment of PZC of S_3 sample.

Table (4): The elemental composition of the investigated clay samples

Sample(S) / Element	S_1	S_2
	Element %	Element %
C	6.38	3.97
O	45.28	36.47
Na	0.38	0.16
Mg	1.18	1.13
Al	8.27	3.30
Si	22.69	19.58
S	0.14	0.0
Cl	0.89	0.0
K	0.92	0.23
Ca	1.08	6.35
Ti	1.14	0.20
Mn	0.0	0.37
Fe	9.13	23.90
Total %	97.49	95.66

Table (5): Total exchangeable metallic cations (TEMC) of the investigated clay samples

Sample	TEMC (meq/100g)
S_1	95
S_2	41

III.5 Elemental analysis of activated carbon

The elemental percentages of the investigated activated carbon sample are shown in table (6). The obtained data show that the numerical ratios of the main constituent atoms (C, H and O) are 4:3:1 and this reveals that the activated carbon is hydrophobic. Also, the atom ratios O/C and H/C are 0.24 and 0.70, respectively. On the bases of these ratios, the value of O/C ratio reveals that the activated carbon has a predominant content of acidic surface centers. The lower value of H/C ratio implies the aromatic character of the surface (**Razvigorova et al., 1998**).

III.6 Mineralogical analyses of the investigated clay samples

The mineralogical composition of the investigated clay samples was carried out by X-ray diffraction (XRD) and the data are given in table (7). The inspection of this table reveals that S_1 contains of smectite as a predominant mineral and the mixed layer of illite and smectite as the most abundant. S_1 has small fraction of gypsum and has no feldspars and siderite. However, S_2 contains of siderite and feldspars as well as calcite as abundant minerals. By comparison between the two clay minerals, it is noticed that the two clay samples have equal amounts of illite and quartz. S_1 has smectite twice that of S_2. The illite/smectite mixed layers in S_1 is about three times that of S_2. Kaolinite, calcite and dolomite are present in S_2 nearly twice that in S_1.

Table (6): The elemental percentages of the investigated activated carbon sample

Element	Element %
C	65.10
H	3.82
S	5.61
P	2.30
O	21.15
Cl	0.55
Ash	1.47
Total	100

Table (7): Mineralogical composition of the investigated clay samples

Sample(S) / Mineral	S_1	S_2
	Mineral Wt %	Mineral Wt %
Smectite	32.9	12
Illite/Smectite-mixed layers	34.8	10.4
Kaolinite	5	9.6
Illite	7.8	7
Quartz	6.8	6.9
Feldspars	0.0	13
Calcite	6	14
Dolomite	4.7	8
Siderite	0.0	11.4
Gypsum	2	0.0

III.7 Sorption characteristics

The different parameters affecting sorption capacity of the investigated samples to sorb the selected contaminants were investigated. These parameters include the effect of sample weight, effect of contact time, pH value of aqueous phase, the metal ion concentration and the competing cations on sorption process.

III.7. 1. Effect of weight variation of the studied samples on removal of the selected contaminants

The effect of weight variation of the investigated samples on removal of radioisotopes, ^{134}Cs, ^{60}Co and ^{89}Sr, from aqueous solutions was studied, under optimized experimental conditions. The experimental data obtained are represented in figures (16-18). Inspection of these figures reveals that the removal % increases with increasing the sample weight up to a certain value, until reaching a saturation level. It is noticeable that 0.05 g, 0.06 g and 0.06 g of S_1, S_2 and S_3, respectively, are sufficient for removal of these ions from radioactive waste solutions. In case of phenol, the experimental data are represented in figure (19). From this figure, it is clear that 0.6 g of either S_1 or S_2 is sufficient for removal of phenol from waste solution and 0.7 g of S_3 is sufficient for removal of phenol from waste solution.

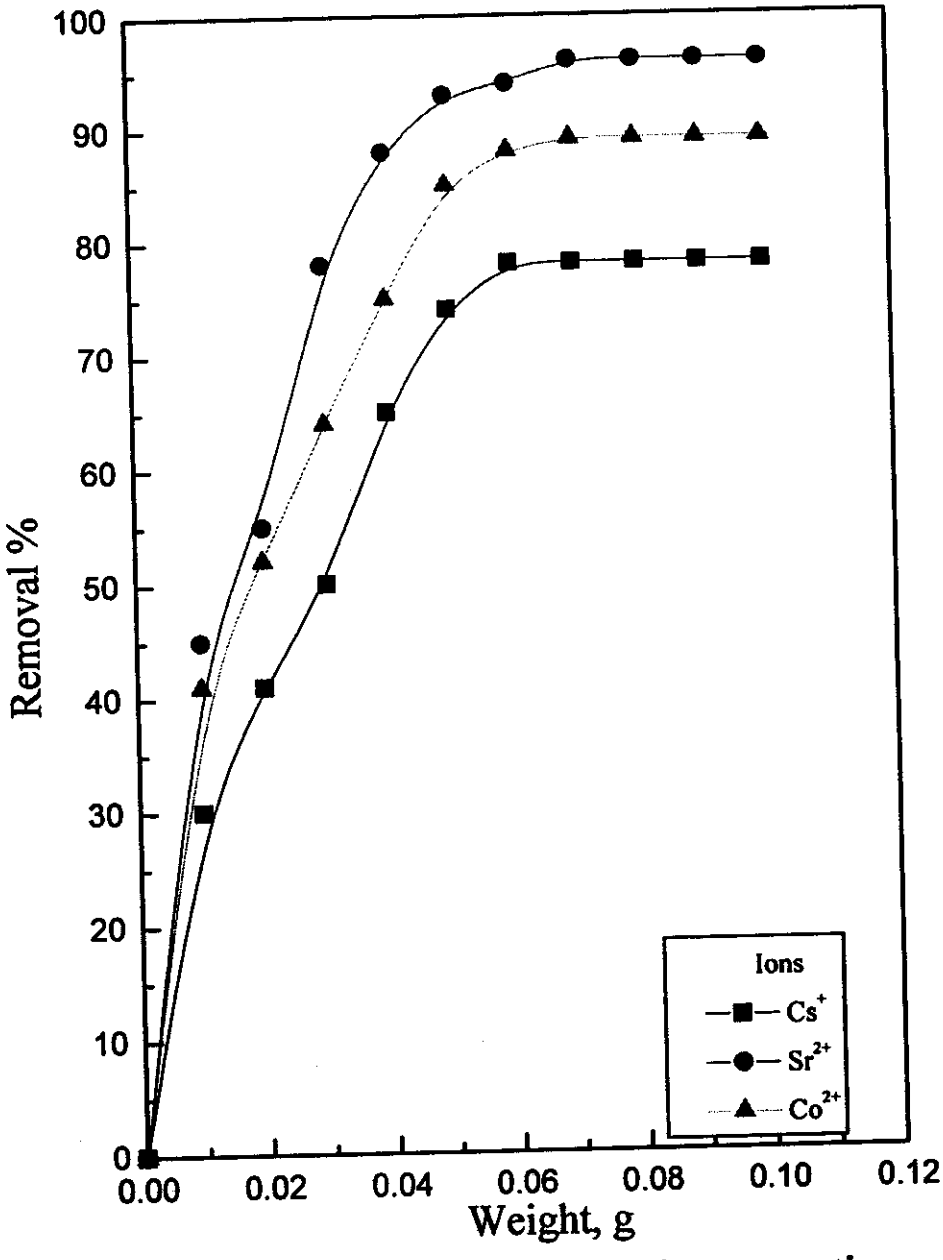

Fig. (16): Effect of S_1 weight on sorption of the selected ions, C_o = 10 mg L^{-1}.

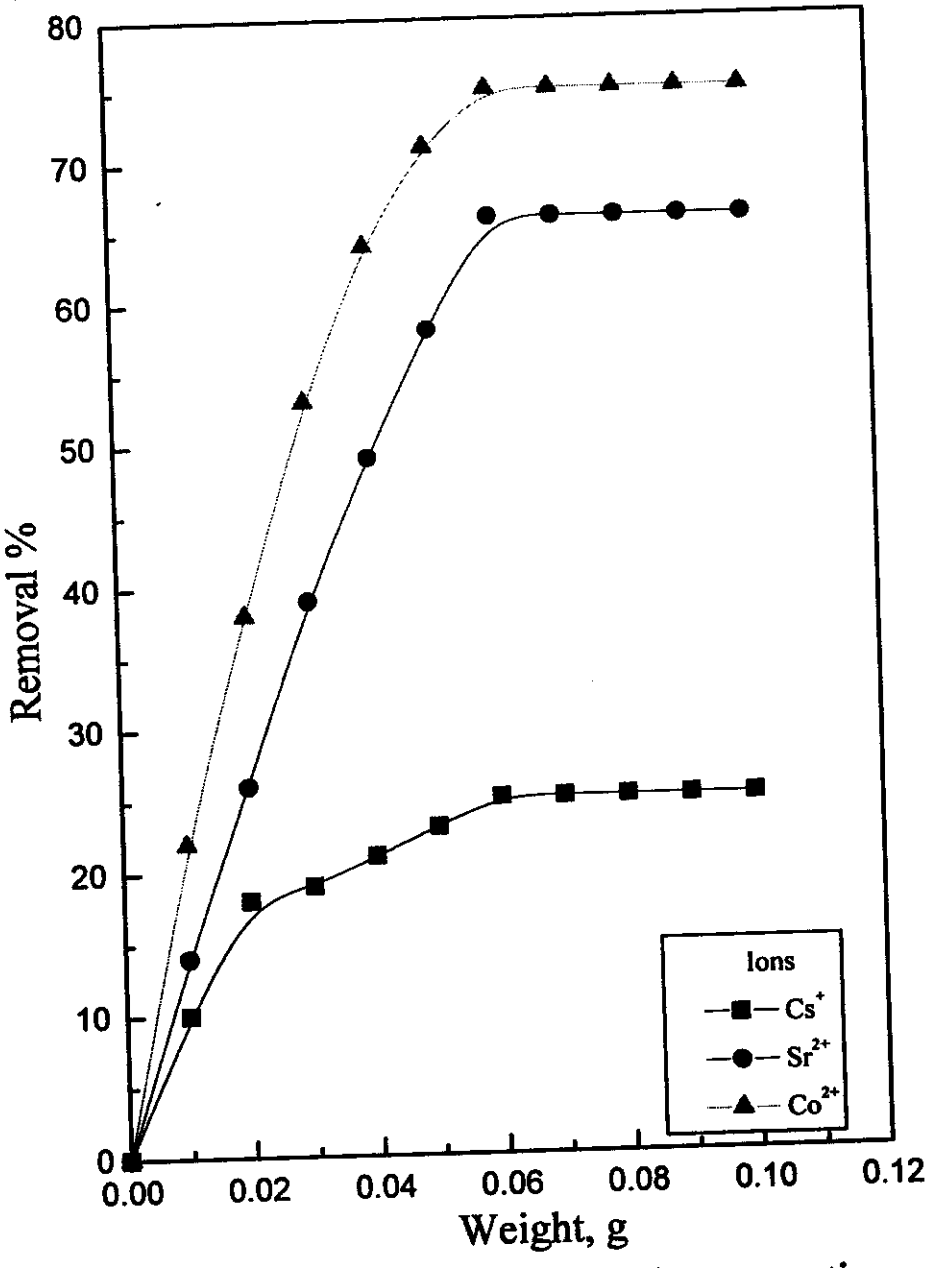

Fig. (17): Effect of S_2 weight on sorption of the selected ions, C_o = 10 mg L^{-1}.

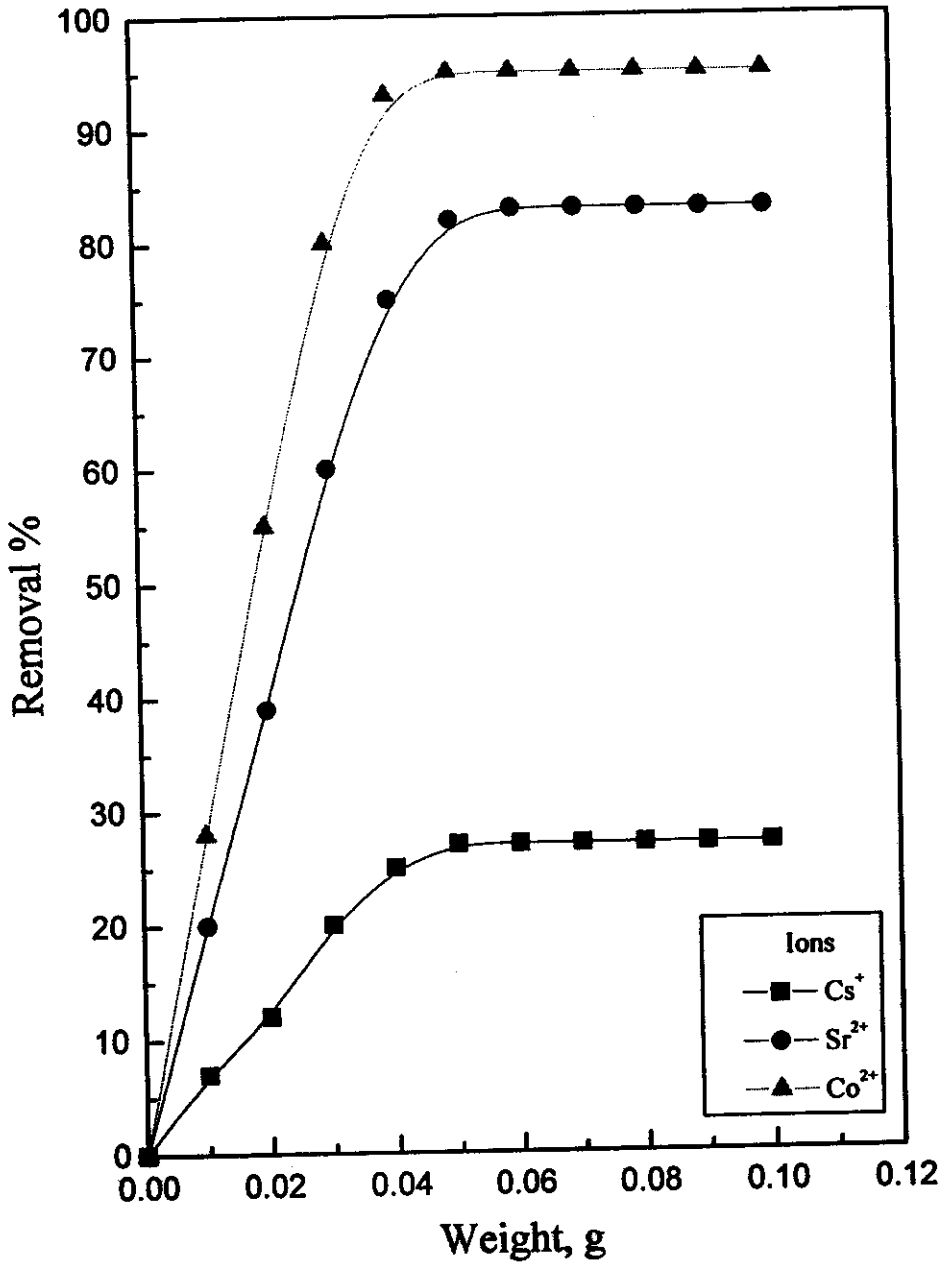

Fig. (18): Effect of S_3 weight on sorption of the selected ions, C_0 = 10 mg L^{-1}.

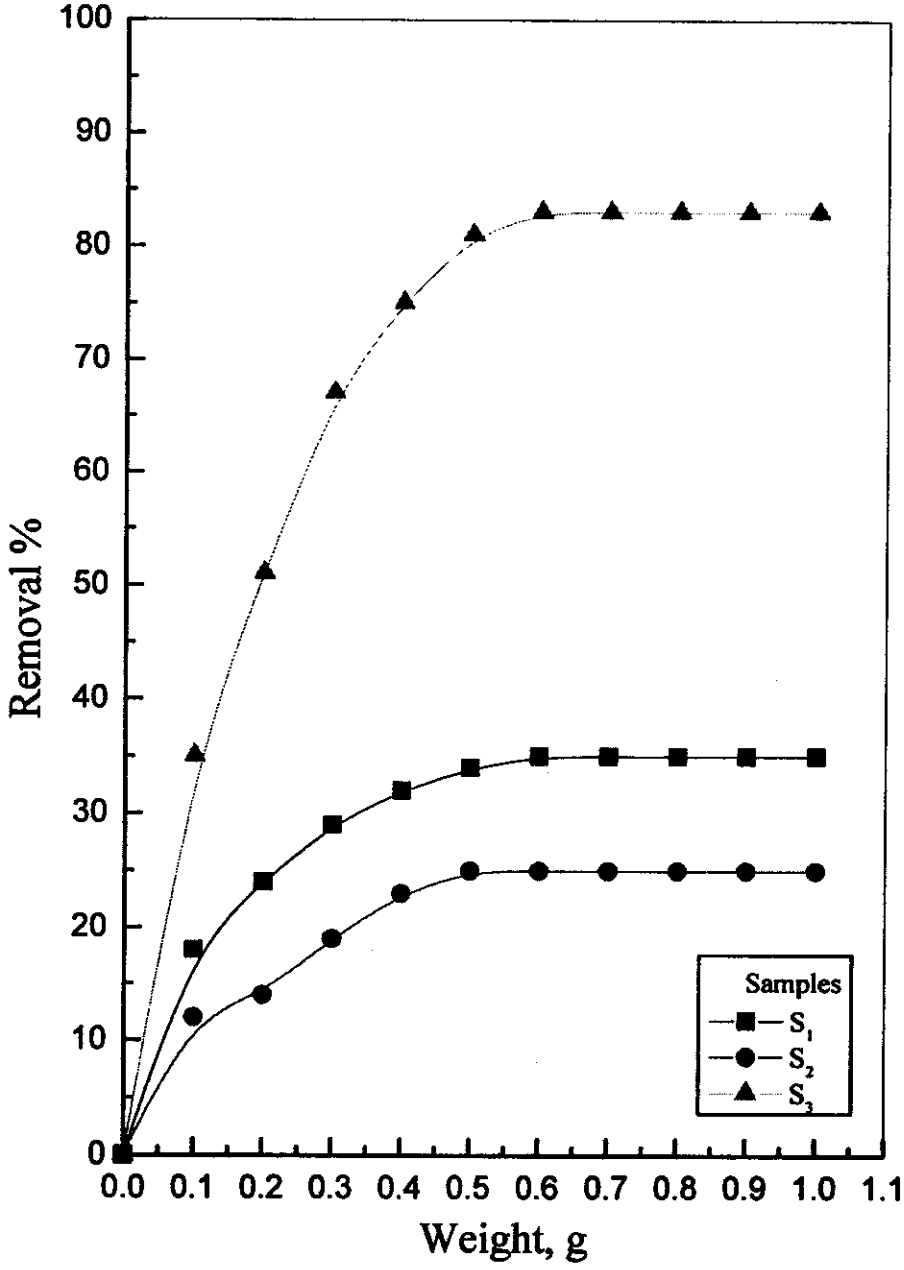

Fig. (19): Effect of sample weight on sorption of phenol onto the investigated samples, [phenol] = 50 mg L^{-1}.

III. 7. 2. Effect of contact time

The effect of contact time on sorption of Cs^+, Sr^{2+} and Co^{2+} by the investigated samples was studied. The variation of the amount sorbed as a function of time is shown in figures (20-22). The figures show that the amount sorbed increase with time, till it reaches a constant value depending on the type of the adsorbate and the nature of the sorbent. The sorption was rapidly increase initially, but then the process slows down and subsequently attains a constant value within 50, 60, and 60 minutes for Cs^+, Sr^{2+} and Co^{2+} ions, respectively i.e., when adsorption equilibrium is established. The slow sorption may be attributed to the diffusion of the ions into the pores of the samples. Therefore equilibrium is nearly established at the same time interval for all the tested ions. Any further increase in shaking period does not significantly affect the amount sorbed. The same trend is observed for sorption of phenol onto the investigated samples and the equilibrium attained within 40 minutes for activated carbon and within 60 minutes for S_1 and S_2 as shown in figure (23). This shaking time period was selected for all subsequent experiments. The variation of amount sorbed values of phenol and the investigated radionuclides depend on the surface area of the grains, the mineralogical and the chemical composition of each studied sample. The uptake % of the investigated cations and phenol by the studied samples are shown in table (8).

The removal of Cs^+, Sr^{2+} and Co^{2+} ions from aqueous solutions by S_1, S_2 and S_3 can be generally described as a four step processes: bulk solution transport, film diffusion transport, pore transport and adsorption (**Carriere et al., 1996**). In bulk solution transport, the adsorbate is transported by diffusion from the bulk solution to the boundary layer of water molecules surrounding the adsorbate particle. Film diffusion transport occurs by molecular diffusion through the stationary layer of water molecules that surround the particle. In pore transport the adsorbate is transported into and around the adsorbent pores to available adsorption sites. Once the adsorbate enters the pores, intraparticle transport may

occur by molecular diffusion either through the solution in the pores (pore diffusion) or along the adsorbate surface (surface diffusion). Adsorption occurs after transport to an available site. This step is reported to be rapid (**Adamson, 1987**) for physical adsorption. So, the preceding diffusion step will control the rate of removal of molecules from solution. However, if adsorption is followed by chemical reaction that changes the nature of the molecule, and the chemical reaction may be slower than diffusion and therefore may in this case control the rate of removal. The rate of amount sorbed of the selected adsorbates is dependent on pore structure of investigated samples and particle size of the adsorbates. From the figures it is clear that the adsorbates are initially relatively rapid indicating some surface uptake. Also, the gradual uptake of the adsorbates after 10 minutes is controlled within the porous structure of micro and meso pores and therefore, the attainment of equilibrium is relatively slow. Similar results were reported by **Abbasi and Streat; 1994, Omar; 2002, Baeza, et al.; 1995, Sheha; 1998** and **Abdel-Aal, et al., 2002.**

Table (8): The uptake % of the investigated cations and phenol by the studied samples

Samples	Contaminants	Uptake %
S_1	Cs^+	78
	Co^{2+}	89
	Sr^{2+}	96
	Phenol	35
S_2	Cs^+	25
	Co^{2+}	74
	Sr^{2+}	66
	Phenol	25
S_3	Cs^+	28
	Co^{2+}	95
	Sr^{2+}	84
	Phenol	83

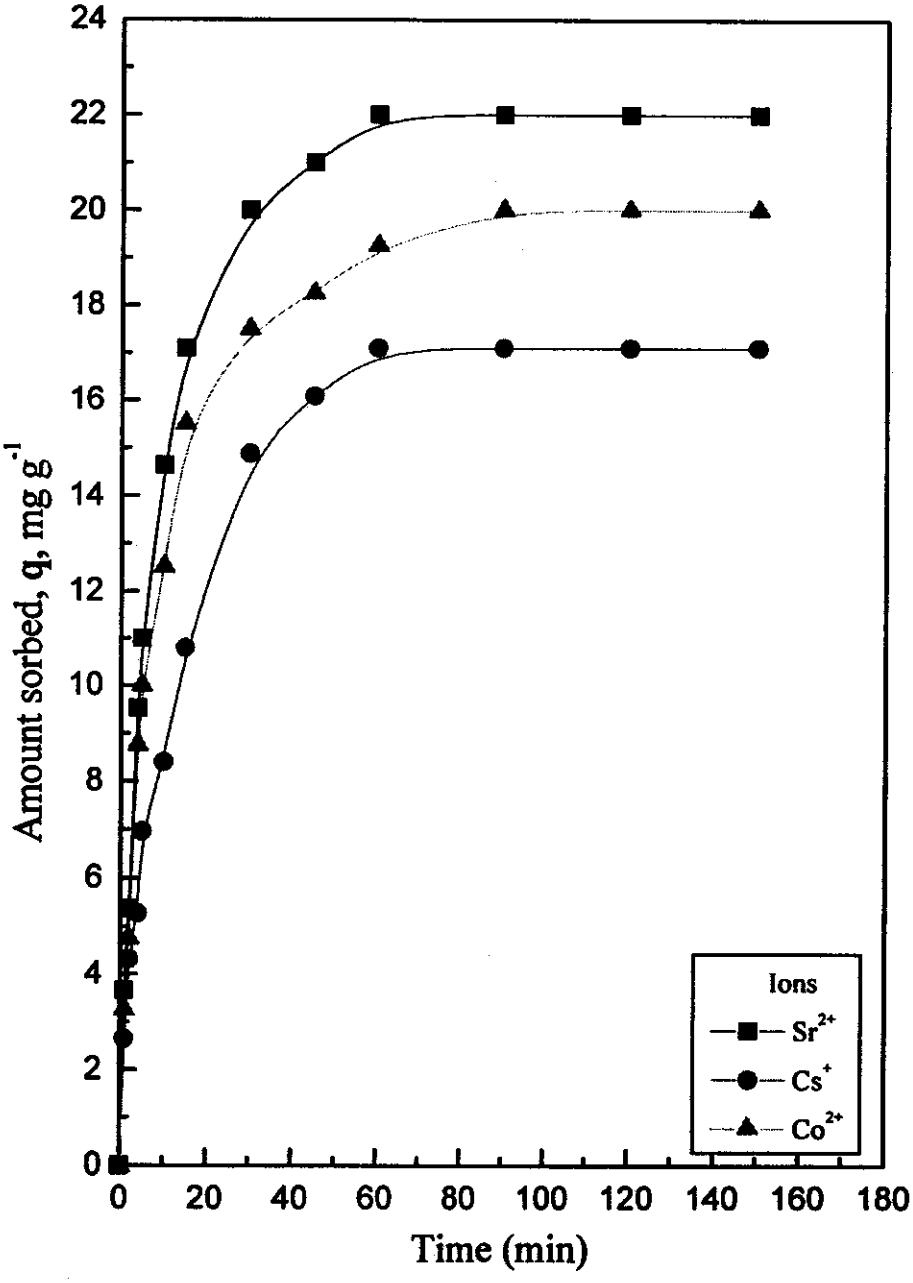

Fig. (20): Effect of contact time on sorption of the selected ions onto S_1; C_0 of metal ion = 10 mg L^{-1}.

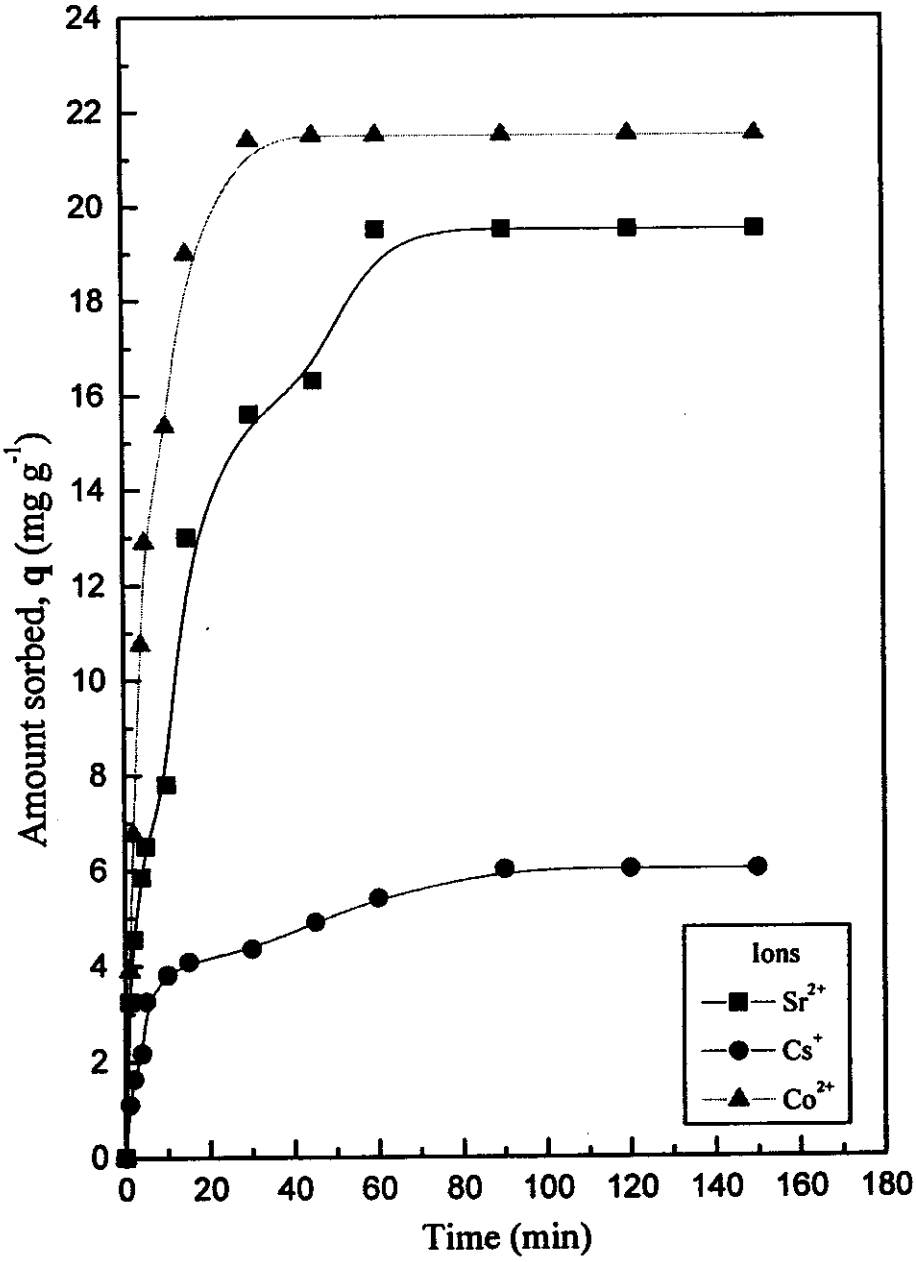

Fig. (21): Effect of contact time on sorption of theselected ions onto S_2, $C_0$of metal ions = 10 mg L^{-1}.

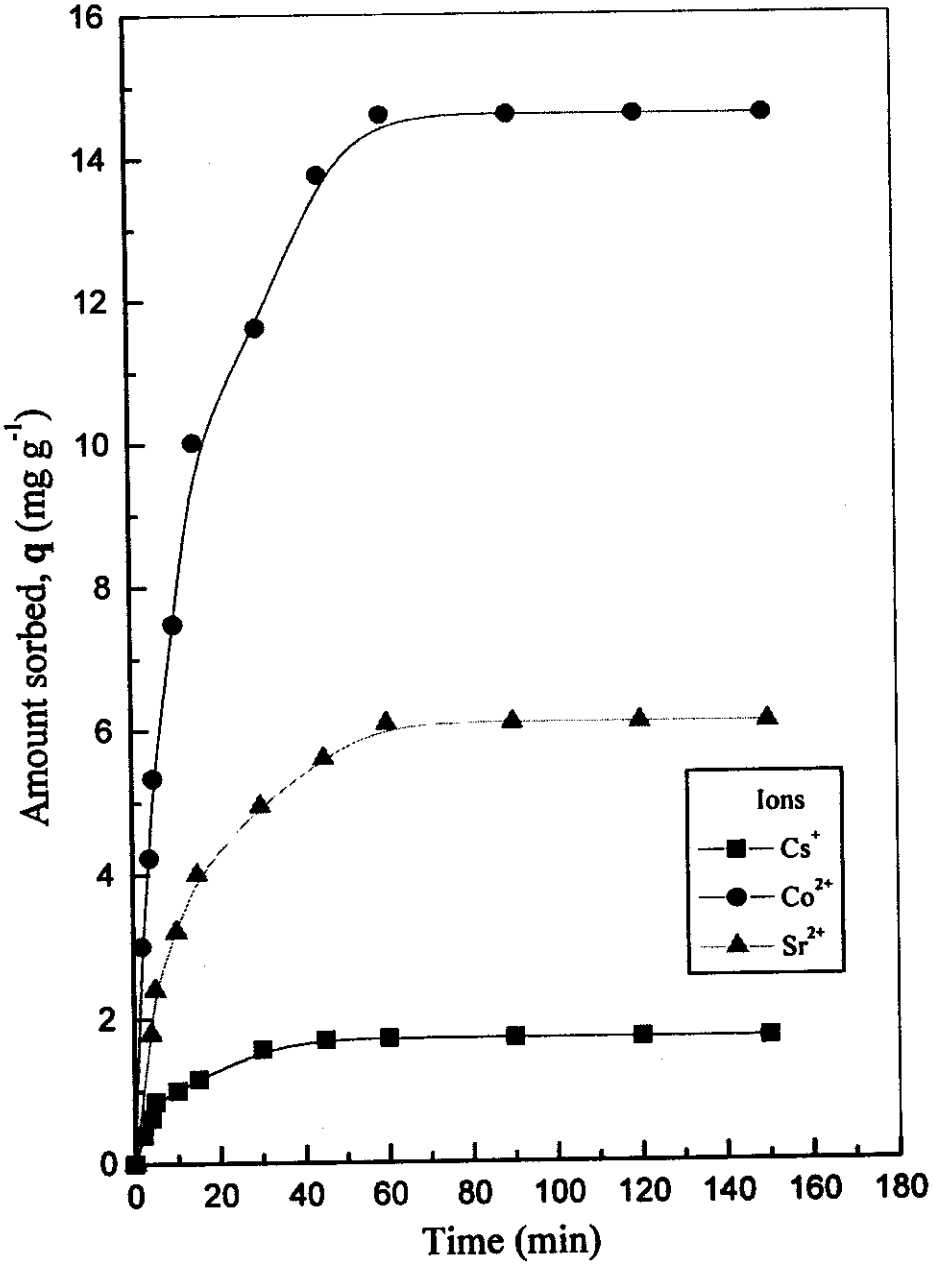

Fig. (22): Effect of contact time on sorption of the selected ions onto S_3, $C_0$of metal ions = 10 mg L^{-1}.

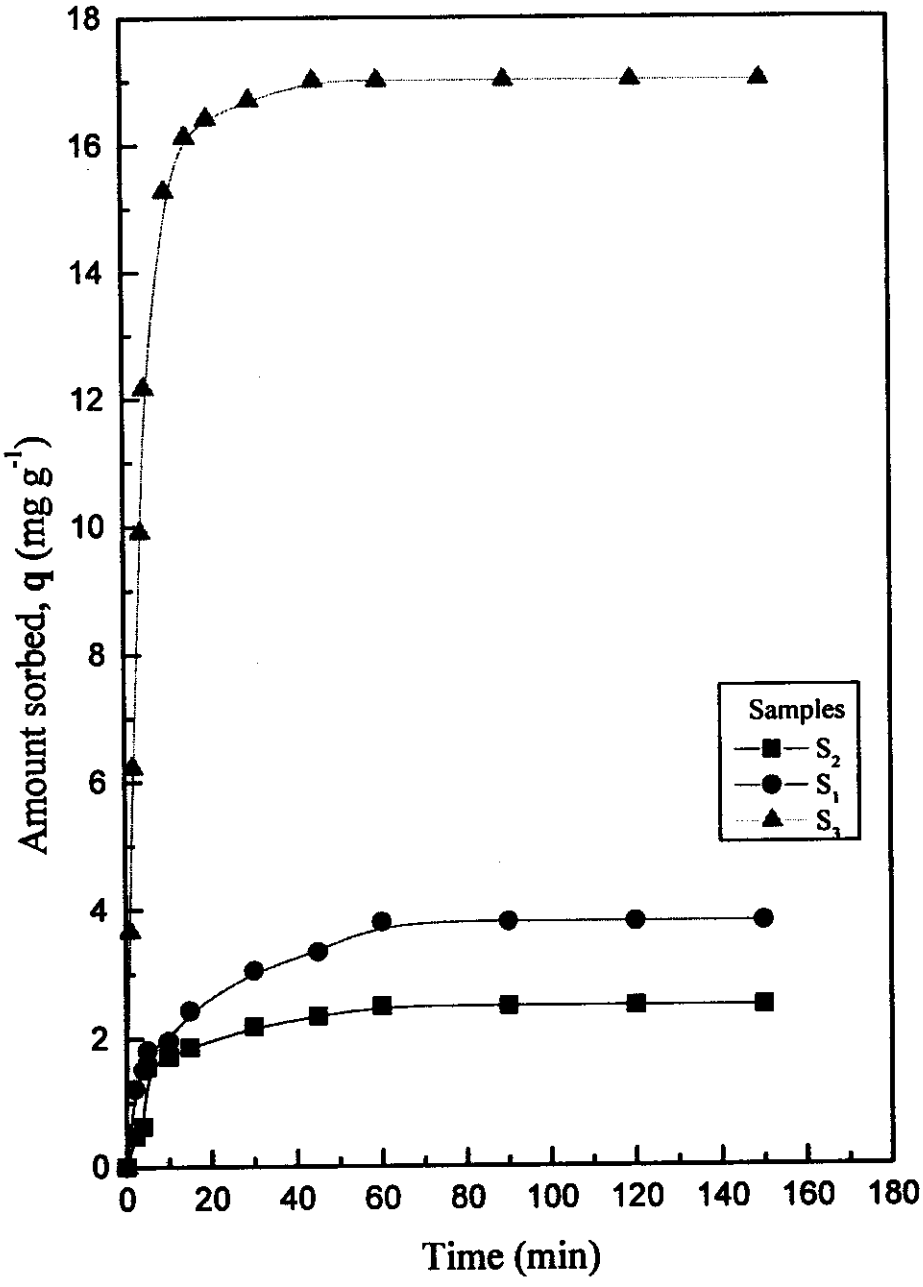

Fig. (23): Effect of contact time on sorption of phenol onto the investigated samples; $C_0$of phenol = 50 mg L^{-1}.

III. 7. 3 Kinetic of sorption reaction

With regard to the sorption kinetics, the sorption rate is quick and decreases with time and ultimately ceases when an apparent equilibrium state is reached. In all cases, the steady state value (q) which is the amount of ion onto the solid phase (mg g^{-1}), was obtained within certain time, as mentioned above. **Lagergren** equation was applied for studying the kinetics of both the selected ions and phenol sorption onto the studied samples, S_1, S_2, and S_3, **(Namasivayam and Ranganathan, 1993).**

$$\log (q_e - q_t) = \log q_e - K_{ad}\, t/2.303 \quad \text{..... (36)}$$

Where;

q_e and q_t are the amount of sorbed species onto the sorbent (mg g^{-1}) at equilibrium time and at time t (minutes), respectively,

K_{ad} is the rate constant of sorption ($minutes^{-1}$).

As shown in figures (24-27), the obtained linear plots of Log (q_e - q_t) vs t indicate that the sorption of all tested ions and phenol onto the investigated samples obey **Lagergren** equation. It is clear that kinetically the sorption is first order reaction. The rate constant (K_{ad}) values for Sr^{2+}, Co^{2+} and Cs^{+} for S_1 calculated from the slopes of the plots are 0.0488, 0.0525 and 0.0519 min^{-1}, respectively. The rate constant (K_{ad}) values of Sr^{2+}, Co^{2+} and Cs^{+} for S_2 are 0.0244, 0.0366 and 0.0403 min^{-1}, respectively. The rate constant (K_{ad}) values of Sr^{2+}, Co^{2+} and Cs^{+} for S_3 are 0.0541, 0.052 and 0.0711 min^{-1}, respectively. The rate constant (K_{ad}) values of phenol sorption onto the investigated sorbents are 0.0403, 0.0451 and 0.1543 min^{-1} for S_1, S_2 and S_3, respectively.

Close inspection of the obtained data reveal that, the sorption rate of Cs^{+} on S_3 is higher than that on the other samples and has the following order: $S_3 > S_1 > S_2$. In case of Co^{2+}, the sorption rate is higher for S_1 and has the following order: $S_1 > S_3 > S_2$. The sorption rate of Sr^{2+} is higher for S_3 and has the following order: $S_3 > S_1 > S_2$. The sorption rate of phenol on the studied samples

has the following sequence: $S_3 > S_2 > S_1$. This quick sorption rate is not constant and may be attributed to the differences in the ratio of V/m and this conclusion is in agreement with several investigators; **Campbell and Davies (1995)** and **Wang Xiangke et al., (2000).**

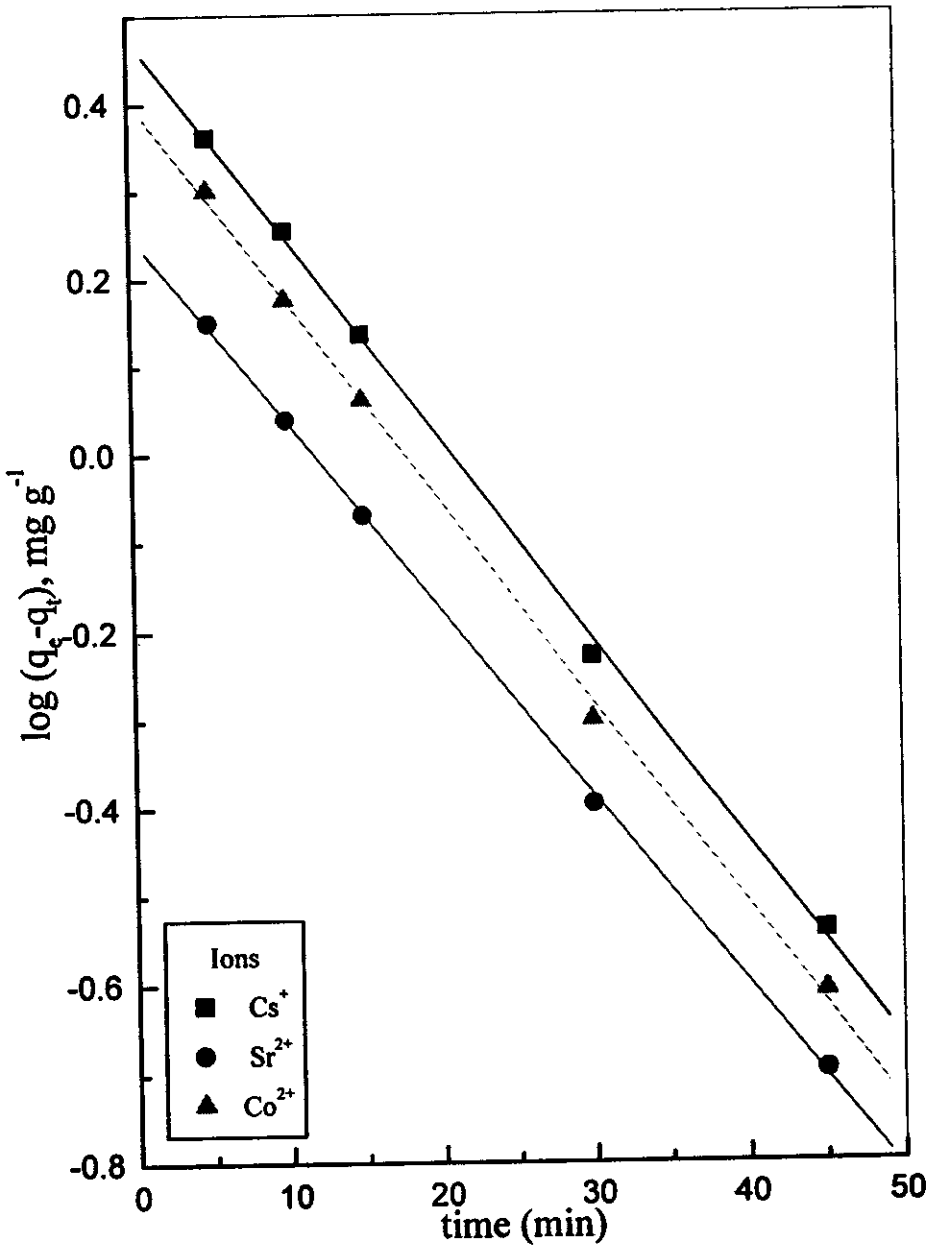

Fig. (24): Plots of $\log(q_e-q_t)$ versus time for ions sorption onto S_1 from aqueous solutions, C_0 of ions = 10 mg L^{-1}.

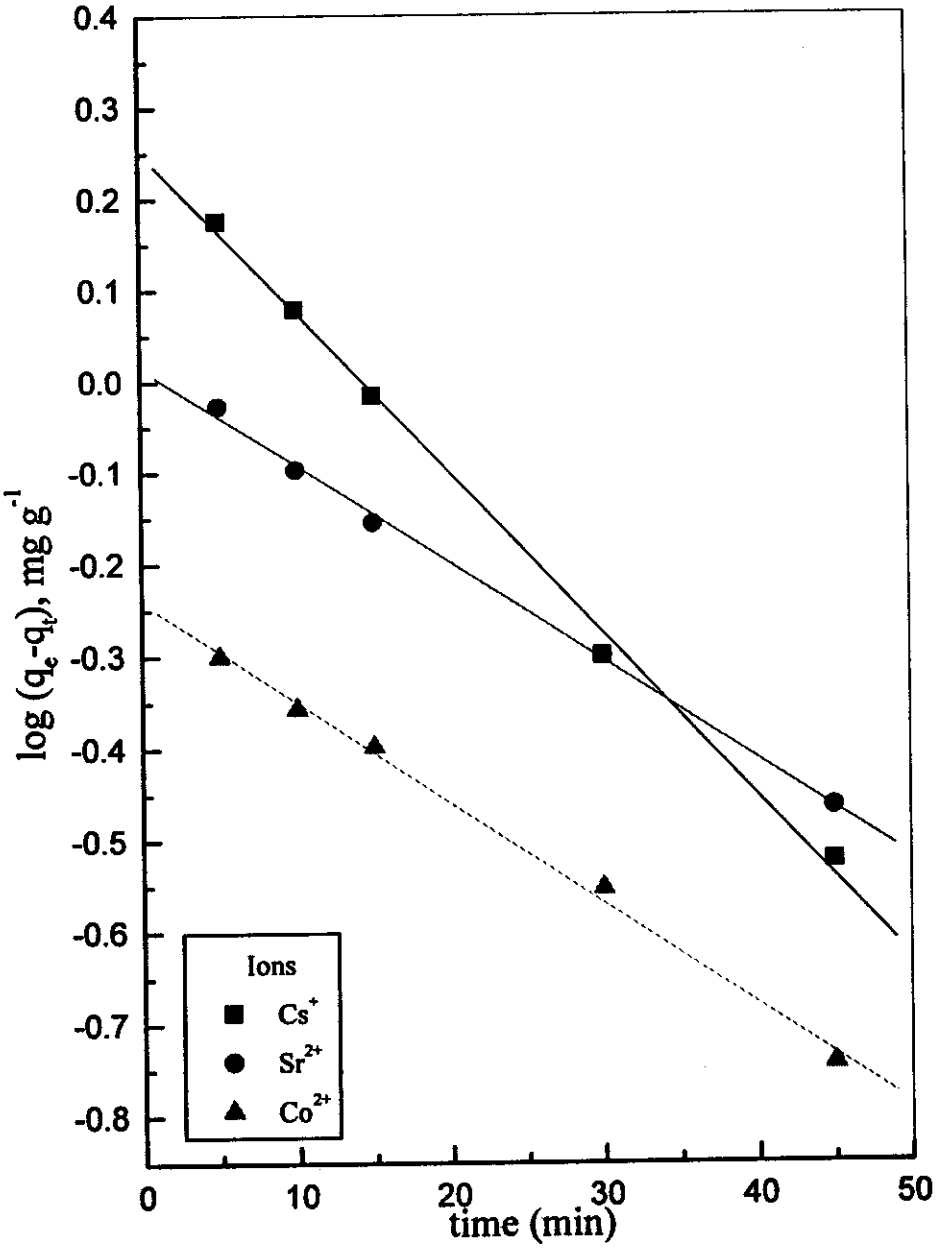

Fig. (25): Plots of $\log(q_e-q_t)$ versus time for ions sorption onto S_2 from aqueous solutions, C_0 of ions = 10 mg L^{-1}.

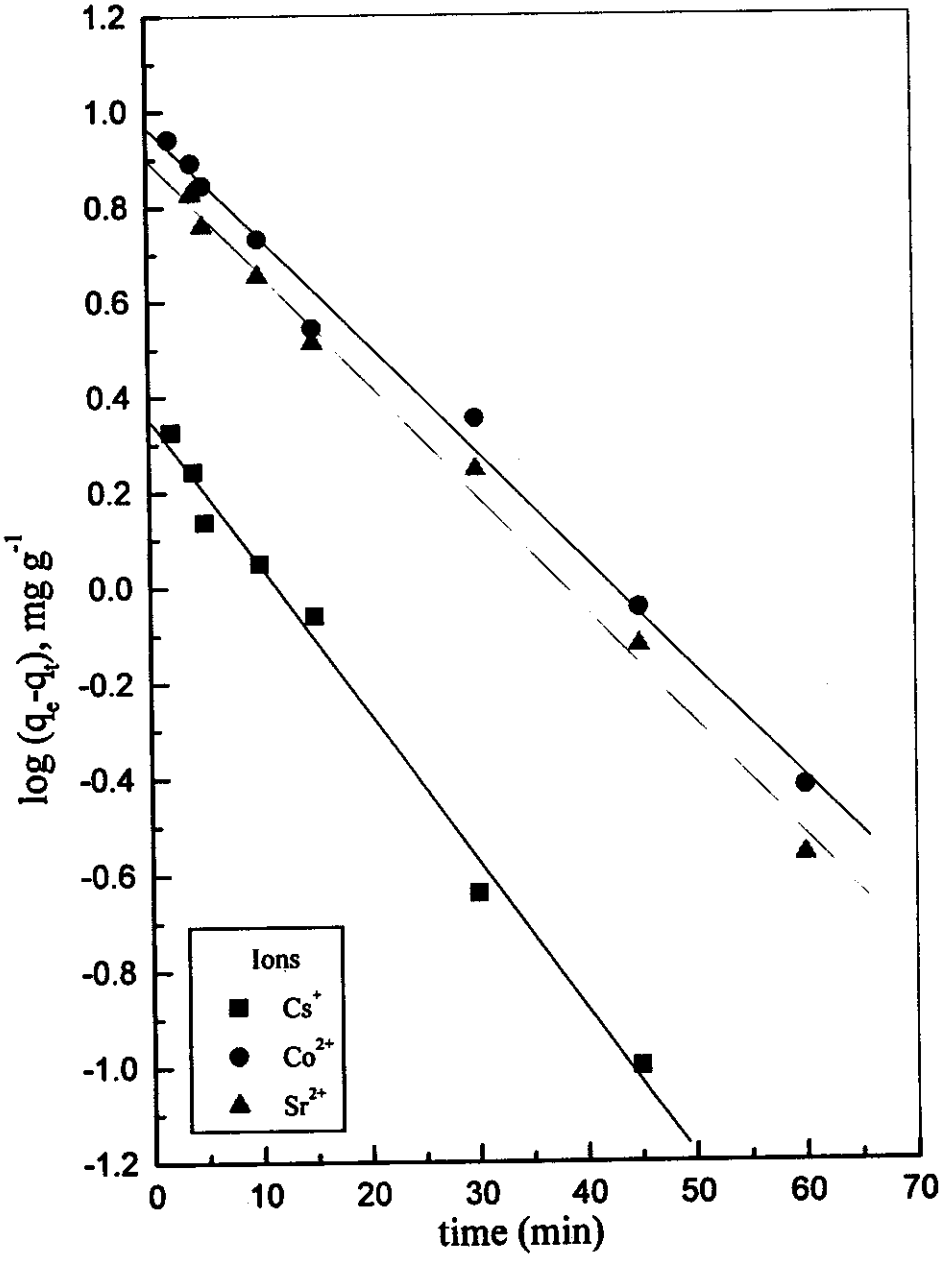

Fig. (26): Plots of log (q_e-q_t) versus time for orption of the selected ions onto S_3 from aqueous solutions, C_o of ions = 10 mg L^{-1}.

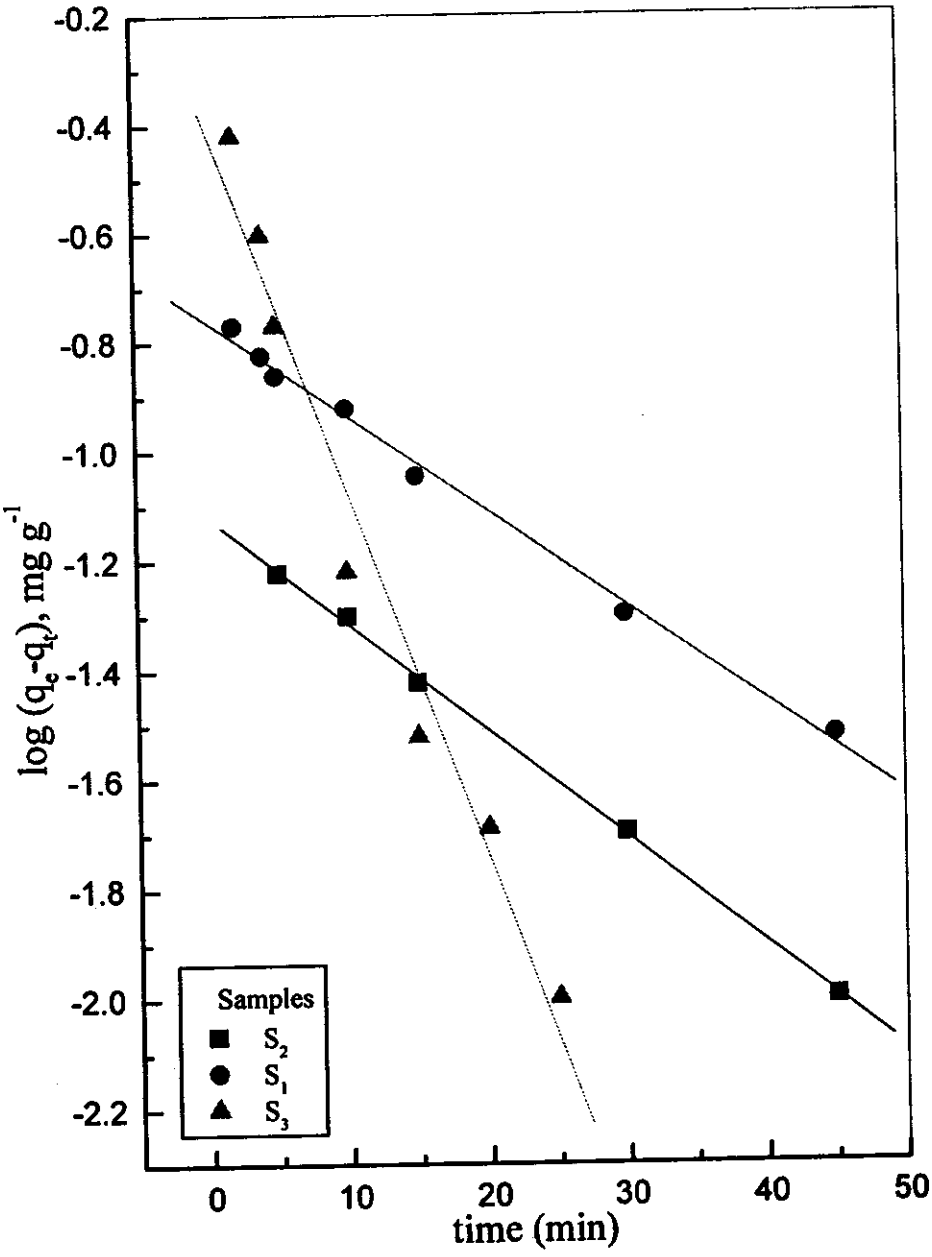

Fig. (27): Plots of $\log(q_e-q_t)$ versus time for phenol sorption onto the investigated samples from aqueous solutions, C_0 of phenol= 50 mg L^{-1}.

III. 7. 4 Effect of pH

The hydrogen ion concentration is one of the most important factors influencing the adsorption of the investigated cations, Cs^+, Co^{2+}, Sr^{2+}, and phenol from aqueous solutions -onto the investigated two clay samples (S_1, S_2) and activated carbon sample, S_3. The pH of the solution affects contaminant removal by influencing the surface charge of the sorbents, by affecting the distribution of the species in the solution and consequently the speciation of the adsorbate species.

III.7. 4. 1 Effect of pH on sorption of the ions onto the samples

The amount sorbed (mg g^{-1}) of the selected radionuclides; ^{134}Cs, ^{60}Co and ^{89}Sr; and phenol onto S_1, S_2 and S_3 is plotted as a function of the pH value as shown in figures (28-30). It is noticeable that, for all samples, the amount sorbed increase with increasing the pH until a maximum uptake of Cs^+, Co^{2+}, Sr^{2+} at certain pH and with a further increase in pH values the amount sorbed falls gradually. By closer inspection, it is observed that, in acidified medium, the amount sorbed of the radionuclides onto the investigated adsorbent samples increase with increasing the pH value and show some slight differences related to the hydrolysis of each individual adsorbates. It is clear that in strongly acidic medium the amount sorbed of the radionuclides by the investigated adsorbent samples are very small or negligible. The amount sorbed of ^{134}Cs, ^{60}Co and ^{89}Sr shows a gradual increase with increasing the pH value till it attains constant value at optimum pH and then it sharply decreases at higher pH values. This decrease in the amount sorbed may be attributed to the amphoteric character of the sorbents **(Stump and Morgan, 1981)**. Closer inspection of figures (28 and 29) shows that the maximum amount sorbed of the selected ions onto both S_1 and S_2 is around a pH value of 7.2, 7.5 and 6.2, ± 0.2 for Cs^+, Co^{2+} and Sr^{2+}, respectively.

A similar trend was observed for sorption of the selected ions onto S_3 sample, as shown in figure (30), but around a pH value of 7.6, 7.2 and 6.5, ± 0.2 for Cs^+, Co^{2+} and Sr^{2+} respectively. Also the amount sorbed of the selected ions onto activated carbon is higher than that onto the clay samples.

The increase of the amount sorbed with increasing the pH value of the medium can be discussed in the light of the exchangeable properties of the hydrogen ions and their competitive effect for the available exchange sites. Since the clay samples have exchange sites of different binding energies; at low pH value the hydrogen ions compete for the available active sites on the adsorbent surface and this negatively affects the amount sorbed of the studied adsorbates. Also, the hydrogen ion has a negative effect on the uptake of the different investigated cations. As the pH value increases, the proton competitive effect decreases due to the hydrogen ion concentration decrease with subsequent increase in the amount sorbed of the different cations (**Peter and Vladimir, 1980**). This explanation is in accordance with that given by **Ezz El-Din, (1995)**; who found that the uptake percent as well as the distribution coefficient (K_d) values for ^{137}Cs and ^{60}Co are gradually increase with increasing pH value to reach a maximum value at pH value of 8.5. **Ezz El-Din et al., (1998)** reported that the amount of Sr^{2+} ions, in percent, that sorbed by different soils shows a slight increase as the ground water pH value increased from pH value of 3 to 8. Similar behaviors are reported by (**Minglu et al., 1993**) and (**Atta, 2001**).

The pH_{max}, where maximum sorption takes place, seems to be related to the hydrolytic properties of the studied metal ion species and their involved sorption mechanism and also may represent the pH value at which the free cationic species (M^{n+}) is the predominant species. The maximum sorption of radiocesium is favored in neutral medium. This is due to the Cesium cations having a large ionic radius and a small hydration number (**Park et al., 1992, Apak et al., 1996**). Thus,

Cs^+ sorption may be attributed to the great polarizability of these cations resulting in their attraction by the induced dipoles of the sorbent surface (**Voyutsky, 1978**). However, the pH value of dispersion medium strongly affects the electrokinetic potential of the adsorbent particles as both H^+ and OH^- ions have great adsorbability, causing spontaneous unipolar orientation of the dipoles of dispersion medium establishing a permanent dipole structure. Since Cs^+ ions are essentially retained by specific sorption via compression of electric double layer, these permanent dipoles caused by H^+ and OH^- ions decrease the amount sorbed of Cs^+ ions in both acidic and alkaline regions down to a level where ion-exchange sorption of Cs^+ prevails.

The decrease in Co^{2+} sorption amount with further pH increase above the value of pH_{max} may be arising from the small ionic radius of Co^{2+} ions. Thus, Co^{2+} penetrate more deeply into the lattice structure of sorbent surface where, it is possible to infer that Co^{2+} ions sorbed mainly by irreversible fixation with a little ion exchange reactions (**Park et al., 1992**). A similar trend was observed by other investigators (**Eskander et al., 2000**, and **Sheha, 2002**).

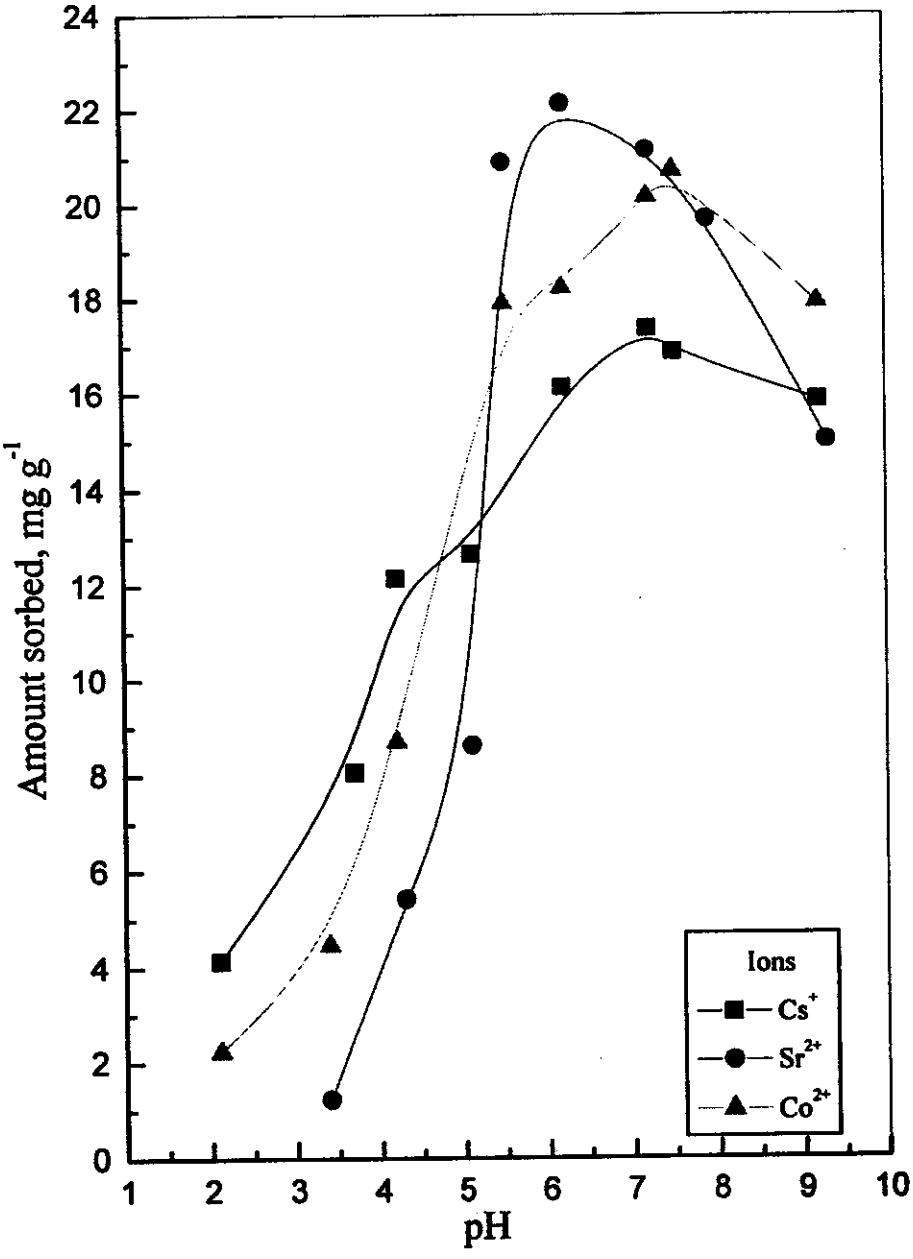

Fig. (28): Effect of hydrogen ion concentration on sorption of the selected ions onto S_1, C_0 of ions = 10 mg L^{-1}.

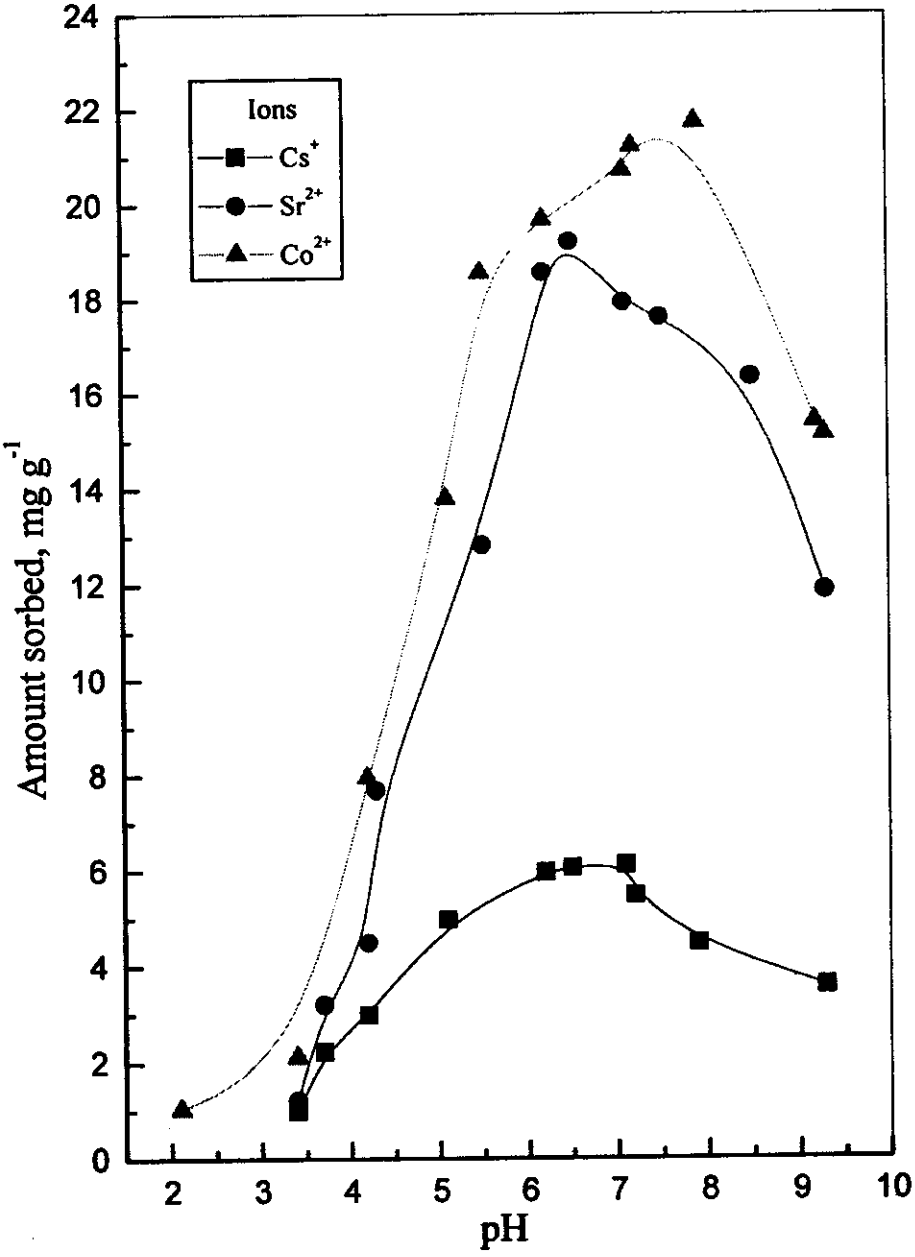

Fig. (29): Effect of hydrogen ion concentration on sorption of the selected ions onto S_2; C_0 of ions = 10 mg L^{-1}.

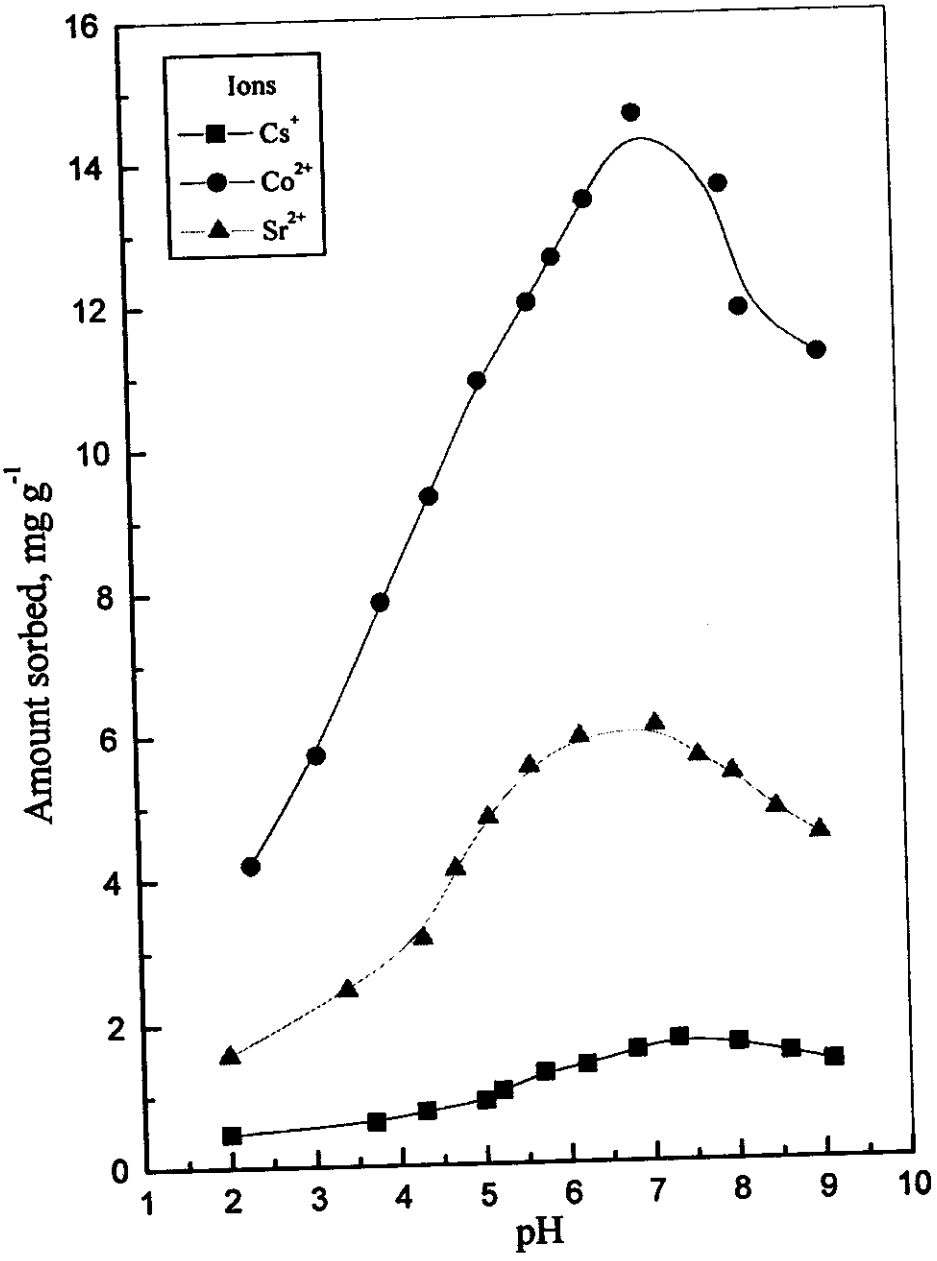

Fig. (30): Effect of hydrogen ion cocentration on sorption of the selected ions onto S_3; C_0 of ions = 10 mg L^{-1}.

III. 7. 4. 2 Effect of hydrogen ion concentration on the distribution coefficient of different metal ions onto the samples

Generally, the mechanism is considered to be predominant of the studied metal ions. This can be explained on the bases of ion exchange process between the metal ion and hydrogen proton (H^+) adsorbed on active sites of adsorbent surface. The cation exchange process between a metal ion M^{n+} and a proton H^+ in a dilute aqueous solution, i.e. activity coefficient $\approx$ 1, is represented by the following equation:

$$M_{aq}^{n+} + n\overline{HR} \leftrightarrow nH^+ + \overline{MR}_n \quad \ldots\ldots\ldots\ldots\ldots\ldots\ldots\ldots (37)$$

Where M_{aq}^{n+} is the cation exchanged in solution and the subscript bar denotes the exchanger phase. The equilibrium constant for such reaction is given by the following equation (**Helfferich, 1962**):

$$K_H^M = \frac{[H_{aq}^+]^n[\overline{MR}_n]}{[\overline{HR}]^n[M_{aq}^{n+}]} \quad \ldots\ldots\ldots\ldots\ldots\ldots\ldots\ldots (38)$$

Where: $[\overline{MR}_n]$ and $[\overline{HR}]^n$ are the concentration of M^{n+} and H^+ ions at adsorbent surface and $[H_{aq}^+]^n$ and $[M_{aq}^{n+}]$ are their concentrations in aqueous solution.

At equilibrium, the distribution coefficient (K_d) is given by:

$$K_d = \frac{[\overline{MR}_n]}{[M_{aq}^{n+}]} \quad \ldots\ldots\ldots\ldots\ldots\ldots\ldots\ldots (39)$$

Substituting equation (38) in equation (39), gives:

$$K_d = K_H^M \frac{[\overline{HR}]^n}{[H_{aq}^+]^n} \quad \ldots\ldots\ldots\ldots\ldots\ldots\ldots\ldots (40)$$

$$\log K_d = \log K_H^M + n\log[\overline{HR}] - n\log[H_{aq}^+] \quad \ldots\ldots (41)$$

Experimentally, the metal ion concentration used is less than the hydrogen ion concentration, i.e. $[\overline{HR}]^n \geq [\overline{MR}_n]$ and $[H_{aq}^+]^n \geq [M_{aq}^{n+}]$ and the term $[\overline{HR}]^n$ is considered constant, therefore equation (41) is reduced to:

$$\log K_d = \text{constant} - n \log [H^+] \quad \ldots\ldots\ldots\ldots\ldots\ldots \quad (42)$$

When log K_d values of n valent metal ions are plotted against log $[H^+]$ of the aqueous solution, a straight line of slope (-n) equals to the charge on the metal ion should be obtained if the sorption process is pure ion exchange process.

The relation between K_d and log $[H^+]$ for sorption of Cs^+, Co^{2+} and Sr^{2+} from aqueous solution onto the investigated sorbent samples are represented in figures (31-33). The plots give straight line relations for all the studied ions. The slopes of these straight lines are not equal to the valence of the sorbed ions. In case of sample S_1, the slopes of the lines are -0.28, -0.52 and -0.43 for Cs^+, Sr^{2+} and Co^{2+}, respectively. In case of sample S_2, the slopes of the lines are -0.18, -0.39 and -0.38 for Cs^+, Sr^{2+} and Co^{2+}, respectively. In case of sample S_3, the slopes of the lines are -0.113, -0.247 and -0.257 for Cs^+, Sr^{2+} and Co^{2+}, respectively. It is recognized that the slopes of these straight lines are not equal to the valence of the sorbed ions. This behavior represents a deviation from the ideal sorption and therefore the mechanism is not pure ion exchange mechanism and other mechanisms may be occurred. This is due to the complexity of the systems involve sorption onto the adsorbent and so the possibility of sharing of more than one mechanism in the sorption process is occurred. A similar case was obtained for the ion exchange of divalent transition metal ions on amorphous hydrous titanium dioxide and hydrous zirconia (**Abe et al., 1980** and **Abe et al., 1978**). And also similar results were reported by **Sheha, (2002)**.

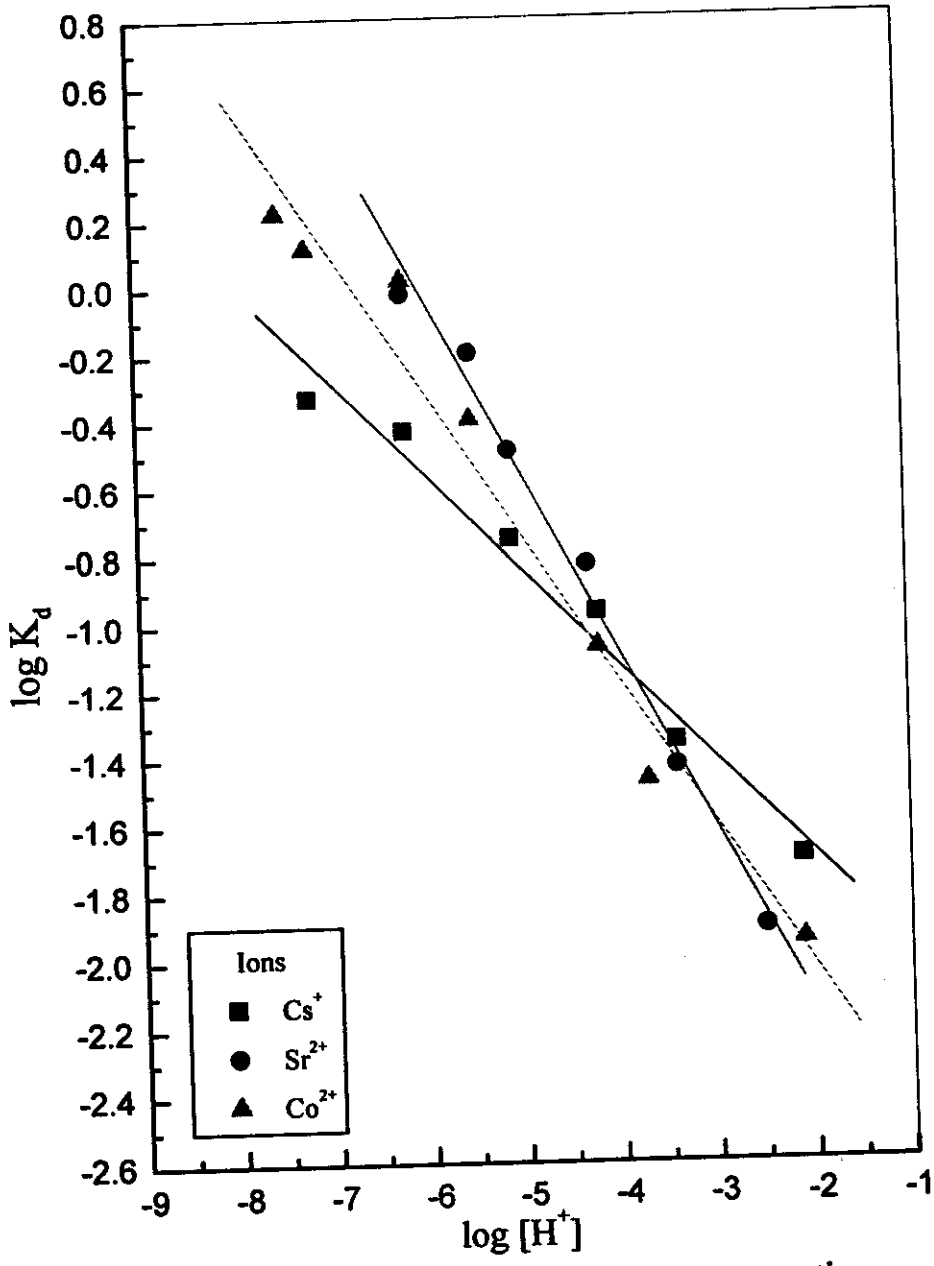

Fig. (31): Effect of hydrogen ion concentration on the distribution coefficient of different metal ions onto S_1; C_o= 10 mg L^{-1}.

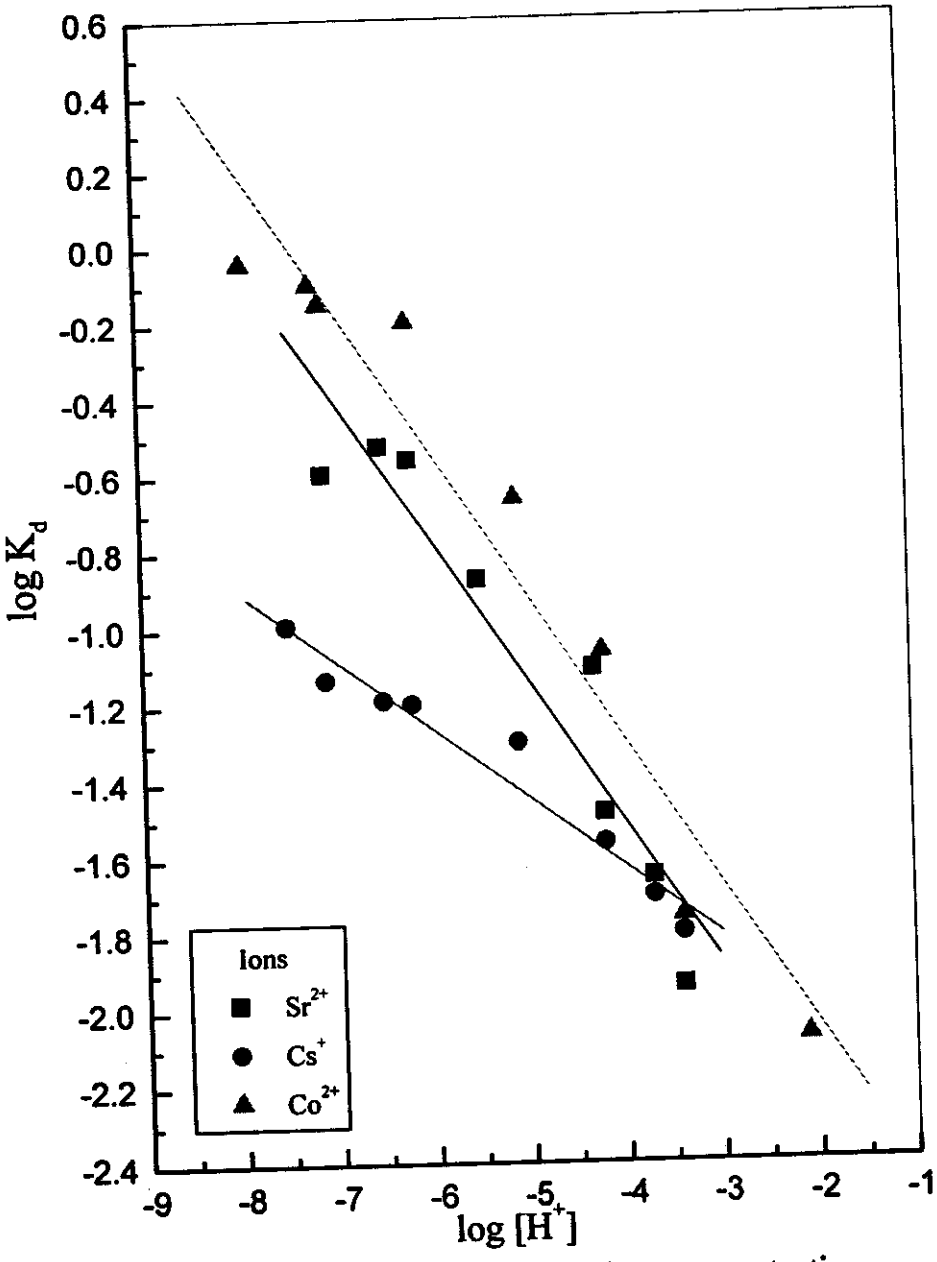

Fig. (32): Effect of hydrogen ion concentration on the distribution coefficient of different metal ions onto S_2;C_o= 10 mg L^{-1}.

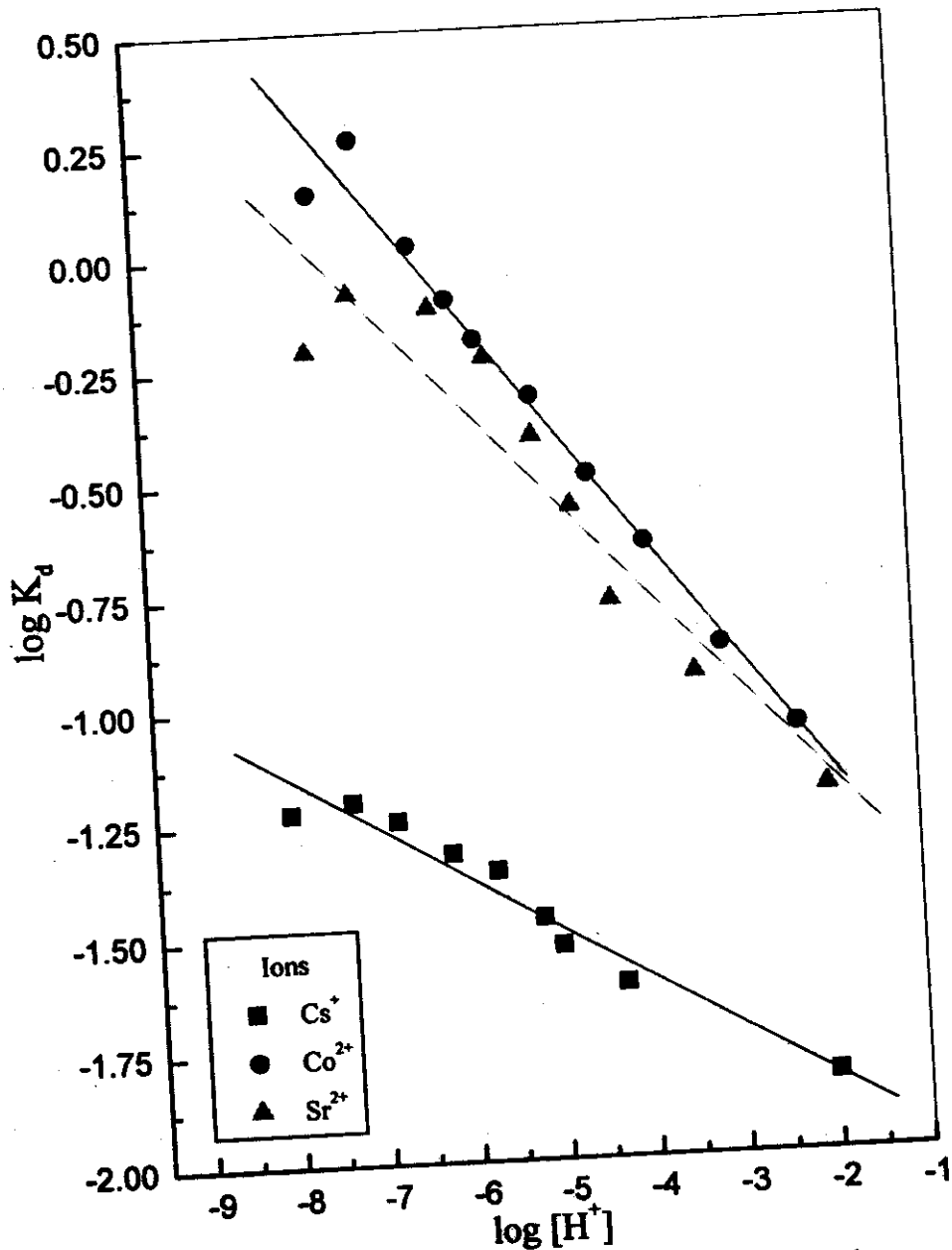

Fig. (33): Effect of hydrogen ion cocentration on the distribution coefficient of different metal ions onto S_3; C_0 = 10 mg L^{-1}.

III. 7. 4. 3 Effect of pH on sorption of phenol onto the samples

The pH of water represents one of the most important factors that influences the sorption capacity of compounds that can be ionized (**Adak and Pal, 2006; Myers and Zolandz, 1981**). Series of experiments were constructed to define the optimum pH value for sorption of phenol onto S_1, S_2 and S_3. Two regions are observed in figure (34), in the first region, the adsorbed amount of phenol increase as the pH increases. The second region has a smooth decrease in the adsorbed amount of phenol as the pH value increases. The maximum sorption capacity of phenol occurs onto S_1 at around pH value ranging between 7.5 and 8.1, onto S_2 at around pH value ranging between 7.3 and 7.9, and onto S_3 at around pH value ranging between 5 and 6.4.

At pH values < 7.5, 7.3 and 5, the sorption capacity of phenol on samples S_1, S_2 and S_3, respectively, is slightly diminished with respect to that at pH_{max} for the investigated sorbents. **Vidic et al., (1993)** reported that the chemisorption of phenol depends on the nature of the adsorbent surface. In this case, chemisorption would be hindered at low pH because of interference of protons with high electronic density centers on S_1, S_2 and S_3 surfaces, which are responsible of adsorptive bindings resulting from the formation of bridge bonds with –OH groups of phenol (**Nevskaia and Guerrero-Ruiz, 2001**) or donor-acceptor complexes as proposed by **Adak and Pal, (2006) and Mattson et al., (1969)**.

At pH values > 8.1, 7.9 and 6.4, a decrease of the amount sorbed of phenol on samples S_1, S_2 and S_3, respectively, was observed likely due to the increase of the concentration of the ionized form of phenol (**Manes, 1981**). A similar behavior was also observed in the adsorption of phenol on montmorillonite at a pH of 5.5 (**Yilmaz and Yapar, 2004**). Also **Saadet and Meric, (2004)** reported that adsorption of phenol onto montmorillonite at around a pH of 8. Similar behavior reported by **Garcia-Araya, et al., (2003)**. The differences observed in the adsorption behaviors of adsorbents may be attributed to the effect of the ionization behavior of phenol at different pH values for each adsorbent as well as to the

different surface structures of each adsorbent. Phenol can dissociate to phenolate and a proton according to the following reaction:

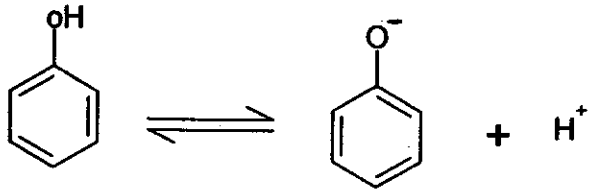

The ratio of phenol to phenolate is a function of pH at constant temperature. However, adsorption proceeds through the polarization of π-electrons and anion exchange. Phenol exists mainly in a neutral molecular form when the pH value equals 3-8 **(Wu and Gschwend, 1986)**, and adsorption through polarization of π-electrons will be dominant in this range in contrast to adsorption by anion exchange at high pH values. Closer inspection, at pH value range of the aqueous medium, it is possible for the adsorption of phenol on a negatively charged surface through the polarization of π-electrons and phenolate through the ion exchange. Since the anion exchange sites of S_1 and S_2 are limited, therefore the amounts sorbed of phenolate are not comparable to the adsorption of phenol molecule. Since phenol molecules interact strongly with water through the hydrogen bonding promoted by the dipole moments of the molecules. The water and phenol, adsorbed amounts depend on the relative magnitudes of water-phenol and phenol-surface interactions **(Saadet and Meric, 2004)**. The effect of water-phenol interaction will be dominant in low concentration due to the decrease in number of water molecules which are available for hydrogen bonding. Thus, the phenol-surface interaction will be dominant. In accordance with the pH findings, isotherm experiments were carried out at a pH value between 7.5 and 8.1, 7.4 and 8, and 5 and 6.4 for S_1, S_2 and S_3, respectively.

Finally, once selected pH conditions a number of adsorption experiments were repeatedly carried out to evaluate reproducibility of results. Data deviations in equilibrium adsorption isotherms lower than 5% were found in all cases.

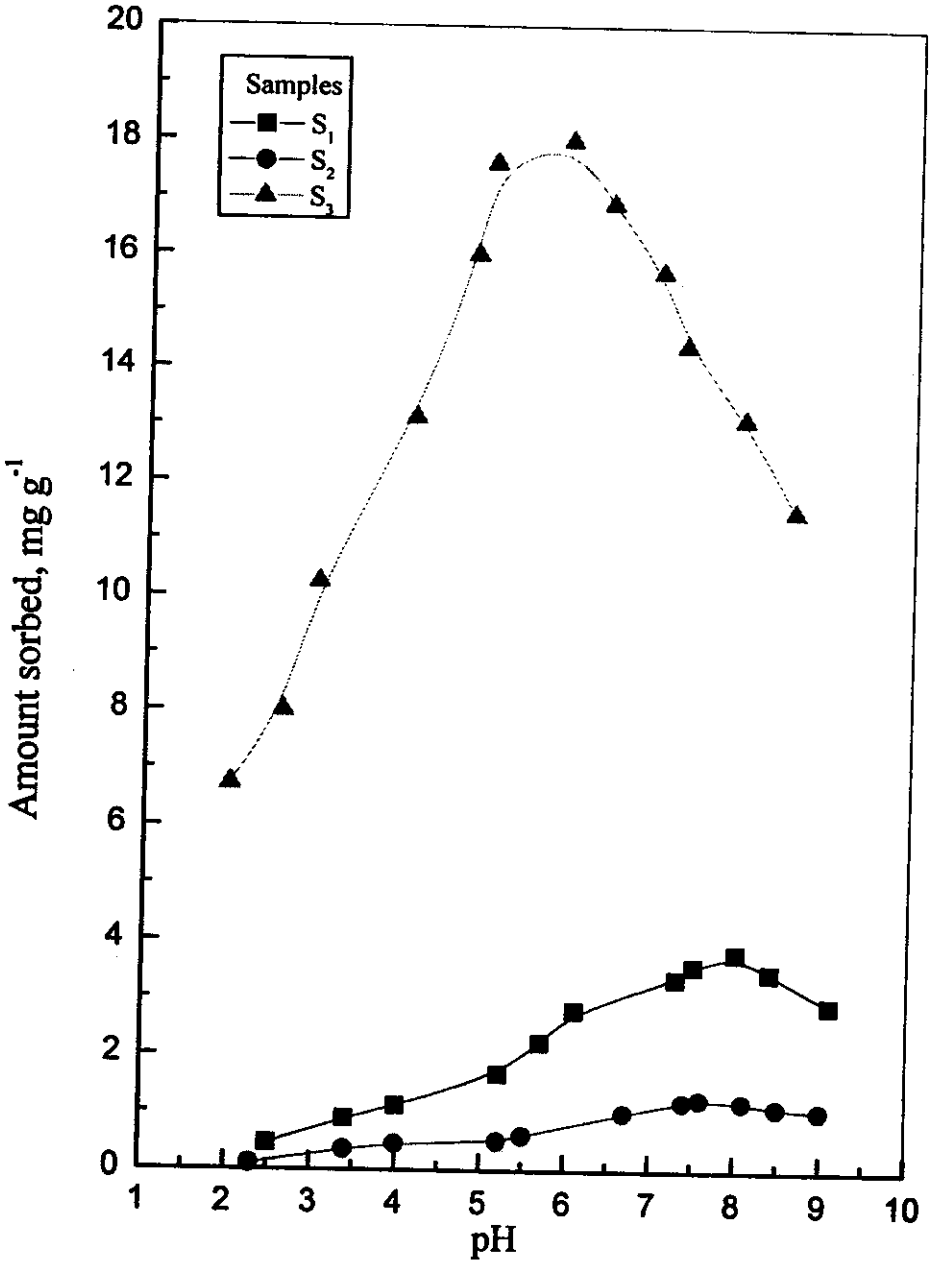

Fig. (34): Effect of hydrogen ion concentration on sorption of phenol onto the investigated samples, C_0 = 50 mg L^{-1}.

III. 7. 5 Sorption isotherms of the selected contaminants onto the studied samples

Adsorption isotherms give a graphical representation of the influence of contaminant concentration on the degree of adsorption. The equilibrium adsorption isotherm of the selected radionuclides onto the clay samples (S_1&S_2) and activated carbon (S_3) at 29°C ±1, pH_{Cs} = 7.2 ± 0.2, pH_{Co} = 7.5 ± 0.2, pH_{Sr} = 6.3 ±0.2, V/m of clay samples = 0.2 L g^{-1}, V/m of activated carbon = 0.25 L g^{-1}, are shown in figures (35-37). The equilibrium adsorption isotherm of phenol onto the investigated sorbents (S_1, S_2, S_3) at 29°C ±1, V/m of activated carbon = 0.016 L g^{-1}, V/m of clay sample = 0.014 L g^{-1}, is shown in figure (38). It is clear that all isotherms are fit in the linearized form for the concentration range used. Concerning these data, the dependence of the amount sorbed on both the sorbent weight and metal ion concentrations have been analyzed by Freundlich isotherm equation.

III. 7. 5. 1 Freundlich-type isotherm

The simple Freundlich-type isotherm model was capable of describing the sorption over the entire concentration range used, according to the following equation (**Gary and Stephen, 2002**):

$$q_e = K_F C_e^{1/n} \quad \text{..... (43)}$$

$$\log q_e = \log K_F + 1/n \log C_e \quad \text{..... (44)}$$

Where:

q_e is the amount of metal ion sorbed per unit weight of adsorbent (mg g^{-1}), C_e is the equilibrium concentration (mg L^{-1}), K_F is the Freundlich constant (mg g^{-1}) and 1/n is Freundlich isotherm exponent constant that is related to the sorption intensity.

Plotting the values of log q_e *vs* log C_e, as shown in figures (39-42), yields a linear relationship. This linearity emphasizes the applicability of Freundlich isotherm model in describing the sorption process in the studied system. From the figures, the constants K_F and 1/n were evaluated from the intercept and the slope of the curve, respectively. Satisfactory linearization is obtained as indicated by the high correlation coefficient (0.9944 – 0.9993). The values of the Freundlich constants K_F and 1/n as well as the correlation coefficient (r) in the above equation for the selected ions were calculated using linear regression analysis and are given in tables (9-12). As the constant K_F in Freundlich isotherm expresses the adsorbent capacity, the larger its value the larger its capacity (**Adak et al., 2005B, Lu and Haghseresht, 1998**). A high value of 1/n indicates that the adsorption is good over the entire range of concentrations studied (**Lu and Haghseresht, 1998**).

Table (9): Freundlich isotherm constants for sorption of Cs^+, Co^{2+} and Sr^{2+} ions onto S_1

Ions	Freundlich constants		r
	K_F (mg g^{-1})	1/n	
Cs^+	17.49	1.60	0.9993
Co^{2+}	20.79	1.39	0.9977
Sr^{2+}	22.28	1.34	0.9972

Table (10): Freundlich isotherm constants for sorption of Cs^+, Co^{2+} and Sr^{2+} ions onto S_2

Ions	Freundlich constants		r
	K_F (mg g^{-1})	1/n	
Cs^+	6.11	0.92	0.9975
Co^{2+}	21.69	1.32	0.9977
Sr^{2+}	19.68	1.53	0.9944

Table (11): Freundlich isotherm constants for sorption of Cs^{+}, Co^{2+} and Sr^{2+} ions onto S_3

Ions	Freundlich constants		r
	K_F (mg g^{-1})	1/n	
Cs^{+}	1.7	1.97	0.9968
Co^{2+}	14.7	4.42	0.9937
Sr^{2+}	6.1	2.54	0.9986

Table (12): Freundlich isotherm constants for sorption of phenol onto the investigated samples

Samples	Freundlich constants		r
	K_F (mg g^{-1})	1/n	
S_1	3.8	3.64	0.9901
S_2	2.5	3.92	0.9924
S_3	17.4	8.44	0.9918

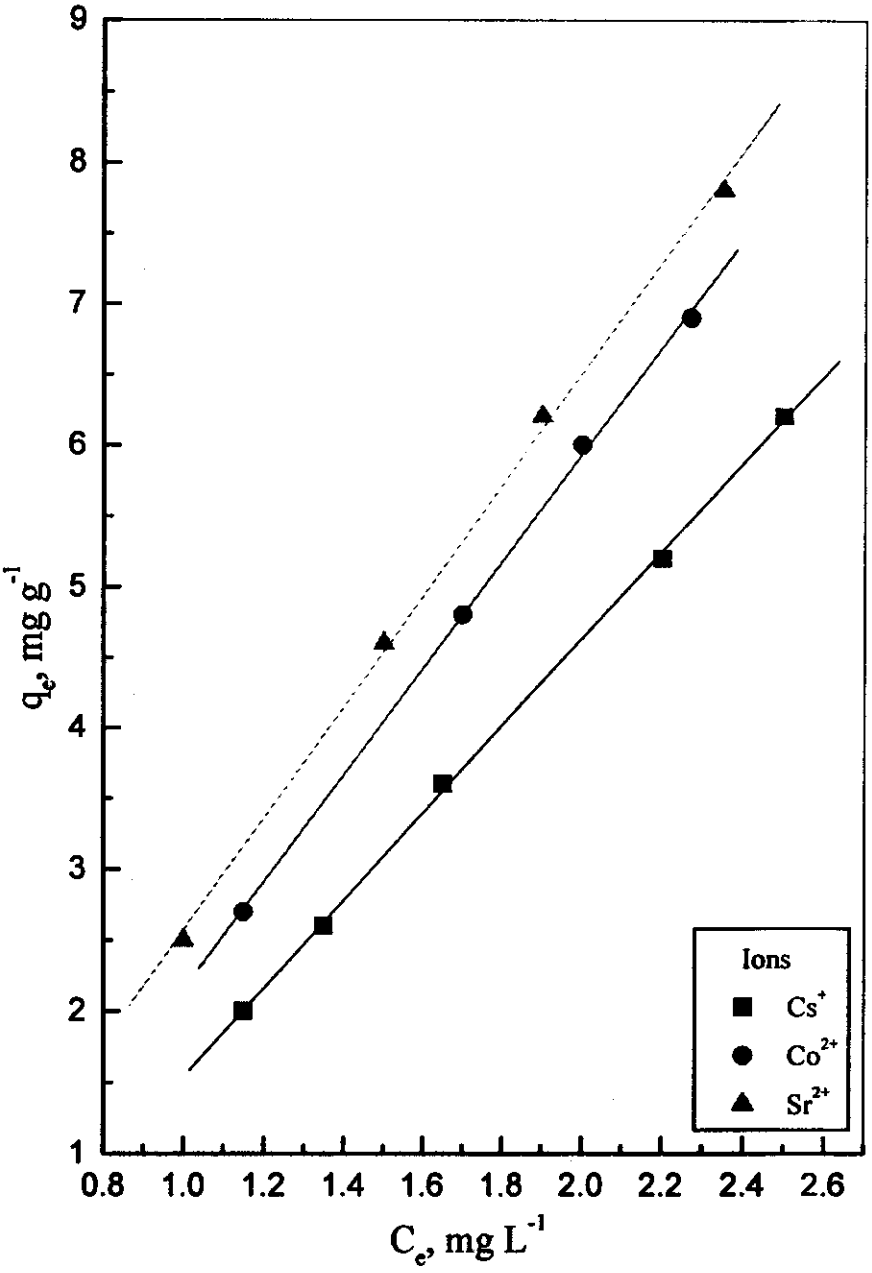

Fig. (35): Sorption isotherm of the selected ions onto S_1;

$T = 29^{\circ}C$, $pH_{Cs} = 7.2$, $pH_{Co} = 7.5$, $pH_{Sr} = 6.3$.

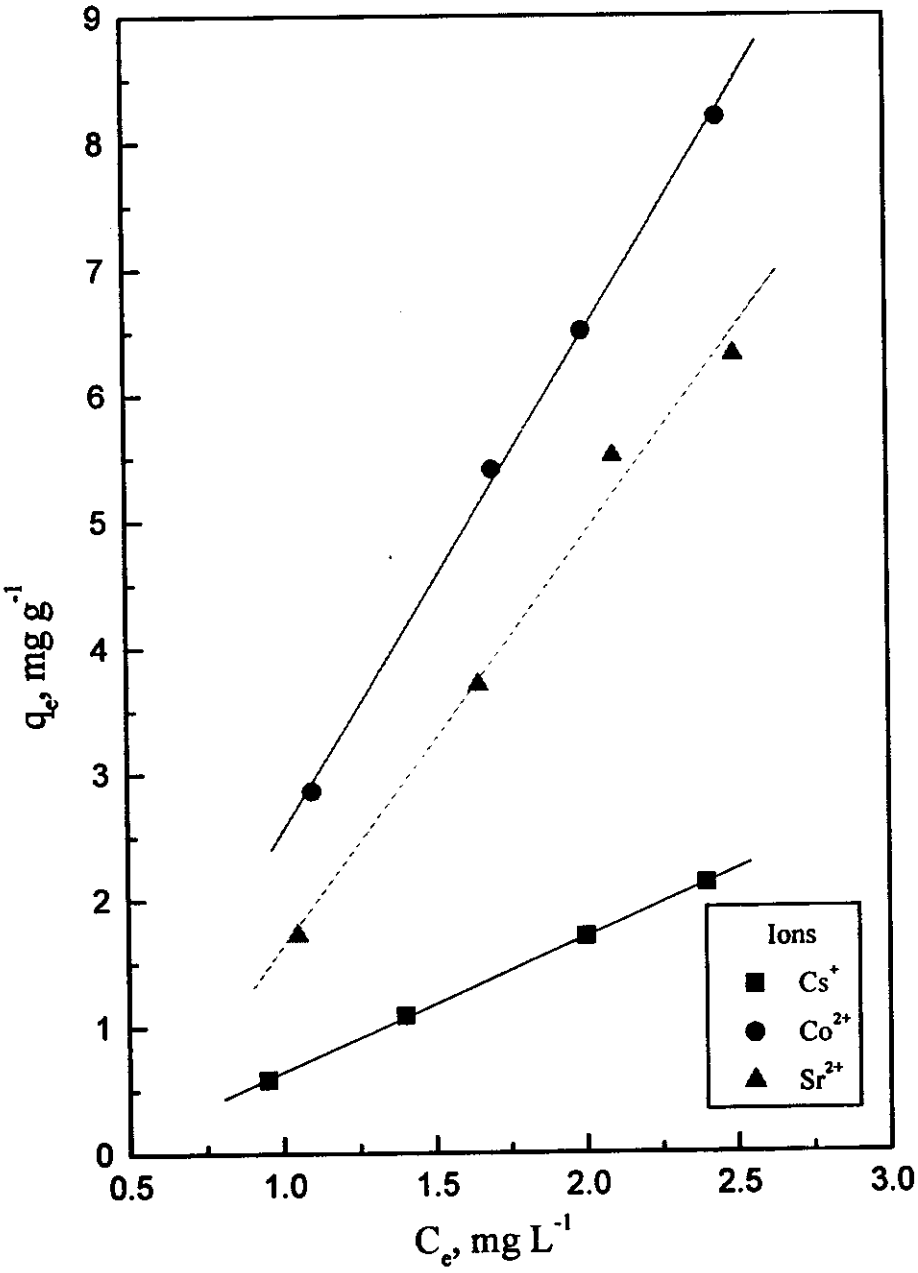

Fig. (36): Sorption isotherm of the selected ions onto S_2;

T=29°C, pH_{Cs} = 7.2, pH_{Co} = 7.5, pH_{Sr} = 6.3.

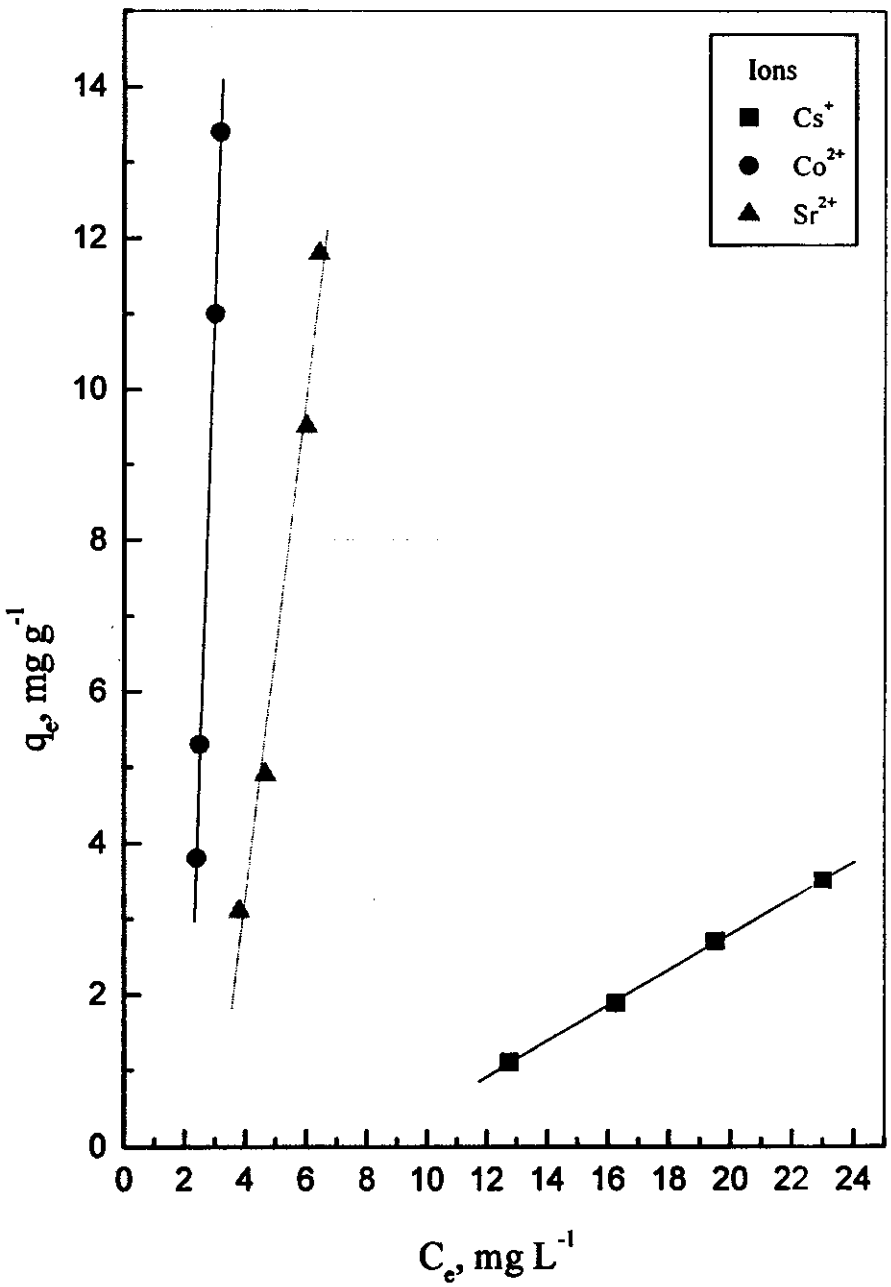

Fig. (37): Sorption isotherm of the selected ions onto S_3, $T = 29^{\circ}C$, $pH_{Cs} = 7.6$, $pH_{Co} = 7.2$, $pH_{Sr} = 6.5$.

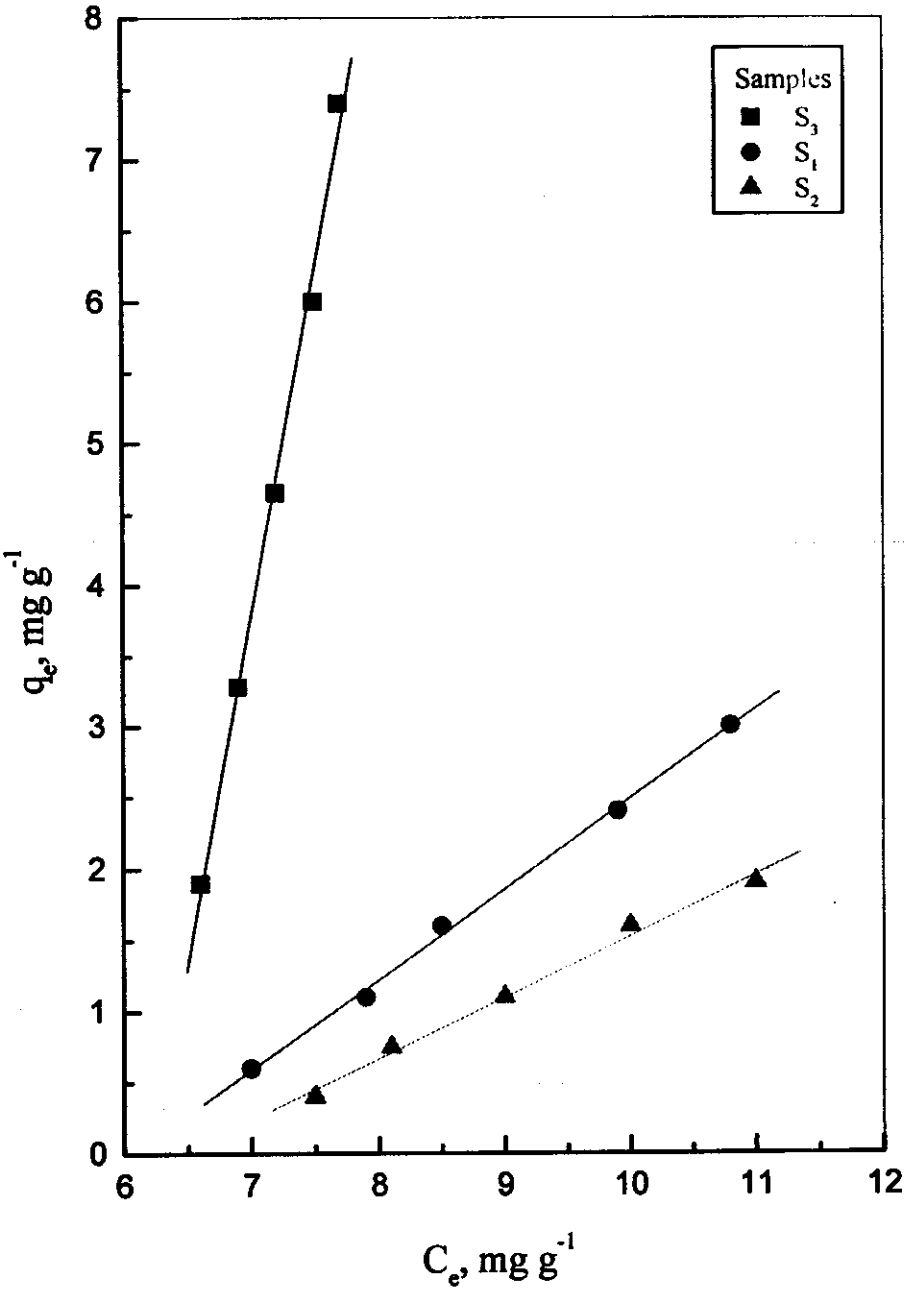

Fig. (38): Sorption isotherm of phenol onto the investigated samples; T= 29°C.

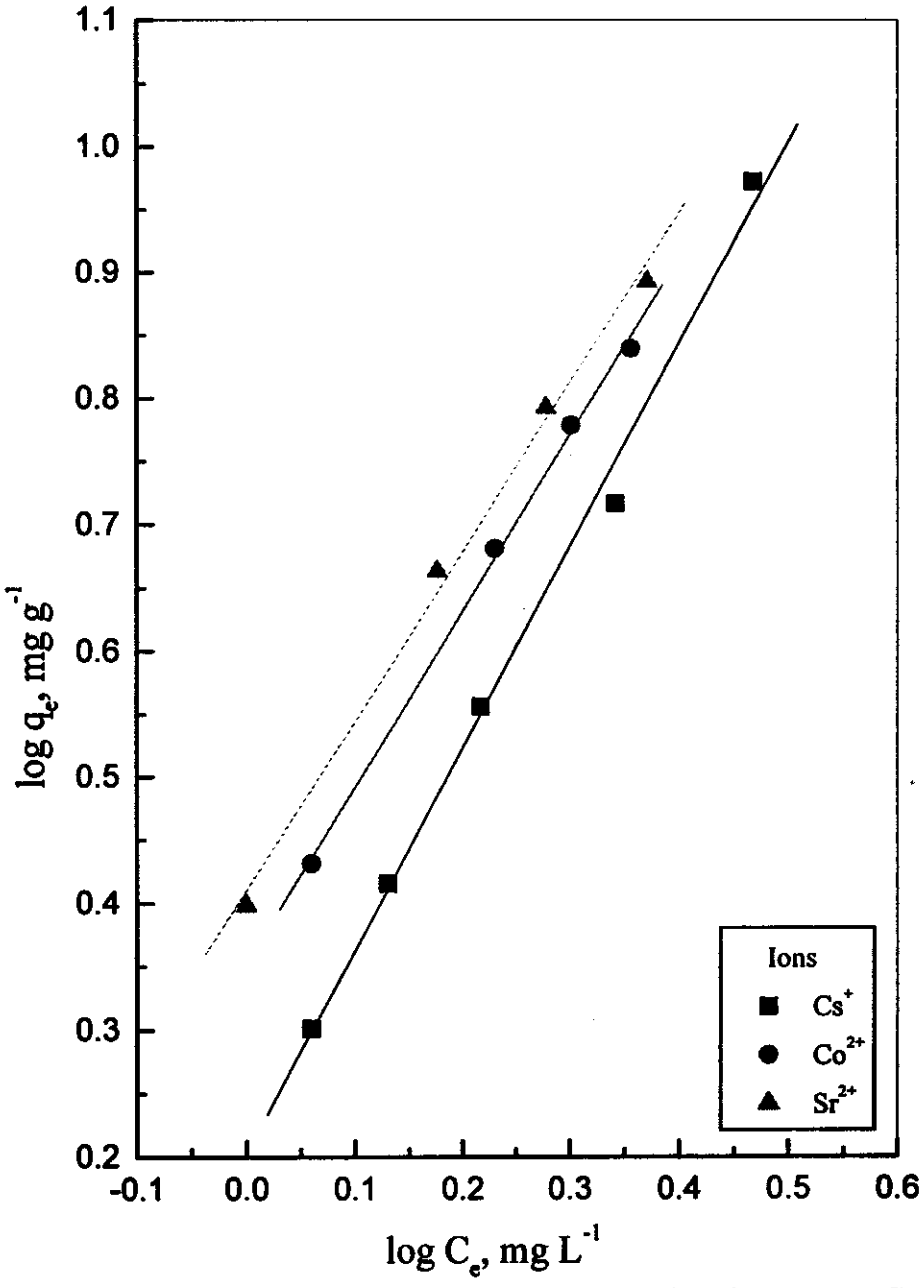

Fig. (39): Freundlich isotherm for sorping ions onto S_1.

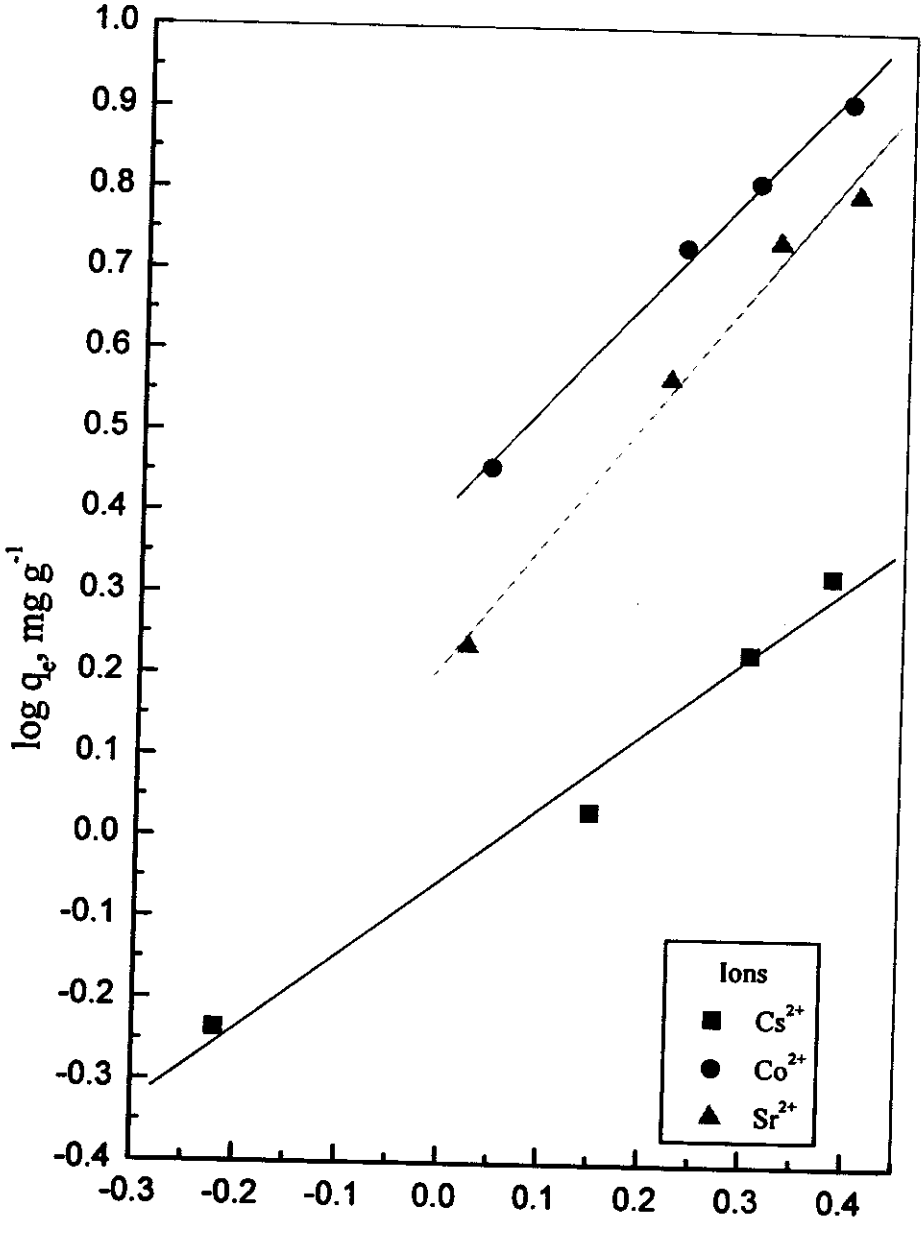

Fig. (40): Freundlich isotherm for sorption of the selected ions onto S_2.

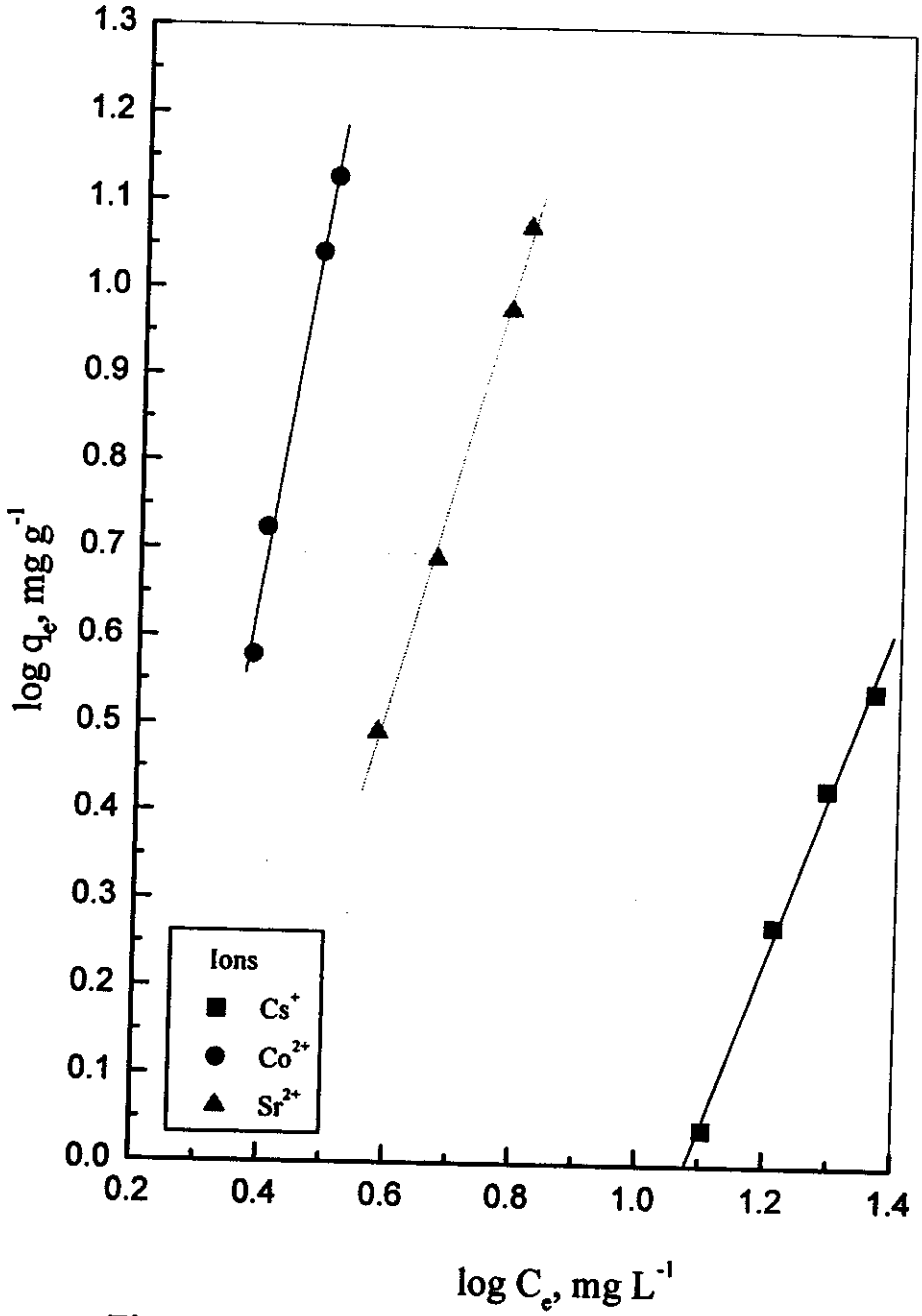

Fig. (41): Freundlich isotherm for sorption of the selected ions onto S_3.

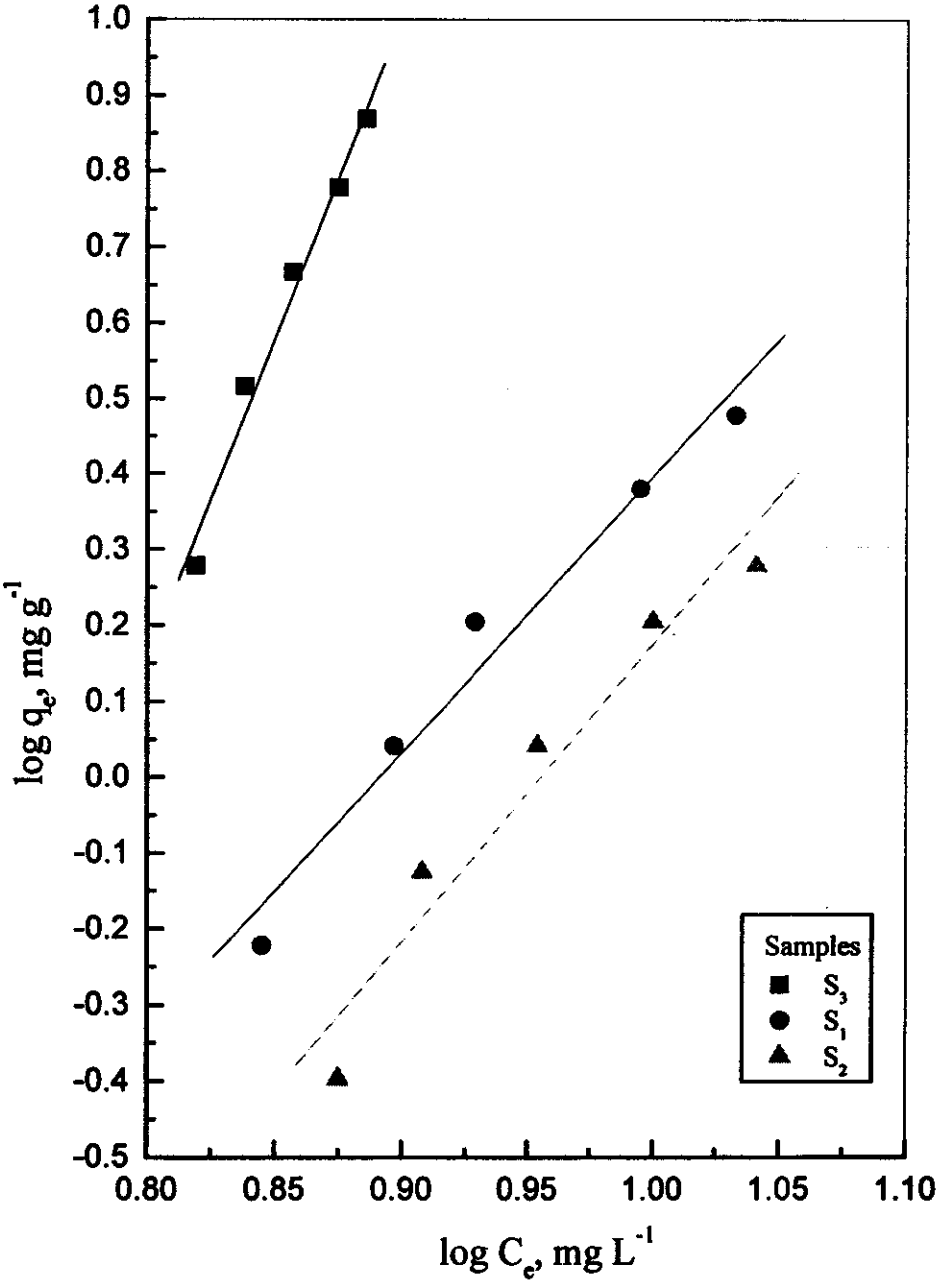

Fig. (42): Freundlich isotherm for sorping phenol onto the investigated samples.

III. 7. 6 Effect of competing ion concentration

The effect of changing the competing cation concentration on sorption of ^{134}Cs, ^{89}Sr and ^{60}Co onto the studied samples was investigated. Two competing cations were used for every selected radioelement. The obtained data were represented in figures (43-51). Generally, it is observed that the presence of K^+ or Ba^{2+} ions as competing cations for Cs^+ reduce the amount sorbed of ^{134}Cs, and also presence of K^+ or Ca^{2+} ions, as competing cations for Sr^{2+}, decrease the amount sorbed of ^{89}Sr. On the other hand, Mg^{2+} or Fe^{3+} ions, as competing cations for Co^{2+}, decrease the amount sorbed of ^{60}Co onto the investigated sorbent samples.

Figure (43) shows the effect of K^+ and Ba^{2+} ions as competing cations on sorption of ^{134}Cs onto S_1. It is clear that as either K^+ or Ba^{2+} ions concentration increased up to 50 mg L^{-1}, the amount sorbed of Cs^+ ions decreased from 17.4 mg g^{-1} to 8.4 mg g^{-1}, in presence of K^+ ions, and from 17.4 mg g^{-1} to 6.0 mg g^{-1}, in presence of Ba^{2+} ions. Figure (44) shows the effect of K^+ and Ba^{2+} ions as competing cations on sorption of ^{134}Cs onto S_2. It is clear that, as either K^+ or Ba^{2+} ions concentration increased up to 50 mg L^{-1}, the amount sorbed of Cs^+ ions decreased from 6.1 mg g^{-1} to 3.25 mg g^{-1}, in presence of K^+ ions, and from 6.1 mg g^{-1} to 2.16 mg g^{-1}, in presence of Ba^{2+} ions. Figure (45) shows the same trend for the effect of K^+ and Ba^{2+} ions as competing cations on sorption of ^{134}Cs onto S_3. It is noticeable that, as either K^+ or Ba^{2+} ions concentration increased up to 50 mg L^{-1}, the amount sorbed of Cs^+ ions is reduced from 1.7 mg g^{-1} to 0.52 mg g^{-1}, in presence of K^+ ions, and from 1.7 mg g^{-1} to 0.37 mg g^{-1}, in presence of Ba^{2+} ions. This indicates that both K^+ and Ba^{2+} ions have a competing effect on sorption of ^{134}Cs onto the investigated sorbent samples. This result may be attributed to the similarity of the ionic radii of K^+, Ba^{2+} and Cs^+ ions; [Cs^+ = 2.25 A°, K^+ = 1.96 A° and Ba^{2+} = 1.98 A°]. It is also noticeable that Ba^{2+}, as a

competing ion, is better than K^+ ion. This may be reported due to the charge density of these ions, where Ba^{2+} ion has two positive charges but K^+ ion has single positive charge i.e. their ionic potential (Z^n /r), where the element of highly charged ions are attracted more strongly to the opposite charged sites in the adsorbent surface than the lower ones when they have the same initial concentration. This result is in agreement with the results obtained by **Khan et al., (1994). Shenber and Johnson, (1992)** and **Stanners and Aston, (1981)** reported that the increase in K^+ ions as a competing cation affect the uptake of Cs^+ ions on soil samples. Presence of Na^+, K^+, Ca^{2+} and Fe^{3+} ions as competing ions decrease the uptake of ^{137}Cs, ^{60}Co, ^{241}Am and $^{(142+154)}Eu$ by the different soil samples (**Ezz El-Din, 1995**).

The obtained data of using either K^+ or Ca^{2+} ions as competing cations for sorption of ^{89}Sr onto the investigated sorbent samples are shown in figures (46-48). The figures illustrate that the amount sorbed of Sr^{2+} ions decrease with increasing the concentrations of either K^+ or Ca^{2+} ions as competing cations.

Figure (46), in case of S_1, shows that as either K^+ or Ca^{2+} ions concentration increased up to 50 mg L^{-1}, the amount sorbed of Sr^{2+} ions decreased from 22.3 mg g^{-1} to 11.03 mg g^{-1} in presence of K^+ ions and from 22.3 mg g^{-1} to 8.09 mg g^{-1} in presence of Ca^{2+} ions. Figure (47), in case of S_2, shows that the amount sorbed of Sr^{2+} ions decreased from 19.6 mg g^{-1} to 7.86 mg g^{-1} in presence of K^+ ions, and from 19.6 mg g^{-1} to 5.22 mg g^{-1} in presence of Ca^{2+} ions. And also, with increasing of either K^+ or Ca^{2+} ions concentration up to 50 mg L^{-1}, the amount sorbed of Sr^{2+} onto S_3 was reduced from 6.1 mg g^{-1} to 3.5 mg g^{-1} in presence of K^+ ions and from 6.1 mg g^{-1} to 2.6 mg g^{-1} in presence of Ca^{2+}ions, as shown in figure (48). This indicates that both K^+ and Ca^{2+} ions have a competing effect on sorption of ^{89}Sr onto the investigated sorbents. This result may be attributed to the similarity of the ionic radii of K^+, Ca^{2+} and Sr^{2+} ions. Although K^+ and Sr^{2+} have

nearly similar ionic radii [K^+ = 1.96 A°, Ca^{2+} = 1.74 A° & Sr^{2+} = 1.92 A°], it is noticeable that Ca^{2+}, as a competing ion, is better than K^+ ion. This could be attributed to their ionic potential (Z^n /r) and the fact that the Ca^{2+} and Sr^{2+} cations have similar chemical properties and chemical charges.

The effect of Mg^{2+} and Fe^{3+} ions as competing cations on sorption of ^{60}Co onto the investigated sorbent samples is shown in figures (49-51). From these figures, it is clear that the competing cations decrease the sorption of radiocobalt. In case of S_1, it is clear that as either Mg^{2+} or Fe^{3+} ions concentration increased up to 50 mg L^{-1}, the amount sorbed of Co^{2+} ions decreased from 20.7 mg g^{-1} to 7.09 mg g^{-1} in presence of Mg^{2+} ions and from 20.7 mg g^{-1} to 5.14 mg g^{-1} in presence of Fe^{3+} ions, as shown in figure (49). The seam trend in case of S_2, it is clear that as either Mg^{2+} or Fe^{3+} ions concentration increased up to 50 mg L^{-1}, the amount sorbed of Co^{2+} ions decreased from 21.7 mg g^{-1} to 4.84 mg g^{-1} in presence of Mg^{2+} ions and from 21.7 mg g^{-1} to 3.28 mg g^{-1} in presence of Fe^{3+} ions, as shown in figure (50). And in case of S_3, the amount sorbed of Co^{2+} ions decreased from 14.7 mg g^{-1} to 9.93 mg g^{-1} in presence of Mg^{2+} ions and from 14.7 mg g^{-1} to 8.72 mg g^{-1} in presence of Fe^{3+} ions, as shown in figure (51). This indicates that both Mg^{2+} and Fe^{3+} ions have a competing effect on sorption of ^{60}Co onto the investigated sorbent samples. This may be attributed to the similarity of the ionic radii of Mg^{2+}, Fe^{3+} and Co^{2+} ions [Co^{2+} = 1.26 A°, Mg^{2+} = 1.30 A° and Fe^{3+} = 1.26 A°]. It is noticeable also that Fe^{3+}, as a competing ion, is better than Mg^{2+} ion of the competition. This may be due to the charge density of these ions, where Fe^{3+} ion has three positive charges but Mg^{2+} ion has two positive charges, i.e. This may be attributed to their ionic potential (Z^n /r). **Murry and Murry (1973)** found that the presence of Mg^{2+} and Ca^{2+} at high concentration reduce the cobalt uptake by soil while the presence of Na^+ or K^+ ions had no effect on the uptake of cobalt. **Ezz El-Din (1995)** reported similar results.

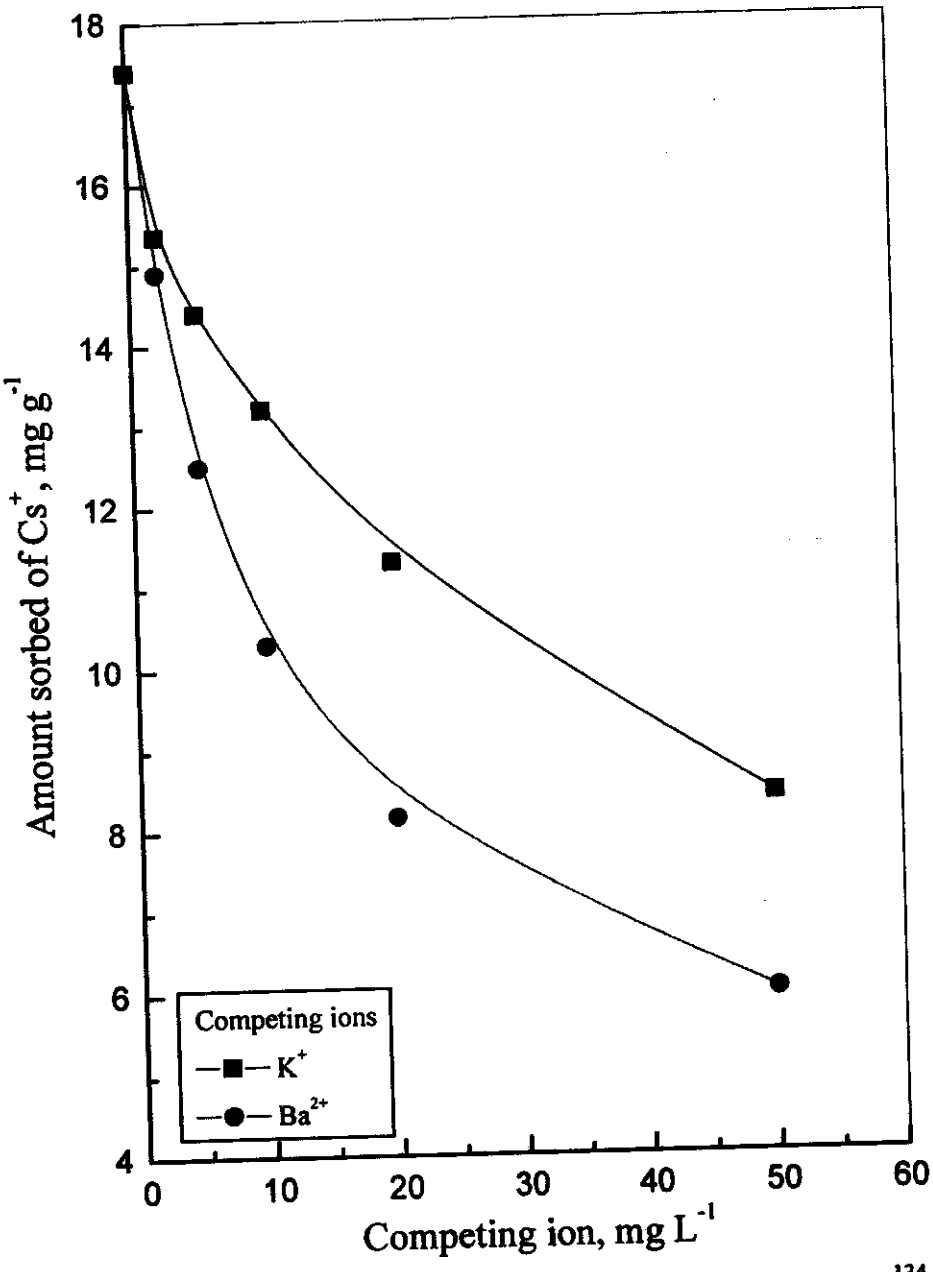

Fig. (43): Effect of competing ions on sorption of ^{134}Cs onto S_1; $[Cs^+]_0 = 10$ mg L^{-1}.

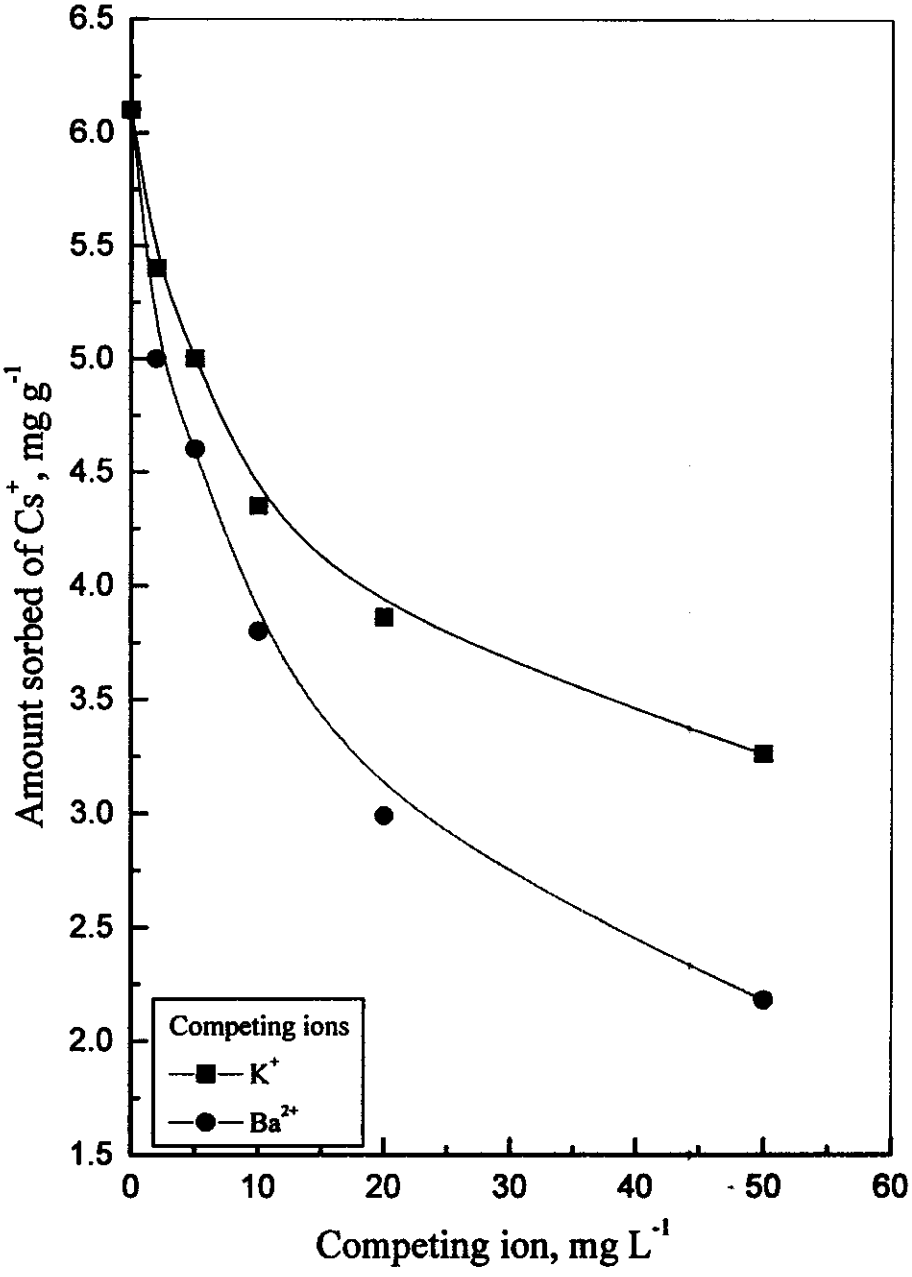

Fig. (44): Effect of competing ions on sorption of ^{134}Cs onto S_2; $[Cs^+]_0 = 10$ mg L^{-1}.

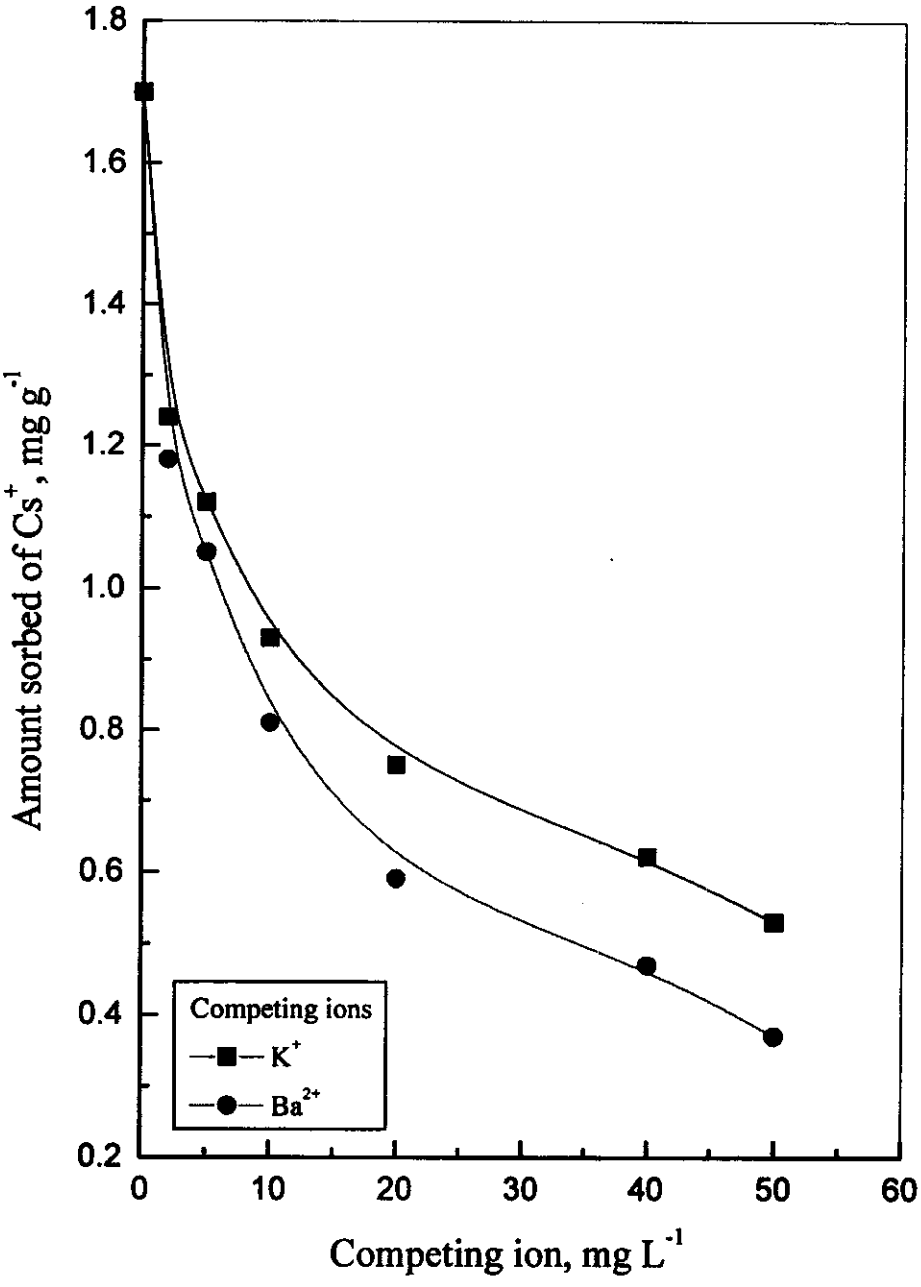

Fig. (45): Effect of competing ions on sorption of ^{134}Cs onto S_3; $[Cs^+]_0$ = 10 mg L^{-1}.

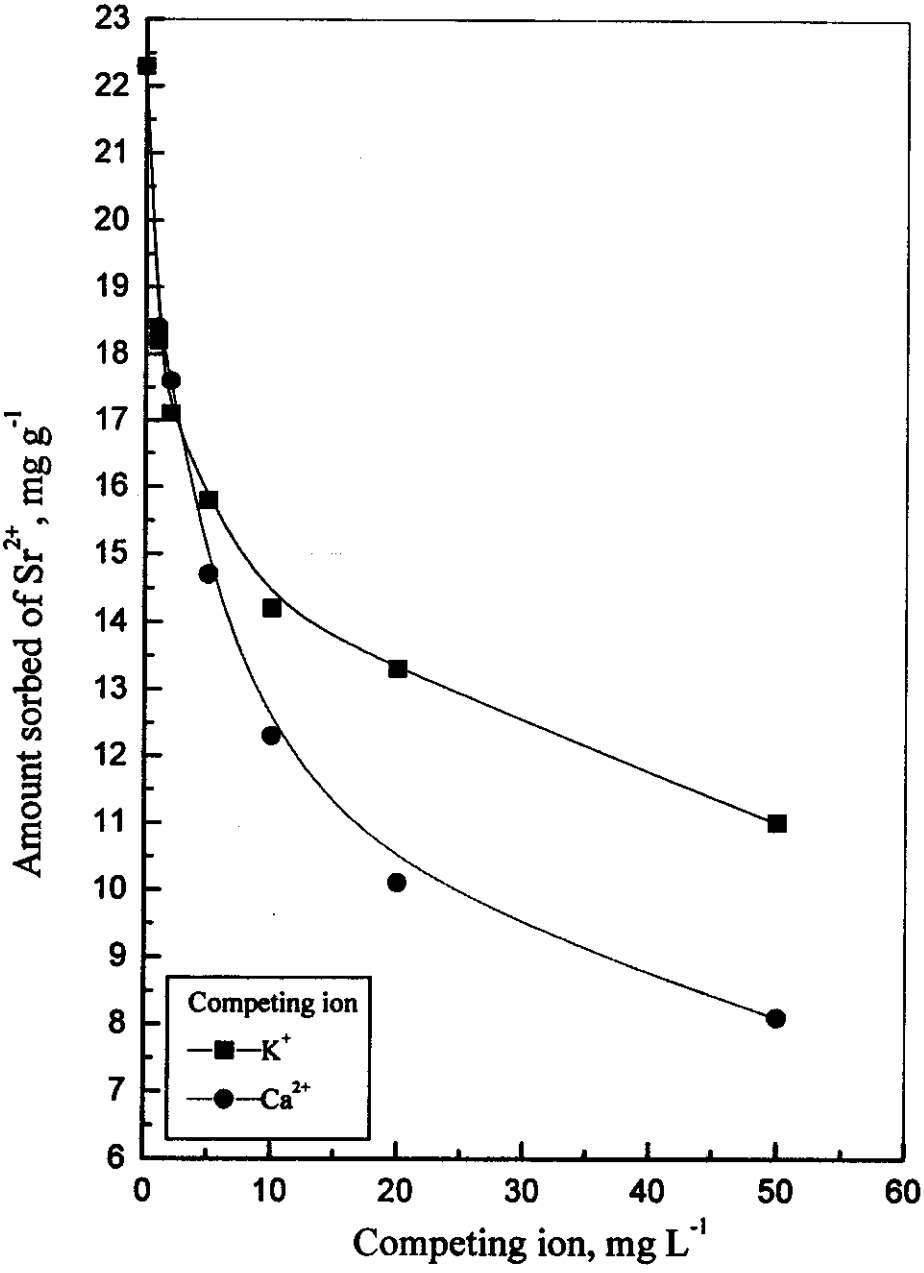

Fig. (46): Effect of competing ions on sorption of ^{89}Sr onto S_1, $[Sr^{2+}]_0 = 10$ mg L^{-1}.

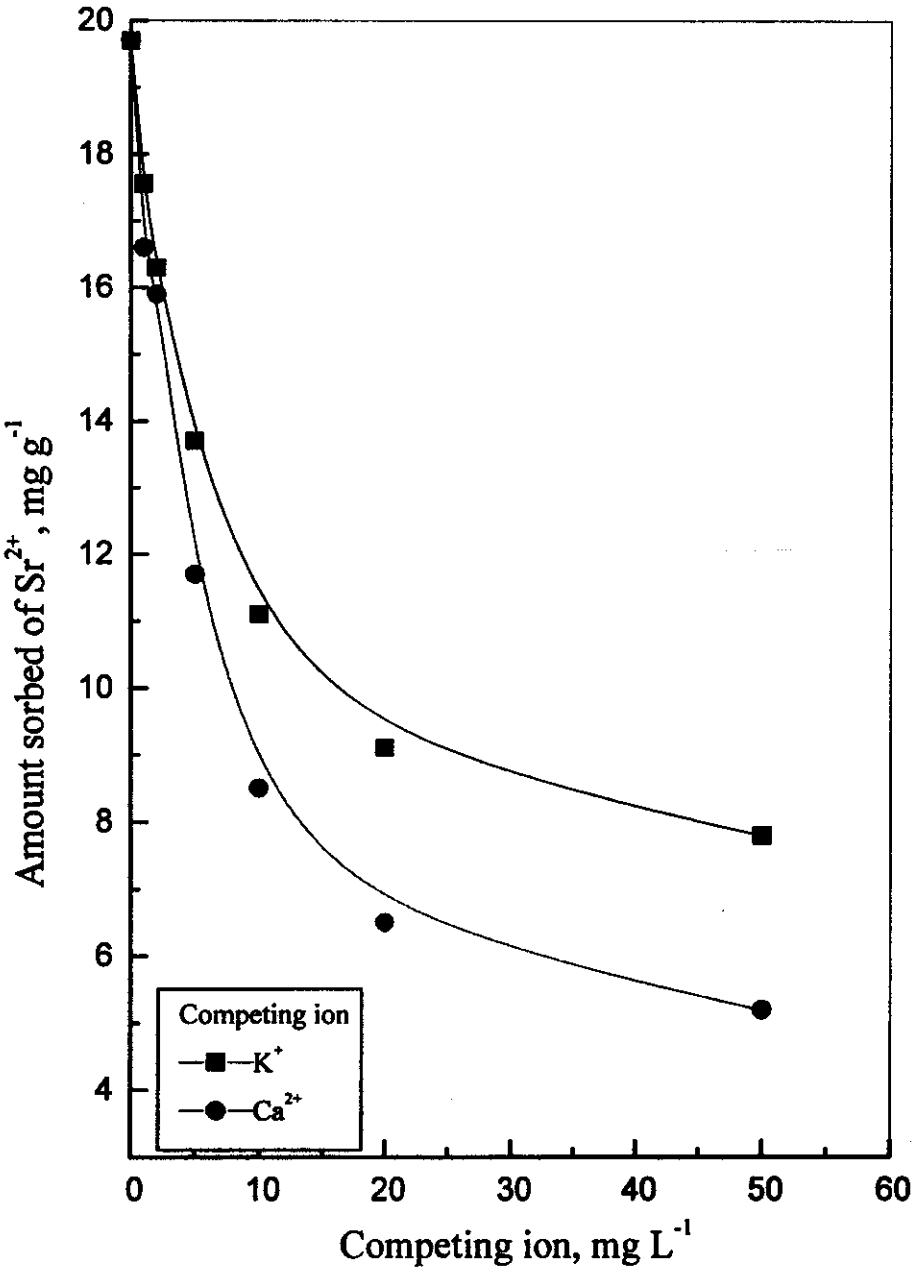

Fig. (47): Effect of competing ions on sorption of ^{89}Sr onto S_2; $[Sr^{2+}]_0 = 10$ mg L^{-1}.

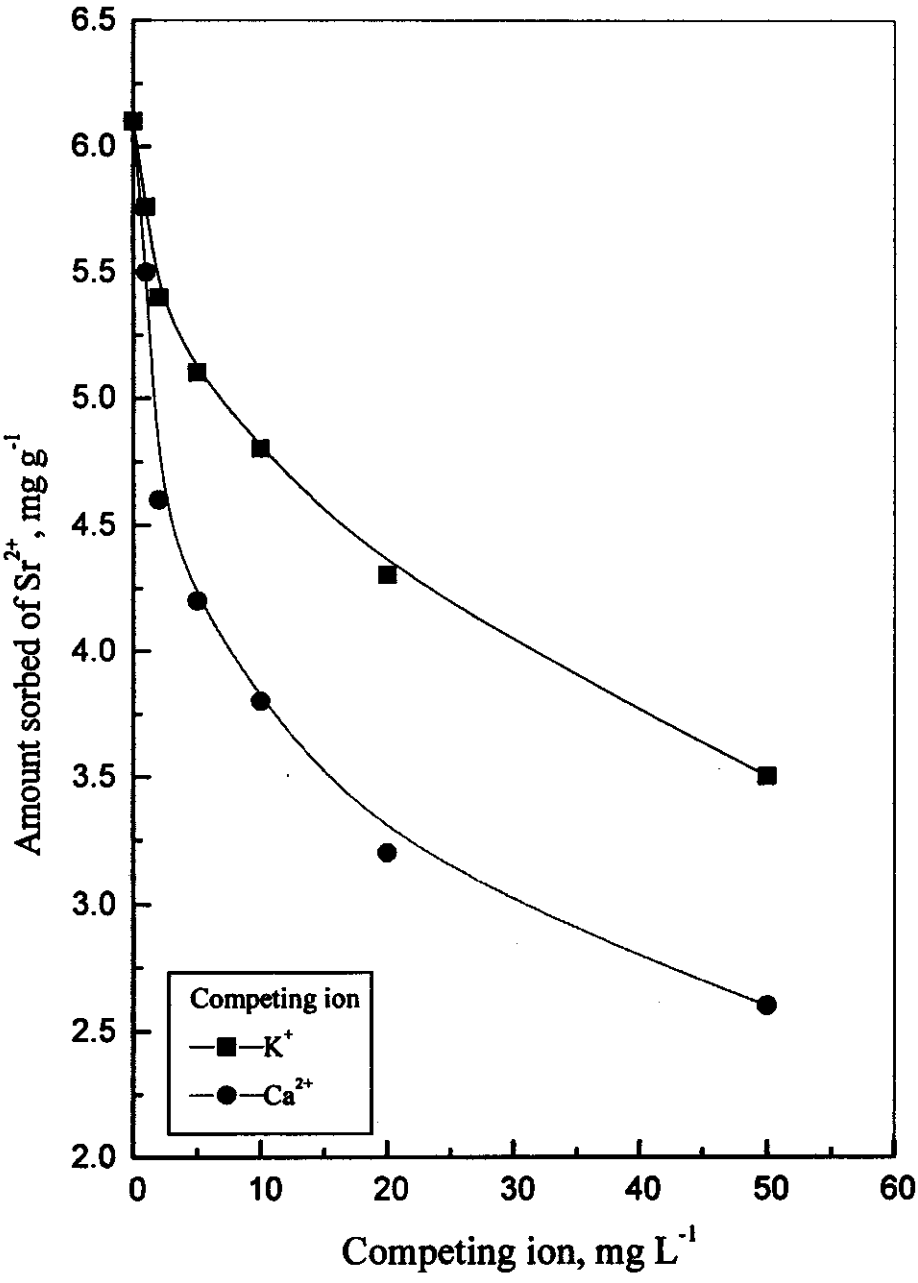

Fig. (48): Effect of competing ions on sorption of ^{89}Sr onto S_3; $[Sr^{2+}]_0 = 10$ mg L^{-1}.

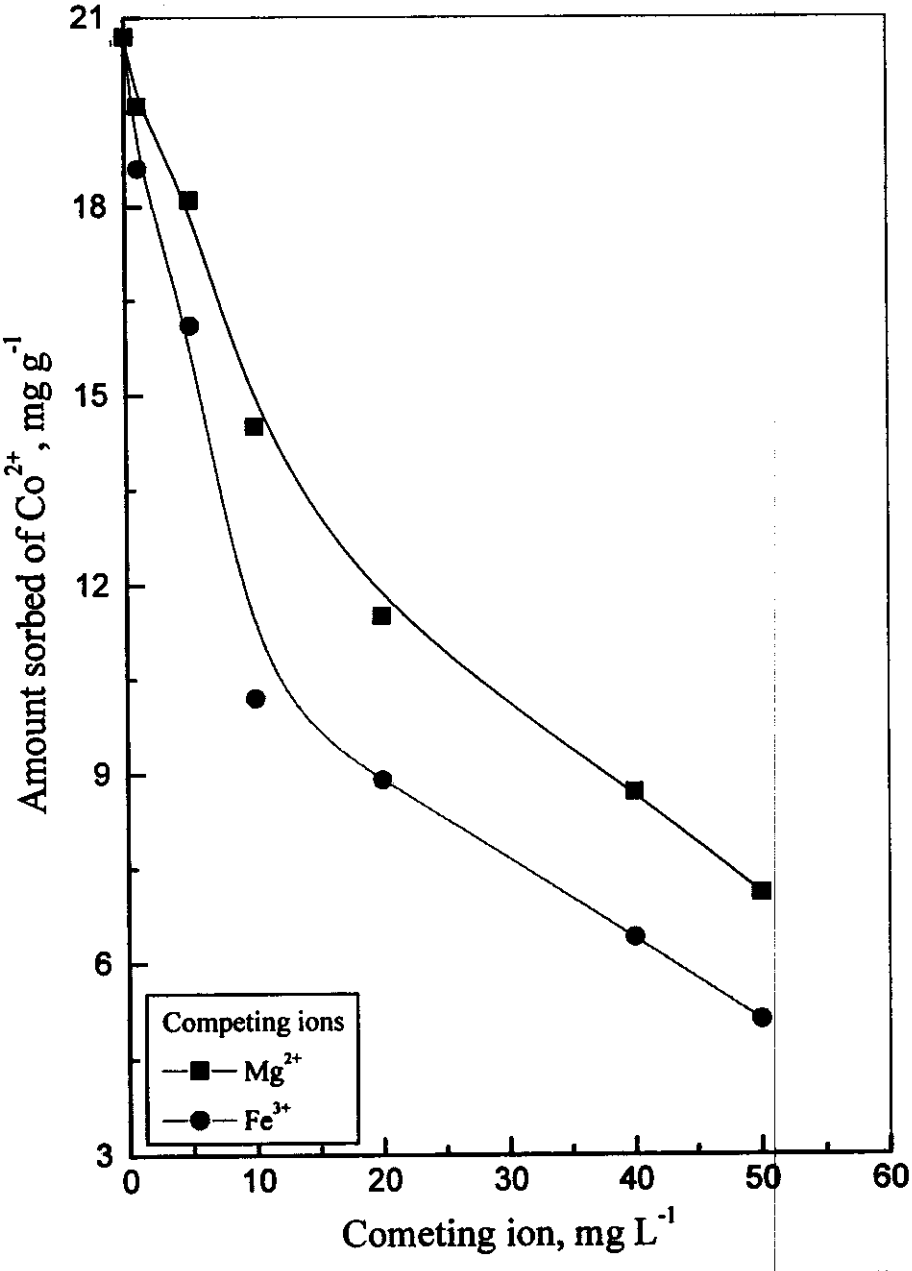

Fig. (49): Effect of competing ions on sorption of ^{60}Co onto S_1; $[Co^{2+}]_0 = 10$ mg L^{-1}.

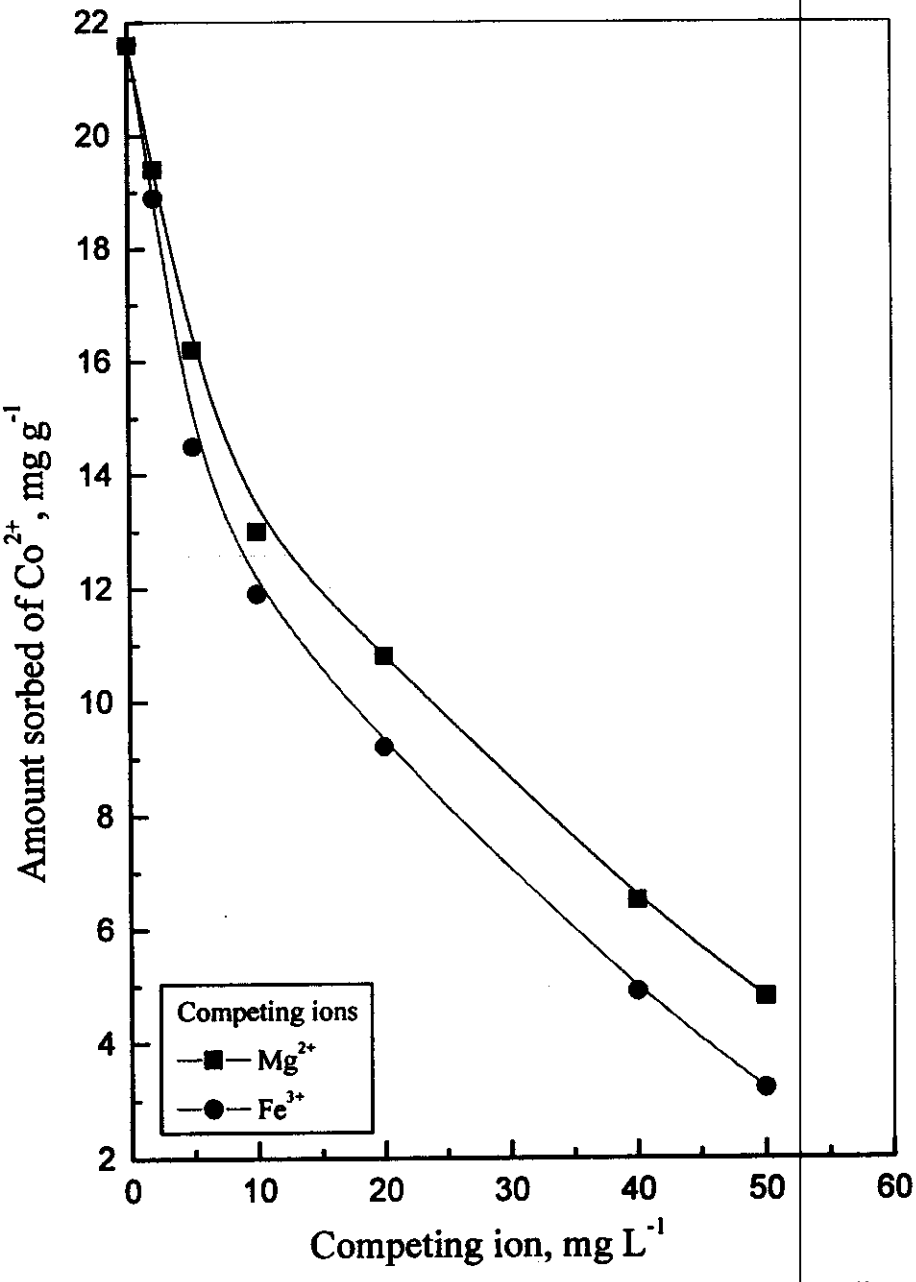

Fig. (50): Effect of competing ions on sorption of ^{60}Co onto S_2; $[Co^{2+}]_0 = 10$ mg L^{-1}.

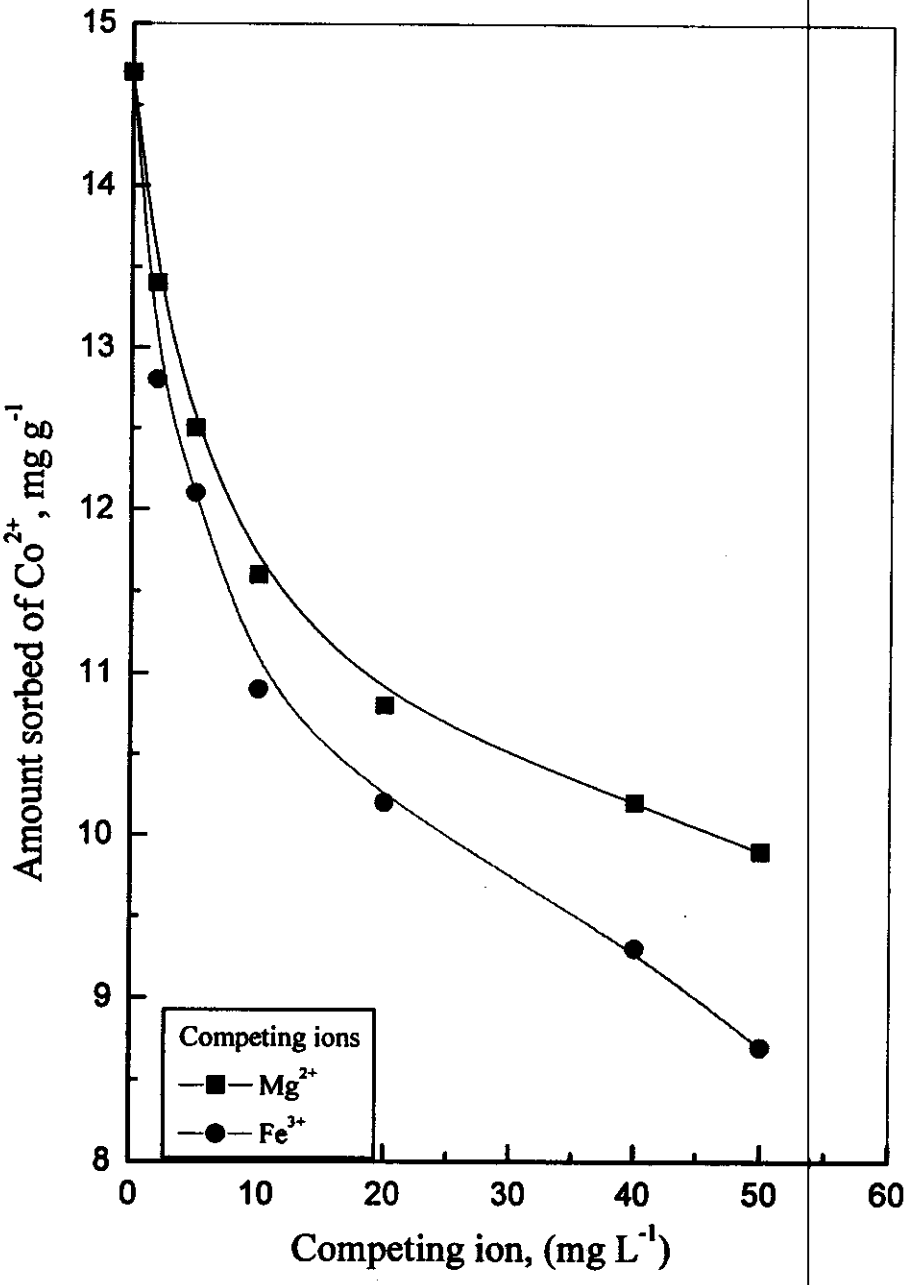

Fig. (51): Effect of competing ions on sorption of ^{60}Co onto S_3; $[Co^{2+}]_0 = 10$ mg L^{-1}.

III. 8 Desorption study

The study of desorption is similar, in many respects, to the adsorption methods. Desorption process of radionuclides and phenol from sorbents is generally much less than the sorption process. Such a study is usually carried out to find either the suitable conditions for the removal of an adsorbed pollutant from sorbents or elucidation of the mechanism of preliminary adsorption i.e. for determination of the nature of the sorption bond and/ or the state of the pollutant on the surface of the adsorbent.

The relative desorption of the selected radionuclides and phenol from the loaded sorbent samples is represented in figures (52 – 55). The desorption percent of ^{134}Cs, ^{60}Co, ^{89}Sr and phenol is plotted as a function of time. Desorption data are obtained after attaining the equilibrium between the loaded sorbent samples and the leaching medium. In case of S_1, it is clear from figure (52) that the maximum desorption percent of ^{134}Cs, ^{60}Co and ^{89}Sr is 19, 24 and 30 %, respectively and this is attained within 120 min. In case of S_2, it is shown from figure (53) that the maximum desorption percent of ^{134}Cs, ^{60}Co and ^{89}Sr is 18, 28 and 33 %, respectively and this is attained within 90 min. In case of S_3, it is shown from figure (54) that the maximum desorption percent of ^{134}Cs, ^{60}Co and ^{89}Sr is 10, 17 and 16 % and this is attained within 120 min. The difference of desorption percent from the loaded sorbents may be attributed to the variation of the surface area of the grains, the mineralogical and the chemical composition of each sorbent sample. Figure (55) shows that the maximum desorption percent of phenol loaded onto S_1, S_2 and S_3 is around 8, 10 and 9 %, respectively and this is attained within 200 min. The variation in desorption percent of phenol from the loaded investigated samples may be attributed to the difference in the nature of the samples.

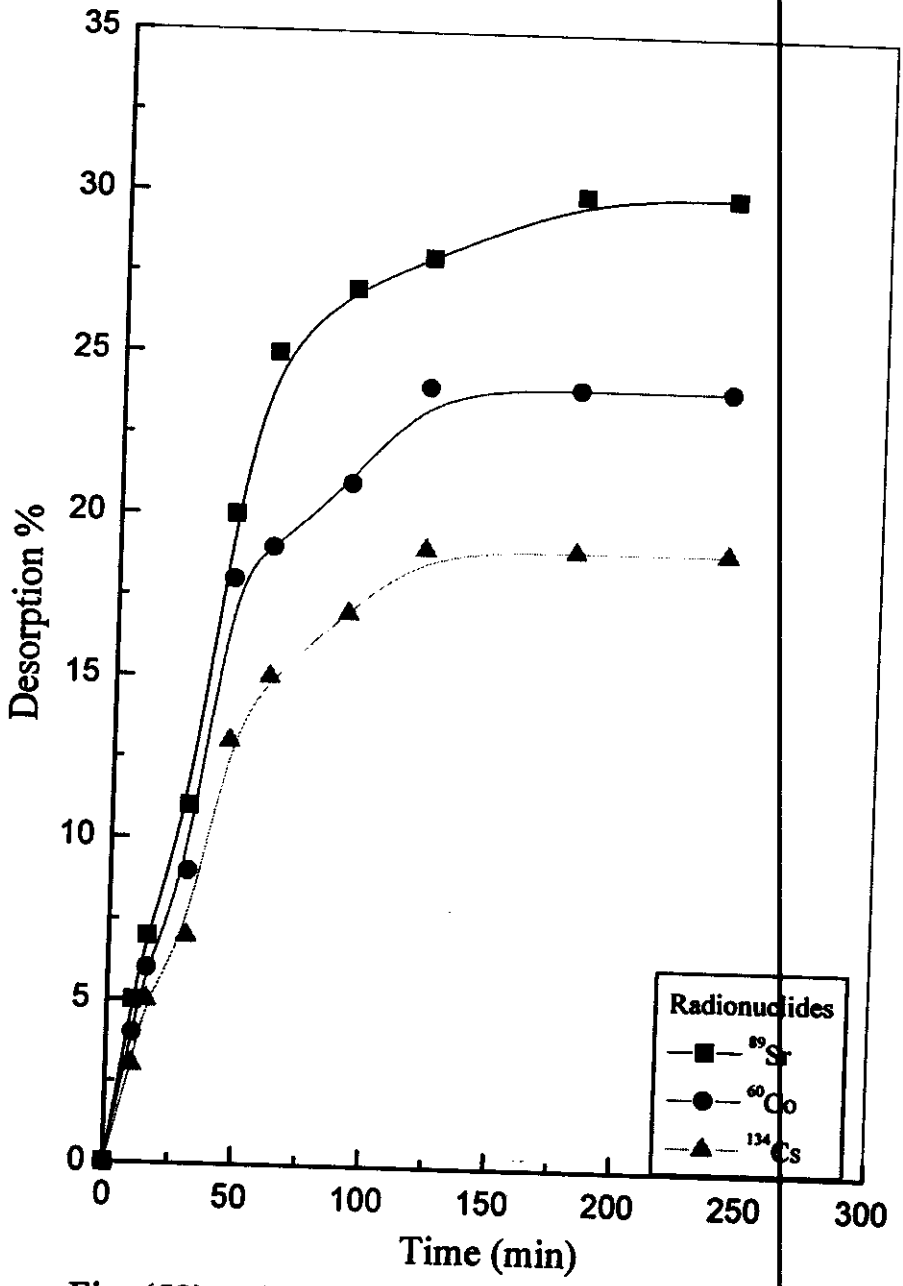

Fig. (52): Effect of contact time on desorption of the investigated radionuclides loaded onto S_1 using H_2O.

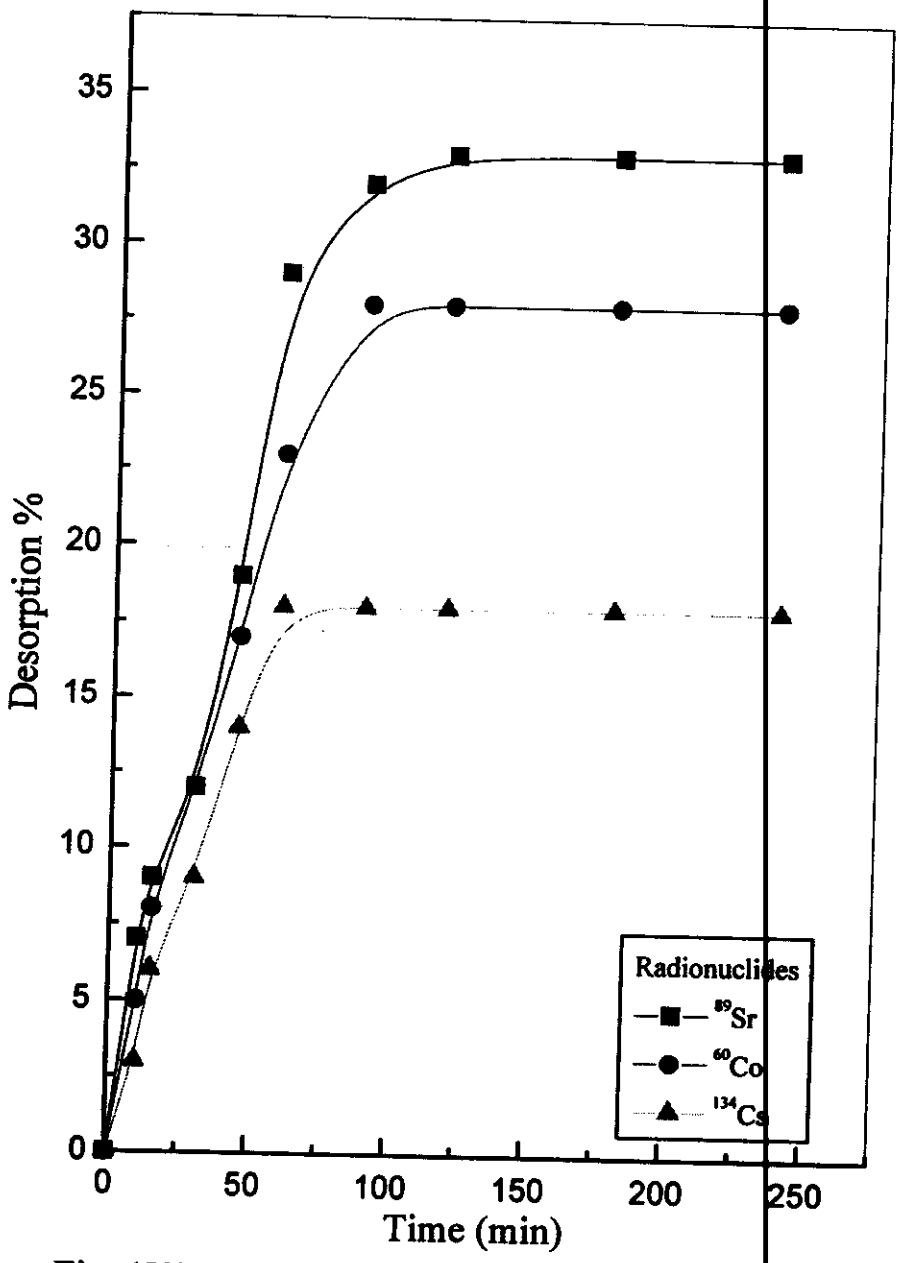

Fig. (53): Effect of contact time on desorption of the investigated radionuclides loaded onto S_2 using H_2O.

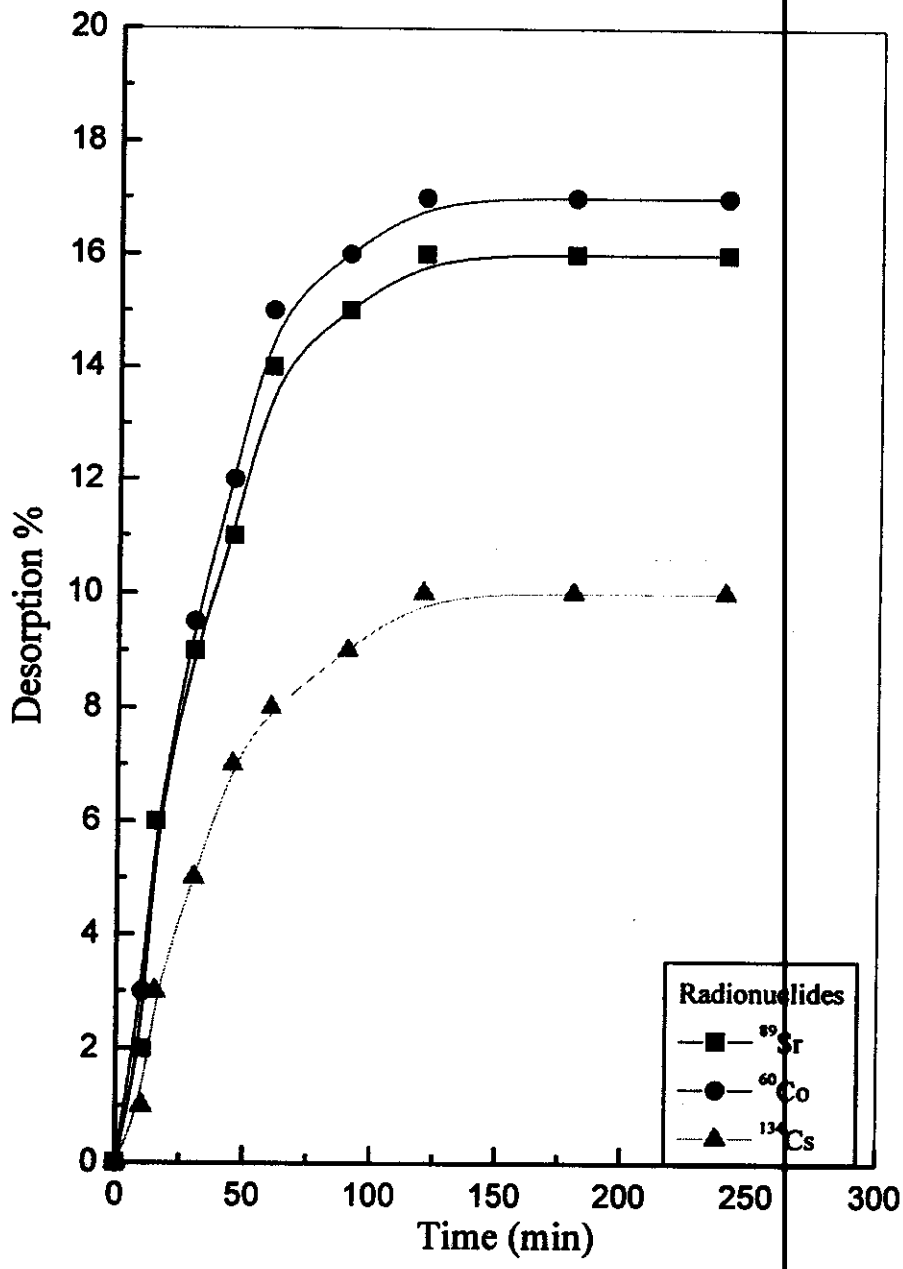

Fig. (54): Effect of contact time on desorption of the investigated radionuclides loaded onto S_3 using H_2O.

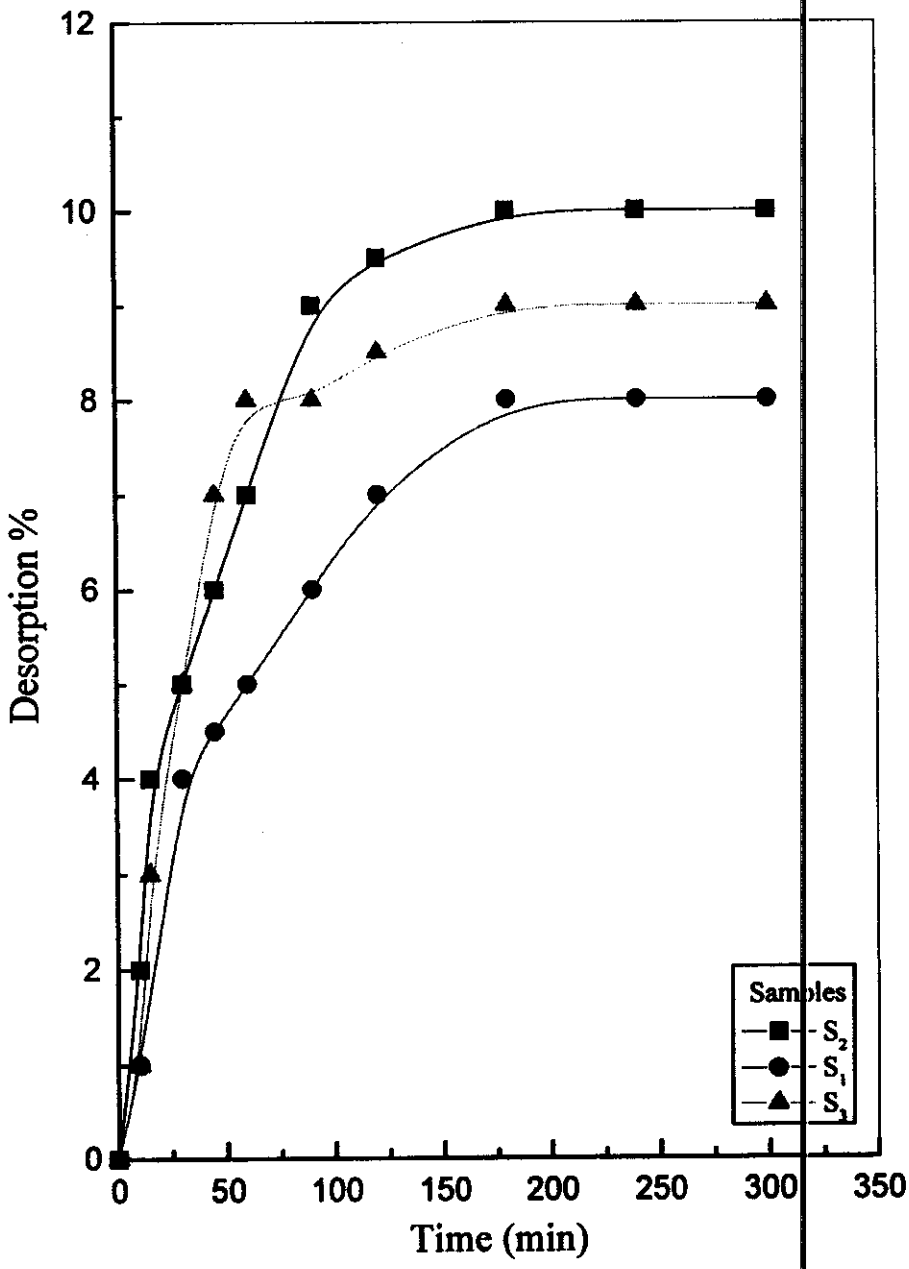

Fig. (55): Effect of contact time on desorption of phenol loaded onto the investigated samples using H_2O.

III. 9 Column investigations

From the previous studies, it was found that activated carbon and the two clay samples have a sorption affinity for some of radionuclides and phenol. Therefore, the studied samples and the selected contaminants (^{134}Cs, ^{60}Co, ^{89}Sr and phenol) are used for column investigations. The solution is percolated through a fixed bed of studied samples operated downwards by running the solution through the exchanger from top to bottom.

In column operation, another expression is used for the filter capacity known as breakthrough capacity which is defined as the amount of ions taken up quantitatively by the column under the condition in question i.e., the number of mg g^{-1} which is retained without any leakage observed. The breakthrough capacity is always lower than the total capacity of the column and is dependent upon a number of different variables, such as particle size, filtration rate and composition of solution.

The following equation was used for the calculation of the sorption capacity of the sorbent in the column **(Communar, et al., 2004, Mansour, 2001, Altin et al., 1999 and El-Assy et al., 1993).**

$$Q = (V_{50\%} - V)\, C_o / m \quad \ldots\ldots\ldots\ldots \quad (47)$$

Where Q: is the sorption capacity in mg g^{-1}.

C_o: is the initial concentration in mg L^{-1}.

$V_{50\%}$: is the average breakthrough volume representing at $(C/C_o)_{50\%}$

V: is the volume void of sorbat in mL.

m: is the mass of a sorbent (g).

In the present study the breakthrough of ^{134}Cs, ^{60}Co and ^{89}Sr in addition to phenol, onto either the two investigated clays or activated carbon sample using a small scale column (1cm internal diameter and 50 cm height) packed with either 4 g of granular activated carbon or 5 g of clay sample. The effluent was

collected in small fractions (of 50 mL) for the solute. The experiments were continued until the solute concentration percolating from the column was the same as the feed solution. The experimental results are shown in figures (56 - 59). The figures show the concentration of the effluent solute as a function of effluent volume. It is clear that the effluent solutions are initially sorbet free until a certain point (the break through point) is attained when the sorbet in the effluent in concentrations which increase with the increase of the effluent until a maximum is reached at which the sorbent samples are fully loaded. The capacity of the samples under the conditions of the experiment can be easily estimated from the data in figures. Results of the uptake of ^{134}Cs, ^{60}Co and ^{89}Sr onto S_1 are plotted in figure (56). The capacity of S_1 to ^{134}Cs, ^{60}Co and ^{89}Sr is about 14.4 mg g^{-1}, 19.6 mg g^{-1} and 20.8 mg g^{-1}, respectively. However, on using clay sample S_2 it was found that its capacity to ^{134}Cs, ^{60}Co and ^{89}Sr is about 7.2 mg g^{-1}, 21.0 mg g^{-1} and 15.6 mg g^{-1}, respectively as shown in figure (57). From figure (58) it is clear that the capacity of S_3 to ^{134}Cs, ^{60}Co and ^{89}Sr is about 1.7 mg g^{-1}, 14.7 mg g^{-1} and 6.1 mg g^{-1}, respectively. Figure (59) shows the sharp s-shape breakthrough curves in sorption of phenol onto the studied samples. It is clear that the sorption capacity of phenol onto S_1, S_2 and S_3 is 3.4 mg g^{-1}, 2.2 mg g^{-1} and 16.5 mg g^{-1}, respectively. These data show the effectiveness of the samples for the removal of the selected contaminants from aqueous solutions.

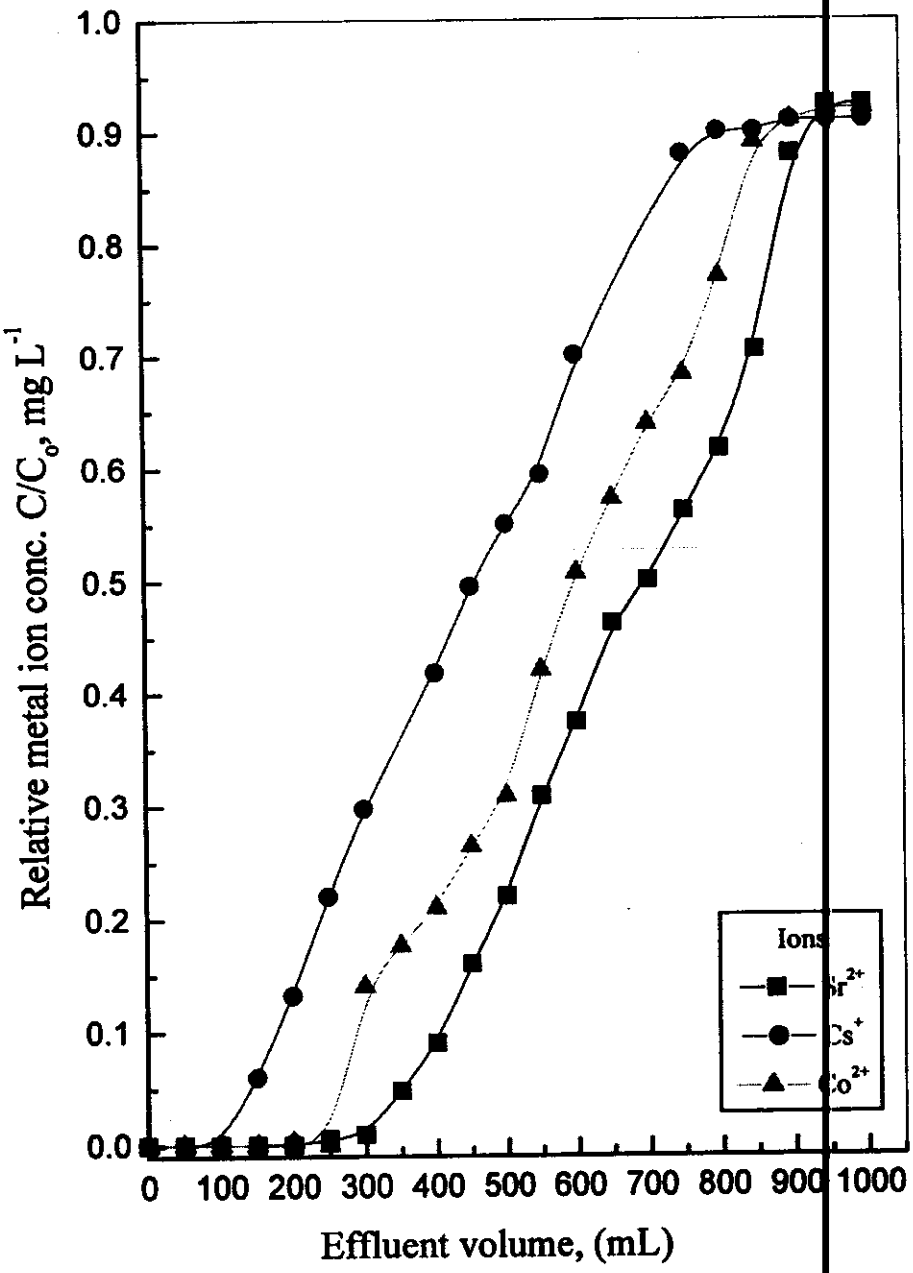

Fig. (56): Breakthrough curves of sorption the selected metal ions onto S_1; $C_0 = 20$ mg L^{-1}.

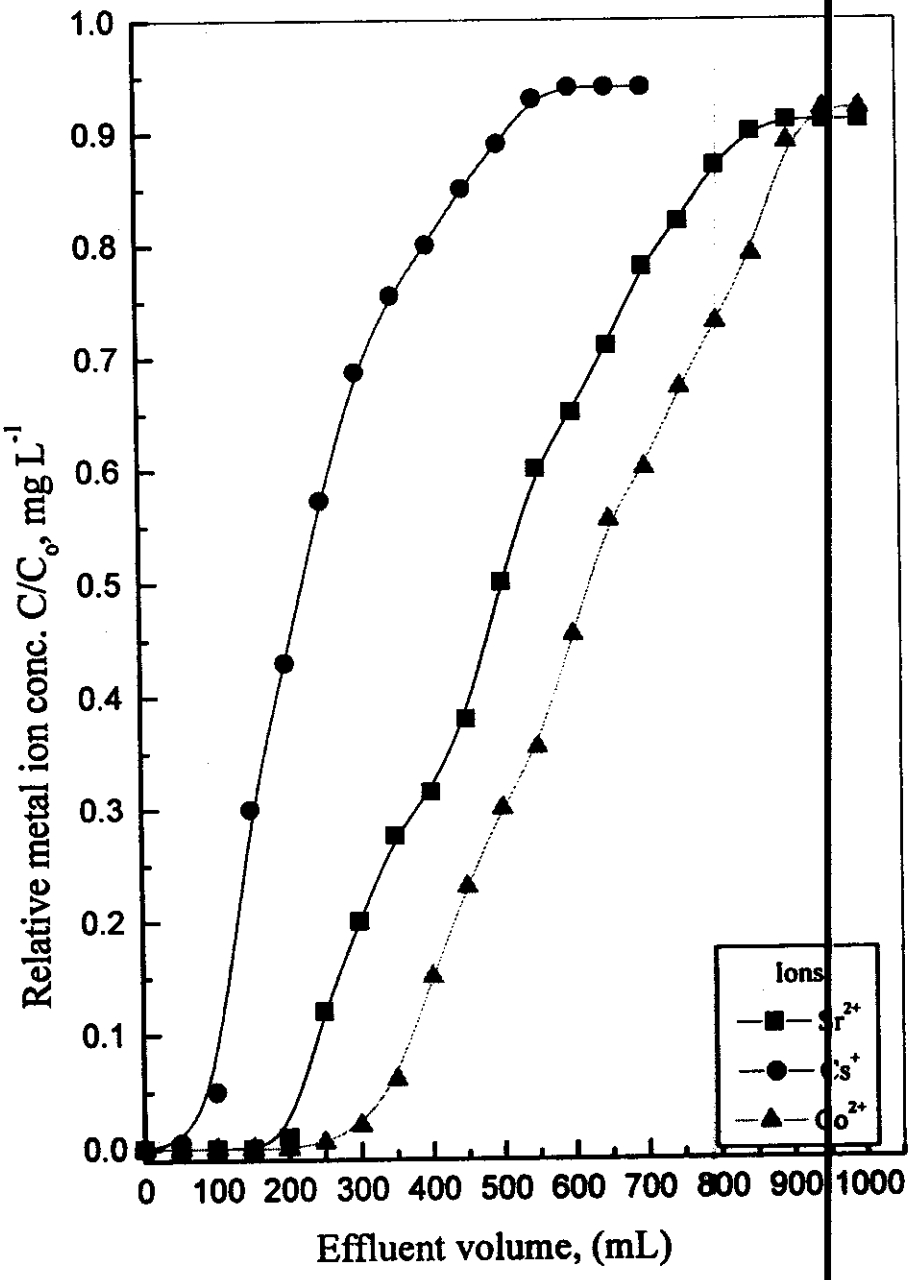

Fig. (57): Breakthrough curves of sorption the selected metal ions onto S_2; C_0 =20 mg L^{-1}.

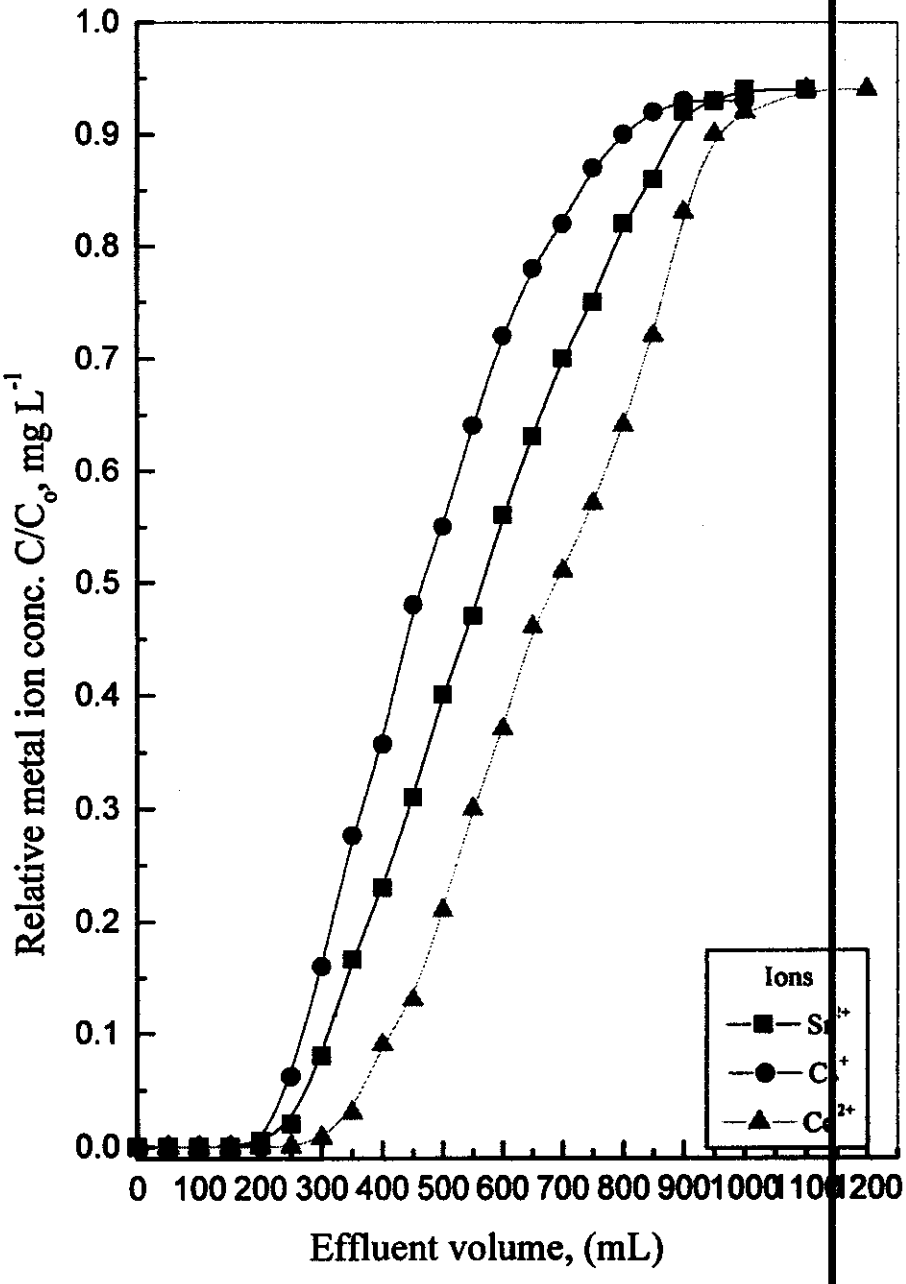

Fig. (58): Breakthrough curves of sorption of the selected metal ions onto S_3; $C_0 = 20$ mg L^{-1}.

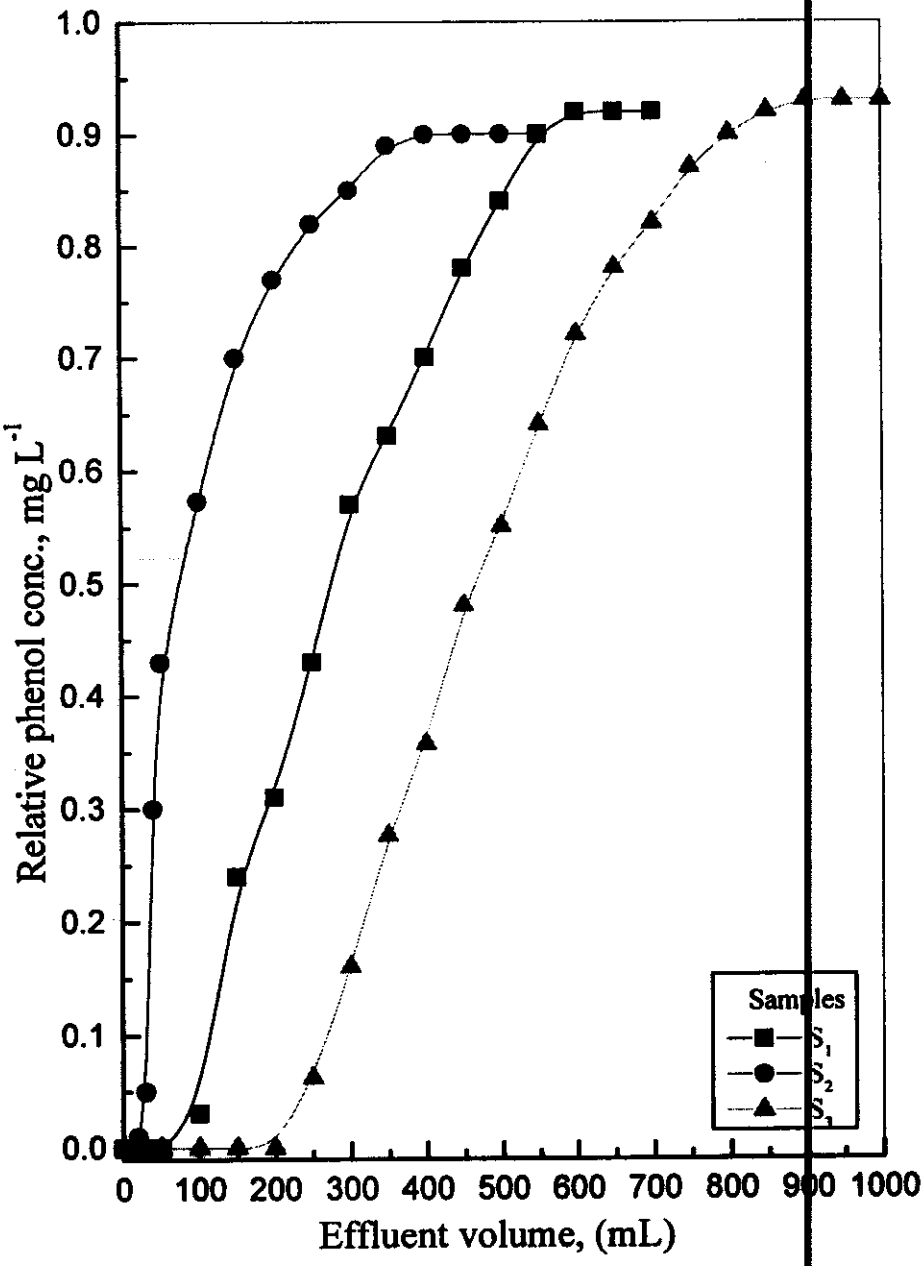

Fig. (59): Breakthrough curves of phenol sorption onto the investigated samples; C_0 = 20 mg L^{-1}.

III. 10 Removal of mixture of the investigated contaminants (Cs^+, Co^{2+}, Sr^{2+} and phenol) from waste solution by the studied samples

The application of radionuclides in research institutions, hospitals and industries generates aqueous waste solutions. The waste solutions should be treated to remove the hazard isotopes prior discharge to the environment. The treatment should reduce the quantities of radioactive contaminants to a level which allows safe discharge according to national and international regulations.

Removal of mixture of Cs^+, Co^{2+} and Sr^{2+} from aqueous waste solution on each studied samples was investigated. The variation of percentage uptake of the mixture of Cs^+, Co^{2+} and Sr^{2+} from the waste solution as a function of contact time is shown in figures (60 - 62). The figures show that the percentage uptake increases with time till attains a constant value depending on the type of the contaminant and the nature of the sample studied (specific area of the grains and the chemical composition). By comparing between these data and that obtained in case of individual elements, it is clear that the percentage uptake values of the selected ions are lower in case of mixture waste solution than that of individual waste solution while the percentage uptake of phenol is similar in the two cases as shown in table (13). This decrease in the percentage uptake of metal ions in mixture may be attributed to the comparative effect of other cations present in the waste solution on available exchange sites within the studied samples and these data are in a good agreement with that reported by **Omar, (2002), Atta, (2001), Ezz El-Din, (1995) and Abdel-Gawad et al., (1981).**

Table (13): The uptake % of the investigated contaminants by the studied samples

Samples	Contaminants	Uptake %	
		Individual contaminant	Mixture of contaminants
S_1	Cs^+	78	66
	Co^{2+}	89	62
	Sr^{2+}	96	69
	Phenol	35	31
S_2	Cs^+	25	18
	Co^{2+}	74	62
	Sr^{2+}	66	55
	Phenol	25	22
S_3	Cs^+	28	21
	Co^{2+}	95	81
	Sr^{2+}	84	70
	Phenol	83	78

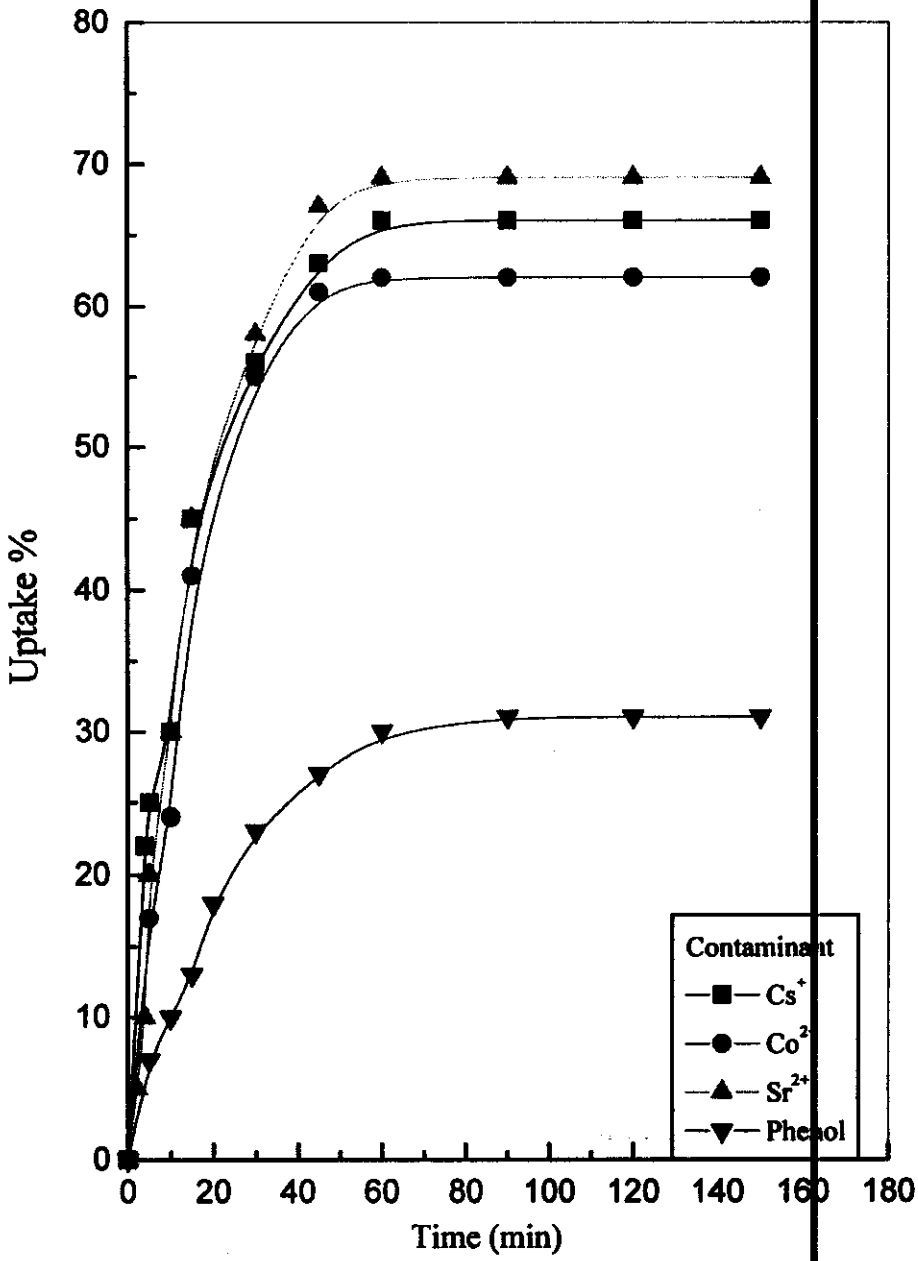

Fig. (60): Variation of uptake % of the studied contaminants onto S_1 as a function of contact time, C_0 of metal ions = 10 mg L^{-1}, C_o of phenol = 50 mg L^{-1}.

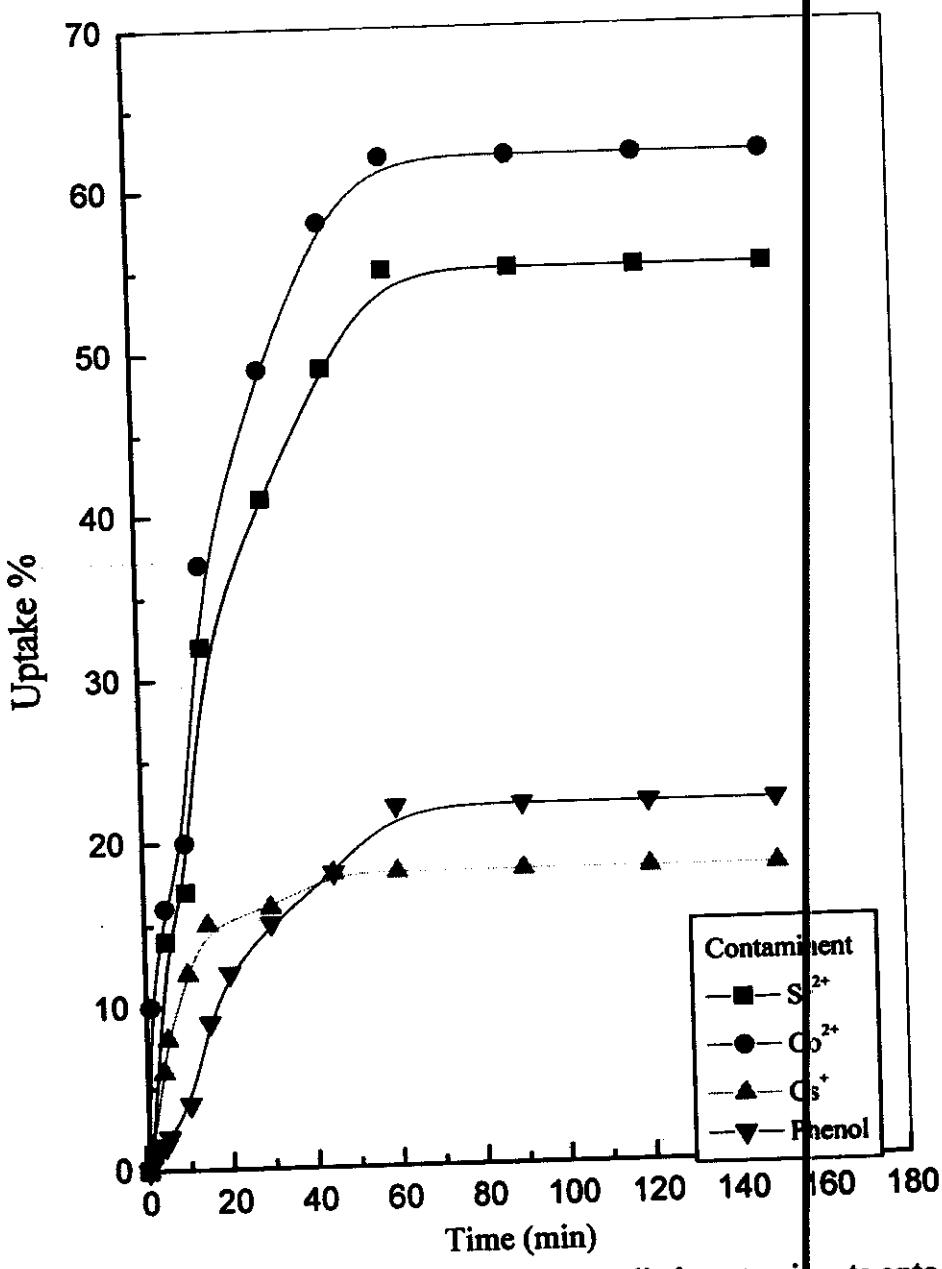

Fig. (61): Variation of uptake % of the studied contaminants onto S_2 as a function of contact time, C_0 of metal ions = 10 mg L^{-1}, C_o of phenol = 50 mg L^{-1}.

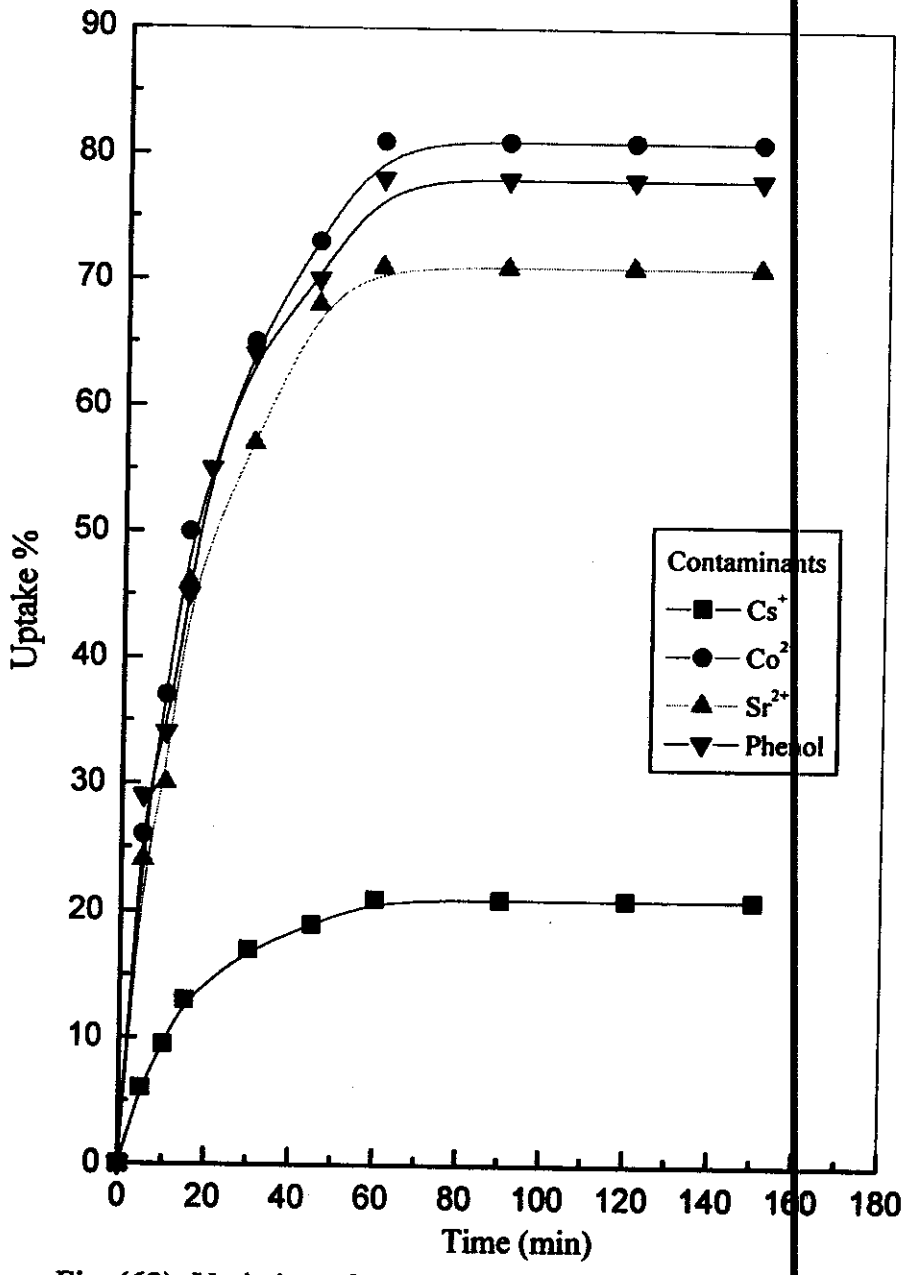

Fig. (62): Variation of uptake % of the studied contaminants onto S_3 as a function of contact time, C_0 of metal ions = 10 mg L^{-1}, C_o of phenol = 50 mg L^{-1}.